THESIS FOR THE DEGREE OF DOCTOR OF PHILOSOPHY

# Cellulose in Quaternary Ammonium-based Solvents

## Dissolution, Modification and Coagulation

SHIRIN NASERIFAR

Department of Chemistry and Chemical Engineering

CHALMERS UNIVERSITY OF TECHNOLOGY

Gothenburg, Sweden 2023

Cellulose in Quaternary Ammonium-based Solvents

Dissolution, Modification and Coagulation

SHIRIN NASERIFAR

ISBN 978-91-7905-918-7



Doktorsavhandlingar vid Chalmers tekniska högskola

Ny serie nr 5384

ISSN 0346-718X

Department of Chemistry and Chemical Engineering

Chalmers University of Technology

SE-412 96 Gothenburg

Sweden

Telephone + 46 (0)31-772 1000

**Front cover:**

Dissolution of cellulose extracted from wood followed by coagulation relevant for application in textiles.

**Back cover:**

Photograph by Soheil Soltani.

Printed by Chalmers Digitaltryck

Gothenburg, Sweden 2023

*To my family*

*"It is not only the question,*

*but the way you try to solve it."*

Maryam Mirzakhani

**Cellulose in Quaternary Ammonium-based Solvents**

Dissolution, Modification and Coagulation

SHIRIN NASERIFAR

Department of Chemistry and Chemical Engineering
Chalmers University of Technology

## Abstract

Processing cellulose through dissolution and regeneration is essential for many applications, yet challenges are posed because it does not readily melt or dissolve in commonly used aqueous and organic solvents. Consequently, extensive efforts have been devoted to developing novel and efficient solvents for cellulose, as well as exploring new functionalization routes. Existing limitations associated with current solvents, such as solution instability, limited dissolution capacity, specific temperature requirements, solvent-related side reactions and a narrow concentration range, are nevertheless significant.

Water-based solvents are of particular interest since they can be applicable in large scales. This thesis mainly focuses on quaternary ammonium hydroxides (QAHs) since they enhance cellulose dissolution compared to extensively studied NaOH(aq) with the aim of gaining deeper insight into the impact of the structural characteristics of the quaternary ammonium-based solvents on cellulose dissolution, modification and coagulation. Initially, cellulose etherification in previously investigated solvents, benzyltrimethylammonium hydroxide, tetramethylammonium hydroxide and NaOH(aq) was investigated *in situ* using spectroscopy and rheology techniques. The results revealed enhanced reagent solubility, improved cellulose solution stability during the reaction and less pronounced cascade reaction in QAHs, either alone or in combination. With the importance of the solvent structure highlighted for cellulose modification and inspired by the industrially used *N*-methylmorpholine *N*-oxide, a series of morpholinium salts with different alkyl chain lengths combined with hydroxide, acetate or chloride counterions were prepared and their ability to dissolve cellulose was investigated. This study aimed to examine the structural properties of the solvent governing dissolution which indeed highlighted the importance of both the cation and anion structures: morpholinium chlorides were incapable of dissolving cellulose whereas morpholinium acetates combined with DMSO and aqueous morpholinium hydroxides functioned as cellulose solvents. While alkyl chains longer than ethyl enabled room-temperature dissolution in aqueous morpholinium hydroxides (likely through improved stabilization of the hydrophobic regions of cellulose), they decreased the dissolution ability of morpholinium acetates in DMSO-based systems. Finally, the behaviour of cellulose solutions in benzyltrimethylammonium hydroxide and two of the newly developed morpholinium hydroxides during coagulation was studied which highlighted the importance of hydrophobic structural motifs for the consistency of the formed gels.

**Keywords**: cellulose, quaternary ammonium hydroxides, dissolution, etherification, gelation.

## Preface

This doctoral thesis serves as partial fulfilment of the requirement for obtaining the degree of Doctor of Philosophy at Chalmers University of Technology, Gothenburg, Sweden. This Ph.D. project was funded by Knut and Alice Wallenberg Foundation within Wallenberg Wood Science Center. The work was conducted mainly at the Division of Forest Products and Chemical Engineering (SIKT) at the Department of Chemistry and Chemical Engineering between July 2019-September 2023 under the supervision of Associate Professor Merima Hasani and Associate Professor Diana Bernin. Part of the third study was conducted at the Institute for Organic Chemistry and Macromolecular Chemistry at Friedrich Schiller University, Jena, Germany, under the supervision of Dr. Andreas Koschella and Professor Thomas Heinze in May-July 2022.

Shirin Naserifar

September 2023

# List of publications

This thesis is based on the following appended papers:

**Paper I.** ***In situ*** **monitoring of cellulose etherification in solution: probing the impact of solvent composition on the synthesis of 3-allyloxy-2-hydroxypropyl-cellulose in aqueous hydroxide systems**
S. Naserifar, P. F. Kuijpers, S. Wojno, R. Kádár, D. Bernin and M. Hasani, *Polym. Chem.*, 2022,13, 4111-4123. https://doi.org/10.1039/D2PY00231K

**Paper II.** **Aqueous *N,N*-dimethylmorpholinium hydroxide as a novel solvent for cellulose**
S. Naserifar, B. Swensson, D. Bernin and M. Hasani, *Eur. Polym. J.*, 2021, 110822. https://doi.org/10.1016/j.eurpolymj.2021.110822

**Paper III.** **Investigation of cellulose dissolution in morpholinium-based solvents: impact of solvent structural features on cellulose dissolution**
S. Naserifar, A. Koschella, T. Heinze, D. Bernin and M. Hasani, *RSC Adv.*, 2023,13, 18639-18650. https://doi.org/10.1039/D3RA03370H

**Paper IV.** **Investigation of cellulose gelation in aqueous hydroxide solutions by $CO_2$(g): Detailed experimental and theoretical approach**
S. Naserifar, N. K. Karna, A. M. Kozlowski, D. Bernin and M. Hasani
Submitted manuscript.

Additional publication not included in the thesis:

***In line*** **monitoring of carbon dioxide capture with sodium hydroxide in a customized 3D-printed reactor without forced mixing**
E. Leventaki, F.M. Baena-Moreno, G. Sardina, H. Ström, E. Ghahramani, S. Naserifar, P. H. Ho, A. M. Kozlowski and D. Bernin, *Sustainability,* 2022, 14, 10795. 10795. https://doi.org/10.3390/su141710795

# Contribution Report

**Shirin Naserifar** has contributed to the papers included in this thesis as follows:

Paper I. **Main author**. Designed and carried out all the experimental work with the exception of the rheology measurements, which were carried out and interpreted at the Industrials and Materials Science Department by MS. Sylwia Wojno and Prof. Roland Kádár, and the NMR measurements which were run at the Swedish NMR Center and interpreted partly by co-supervisor Assoc. Prof. Diana Bernin. Dr. Paul Kuijpers, a consultant at Metler-Toledo, contributed to the design and interpretation of the *in situ* IR study measurements. Evaluated the results with the support of the co-authors, wrote the paper and revised it after receiving co-authors' feedbacks.

Paper II. **Main author**. Designed and performed all the experiments except for the intrinsic viscosity measurements, which were partially done together with Dr. Beatrice Swensson. Dynamic light scattering (DLS) measurements were run and interpreted by Dr. Beatrice Swensson and size exclusion chromatography (SEC) measurements were run by Ms. Christina Wedin at MoRe Research. Evaluated the results with the support of the co-authors, wrote the paper except for the DLS part, and revised it after receiving the co-authors' feedback.

Paper III. **Main author**. Designed and performed all the experiments except for the elemental analysis and Karl-fisher titration which were performed by Ms. Sandra Köhn and Ms. Beate Fähndrich, respectively, at Friedrich Schiller University Jena, Germany. SEC measurements were performed by Ms. Christina Wedin at MoRe Research, liquid state NMR measurements were run by Assoc. Prof. Diana Bernin, and solid-state NMR measurements were conducted by Dr. Tobias Sparrman at Umeå University. Evaluated the results with the support of the co-authors. Wrote the paper and revised it after receiving the co-authors' feedback.

Paper IV. **Main author**. Designed and carried out all the experiments. MD simulations were run, interpreted, and written by Dr. Nabin Kumar Karna and solid-state NMR measurements were run by Dr. Tobias Sparrman at Umeå University and partially interpreted by Assoc. Prof. Diana Bernin. Evaluated the results with the support of the co-authors, wrote the paper and revised it after receiving feedback from the co-authors.

**Parts of the results have also been presented at:**

- The 7th International Polysaccharides Conference (EPNOE)
  **Probing the impact of the hydroxide base composition on the etherification of cellulose**
  Oral presentation, Nantes, France, 11-15 October, 2021.

- The 21st International Symposium on Wood, Fiber and Pulping Chemistry
  **Investigation of cellulose dissolution in morpholinium-based solvents**
  Oral presentation, Venice, Italy, 4-7 July, 2023.

- The 8th International Polysaccharides Conference (EPNOE)
  **Gelation of cellulose in aqueous alkaline solutions by $CO_2$(g)**
  Oral presentation, Graz, Austria, 18-22 September, 2023

- Chalmers Science and Technology Day
  **Investigation of cellulose dissolution in morpholinium-based Solvents**
  Poster presentation, Gothenburg, Sweden, 16 May, 2023

- Biannual Wallenberg Wood Science Center Workshops
  Pitches and poster presentations, Sweden, 2019-2023

## List of Abbreviations

| | |
|---|---|
| AGU | Anhydroglucose unit |
| AGE | Allyl glycidyl ether |
| AHP-cellulose | 3-allyloxy-2-hydroxypropyl-cellulose |
| AMIMCl | 1-allyl-3-methylimidazolium chloride |
| AMMorCl | *N*-allyl-*N*-methylmorpholinium chloride |
| AMMorOAc | 4-allyl-4-methylmorpholinium acetate |
| BMIMCl | 1-butyl-3-methylimidazolium chloride |
| BMMorOAc | *N*-butyl-*N*-methylmorpholinium acetate |
| BMMorOH | *N*-butyl-*N*-methylmorpholinium hydroxide |
| CA | Cellulose acetate |
| CMC | Carboxymethyl cellulose |
| CP/MAS | Solid-state Cross-Polarization Magic Angle Spinning |
| $CS_2$ | Carbon disulfide |
| DLS | Dynamic light scattering |
| DMAc/LiCl | *N,N*-dimethylacetamide/lithium chloride |
| DMAP | 4-dimethylaminopyridine |
| DMSO | Dimethyl sulfoxide |
| DMSO-$d_6$ | Deuterated dimethyl sulfoxide |
| $D_2O$ | Deuterium oxide |
| DP | Degree of polymerization |
| EMIMAc | 1-ethyl-3-methylimidazolium acetate |
| EMMorCl | *N*-ethyl-*N*-methylmorpholinium chloride |
| EMMorOAc | *N*-ethyl-*N*-methylmorpholinium acetate |
| EMMorOH | *N*-ethyl-*N*-methylmorpholinium hydroxide |
| GTAC | Glycidyltrimethylammonium chloride |
| HMMorOAc | *N*-heptyl-*N*-methylmorpholinium acetate |
| HMMorOH | *N*-heptyl-*N*-methylmorpholinium hydroxide |
| HPC | Hydroxypropyl cellulose |
| HSQC | Heteronuclear single quantum coherence |
| IL | Ionic liquid |

| | |
|---|---|
| MC | Methyl cellulose |
| MD | Molecular dynamics |
| MCC | Microcrystalline cellulose |
| MorCl | Morpholinium chloride |
| MorOAc | Morpholinium acetate |
| MorOH | Morpholinium hydroxide |
| MPMorCl | *N*-methyl-*N*-propylmorpholinium chloride |
| MPMorOAc | *N*-methyl-*N*-propylmorpholinium acetate |
| MPMorOH | *N*-methyl-*N*-propylmorpholinium hydroxide |
| MS | Molar substitution |
| $M_w$ | Molecular weight |
| NDMMCl | *N,N*-dimethylmorpholinium chloride |
| NDMMOH | *N,N*-dimethylmorpholinium hydroxide |
| NMMO | *N*-methylmorpholine N-oxide |
| NMR | Nuclear magnetic resonance |
| PD | Polydispersity |
| PEG | Polyethylene glycol |
| QAH | Quaternary ammonium hydroxide |
| QAF | Quaternary ammonium flurides |
| RHS | Right hand side |
| SEC | Size exclusion chromatography |
| TBAH | Tetrabutylammonium hydroxide |
| TEAOH | Tetraethylammonium hydroxide |
| TMAH | Tetramethylammonium hydroxide |
| Triton B | Trimethylbenzylammonium hydroxide |
| Triton F | Dimethyldibenzylammonlum hydroxide |

## Table of Contents

# 1

# Introduction

Today, the planet faces major environmental challenges stemming from a significant population increase and a continued reliance on petroleum-based resources to fulfil human needs. Many industries depend heavily on fossil feedstock to manufacture everyday products. The growing need to transit towards renewable alternatives has, however, attracted tremendous attention towards the use of biomass to meet the escalating demands for materials and chemicals. One particularly invaluable material in this context is cellulose which is the most available biopolymer on Earth. Cellulose has gained increasing attention due to its wide-ranging applications in various end-use products, including paper, textiles, cellulose derivatives for food and pharmaceuticals, etc. As the demand for cellulose continues to rise in diverse areas, there is a serious need to explore and enhance ways of processing cellulose, and to develop a range of structural modifications through extensive research.

Cellulose poses challenges in processing due to not only its inability to melt (it degrades before melting) but also to its resistance to dissolve in conventional organic and aqueous solvents, making it difficult to be used in many applications. Certain solvent systems capable of dissolving cellulose (with or without cellulose derivatization) have been developed in order to address this issue, two of which are used extensively on an industrial scale: aqueous carbon disulphide-sodium hydroxide ($CS_2$-NaOH(aq)) and *N*-methylmorpholine *N*-oxide (NMMO), which are used in viscose and Lyocell processes, respectively. The drawbacks associated with these solvents, namely toxicity, instability, low dissolution capacity, undesired side reactions, cellulose degradation [1,2] and a limited range of textile fibre properties have, however, called for further research to overcome these limitations and explore the development of novel solvents that can offer improved capabilities for processing cellulose. Of particular interest are those offering the possibility of processing in water systems or ionic liquids such as quaternary ammonium-based salts. Despite the significant amount of research already conducted on cellulose dissolution, there remains a lack of comprehensive

understanding regarding the significance of the structural motifs of the solvent, especially the influence of the cation structure on the dissolution of cellulose in salt systems as well as on coagulation, and the resulting characteristics of the coagulated material.

Furthermore, three reactive OH groups present in the cellulose backbone offer the opportunity for chemical modification and the creation of numerous derivatives with diverse properties and applications. Among these derivatives, cellulose ethers have garnered significant attention due to their non-toxic nature and often water-soluble characteristics. Despite considerable research conducted on cellulose ethers, there is still insufficient knowledge and understanding concerning the course of the etherification reaction, specifically when homogeneous modification is performed in aqueous media. This particularly involves the various side reactions that occur during aqueous processing and the potential of controlling the properties of the products by adjusting reaction conditions. A major challenge contributing to the limited understanding of cellulose etherification lies in the difficulty of *in situ* monitoring of these reactions.

### 1.1 Objectives

The main objective of this work was set to investigate and gain deeper insight into cellulose dissolution, etherification and coagulation in quaternary ammonium-based solvents. More specifically, the studies conducted have aimed at:

- Developing a methodology for *in situ* monitoring of cellulose etherification in a homogeneous aqueous system
- Gaining insight into the influence of the solvent composition on the course and outcome of etherification
- Developing novel quaternary ammonium-based solvents for cellulose, and elucidating the solvent structural features required for cellulose dissolution
- Investigating the structural impact of the solvent on the stability and gelation of cellulose dissolved in quaternary ammonium hydroxides

### 1.2 Scope

The initial focus of this work was on cellulose etherification in two well-known aqueous quaternary ammonium hydroxides: tetramethylammonium hydroxide (TMAH) and benzyltrimethylammonium hydroxide (Triton B) as wells as NaOH(aq). These solvents were studied both individually and in different combinations for their impact on the cellulose etherification process as well as the obtained product, with the emphasis on *in situ* monitoring. Since the crucial role of the solvent in these reactions, indeed was highlighted in this study, the work that followed aimed at developing novel quaternary ammonium-based solvents inspired by the commercially employed *N*-methylmorpholine *N*-oxide (NMMO) and based on the morpholinium cation

combined with hydroxide, acetate or chloride counter ions to identify the structural requirements for enhanced cellulose dissolution. After proving the dissolution power of morpholinium hydroxides and morpholinium acetates, the final study investigated the effect of cation structure in morpholinium hydroxides on the stability of cellulose in the dissolved state against gelation by $CO_2$(g), as well as on the properties of the systems after gelation.

### 1.3 Outline

This thesis is based on the four appended papers. Chapter 2 covers the background of cellulose: its structure, dissolution, modification and regeneration. Chapter 3 presents materials and general methods used to perform the experiments and characterisation. Results and discussions of the studies on cellulose etherification, development of novel quaternary ammonium-based solvents and cellulose gelation in quaternary ammonium hydroxides are outlined in Chapter 4, followed by conclusions in Chapter 5. Finally, some suggested future works are presented in Chapter 6.

# 2

# Background

This chapter presents an introduction to cellulose structure, solvents, chemical modification and regeneration.

## 2.1 Cellulose

The discovery of cellulose can be traced back to 1838, when the French chemist Anselme Payen observed a solid fibrous material left as a residue after plant tissue was treated with acid or ammonia and then subjected to subsequent extraction with water, alcohol and ether [3,4]. Through elemental analysis, he determined its chemical formula to be $C_5H_{10}O_5$. The term "cellulose" was initially used in a report on Payen's findings in 1839 [5]. Later, in 1920, Hermann Staudinger discovered the polymer structure of cellulose [6], which is currently known as a linear homopolysaccharide. Today, cellulose is widely recognised as the most abundant biopolymer on Earth, being a major component of plant cell walls, which can also be found in various living organisms such as algae, tunicates and bacteria.

## 2.2 Cellulose structure, ultrastructure and morphology

Cellulose exhibits a consistent molecular structure irrespective of its biological origins. It is comprised of D-anhydroglucose units (AGU) linked together through β-1,4-glycosidic linkages, with every second AGU rotated 180 °C around it (Figure 1). The degree of polymerisation (DP), which indicates the number of connected D-glucose units varies depending on the source and the extraction process from which cellulose is derived [7], for instance in native wood the DP is estimated to be between 9000 to 10000 [8]. Each end of a cellulose chain is chemically distinct: a reducing end where the free anomeric carbon can potentially convert to an aldehyde, and a non-reducing end where the anomeric carbon atom is involved in a glycosidic bond (Figure 1).

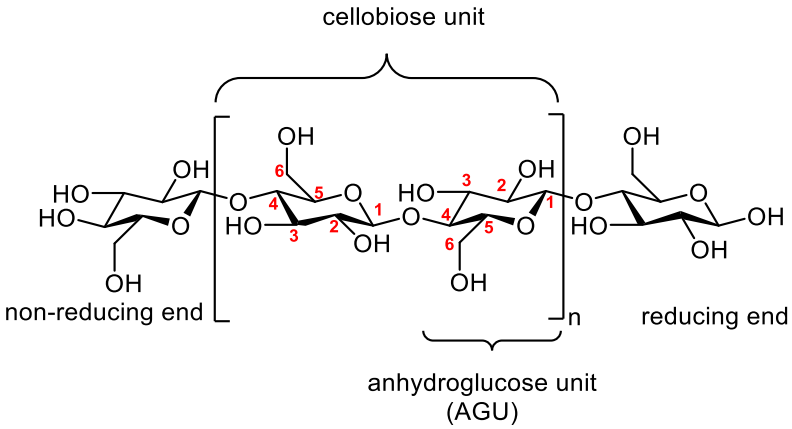


Figure 1. Structure of the cellulose chain.

Each D-anhydroglucose unit (AGU) in the cellulose chain possesses three equatorial OH groups located on the C2, C3, and C6 positions while C-H groups are positioned axially, giving cellulose amphiphilic characteristics. Cellulose hydroxyl groups contribute to the formation of intra- and intermolecular hydrogen bonding within and between the chains. The flat conformation of the cellulose chain is stabilised by the intramolecular hydrogen bonds, resulting in chain rigidity and a high propensity for crystallisation. The intermolecular hydrogen bonds, on the other hand, lead to the alignment of cellulose chains side by side, thereby creating a sheet-like structure. Additionally, as previously mentioned hydrogens are axially linked to the carbons of the pyranose ring, forming hydrophobic regions above and below the ring planes. Cellulose sheets stack on top of each other due to additional forces namely via van der Waals interactions between hydrophobic regions resulting in formation of microfibrils. These microfibrils then aggregate into larger structures, known as macrofibrils, within the cell wall. These, in turn, are deposited in different layers of the cell walls and thus form the cellulose part of a fibre.

Similar to most polymers, cellulose microfibrils are regarded as not being entirely crystalline: they are, in fact, semi-crystalline in structure, containing both ordered and less-ordered regions which has been described by the fringed fibrillar model [9] (Figure 2). The proportions of crystalline and amorphous regions in cellulose vary, depending on its origin [10,11].

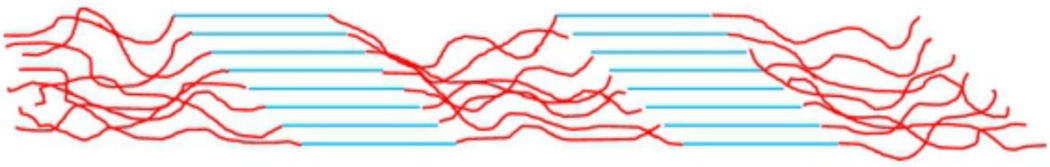

Figure 2. The organisation of cellulose chains in a microfibril [12]. Reprinted under the Creative Commons license (CC BY 3.0).

Since cellulose can exhibit different types of crystallinities, extensive studies have led to the identification of four crystalline allomorphs: Cellulose I, II, III and IV. The crystalline structure of native cellulose, formed during biosynthesis, is referred to as cellulose I and is comprised of a combination of two crystal forms: Iα and Iβ. In cellulose derived from wood, the Iβ form predominates [13]. In cellulose I, the intramolecular hydrogen bonds are typically formed between the C3 hydroxyl groups and the ring oxygen in the adjacent AGU, as well as between the C2 hydroxyl groups and the hydroxyl group on the C6 position of the neighbouring AGU [14]. On the other hand, the interchain hydrogen bonds occur between the hydroxyl group on C6 and the hydroxyl group on C3 of the neighbouring chain [14] (Figure 3). Cellulose II, a crystalline structure that is thermodynamically more stable, is obtained by treating native cellulose (cellulose I) with alkali or regenerating it from a dissolved state [15]. While the polymer chains in cellulose I are arranged in a parallel configuration, they are believed to undergo a transformation into an antiparallel arrangement with a different hydrogen bonding pattern in cellulose II. For instance, cellulose II only consists of intramolecular hydrogen bonds between the C3 hydroxyl groups and the ring oxygen in the adjacent AGU as well as intermolecular hydrogen bonds between hydroxyl group on C6 and hydroxyl group on C2 [10] (Figure 3).Cellulose III, formed by treating native cellulose with liquid ammonia or anhydrous ethylamine, is known to contain a relatively high amount of less ordered material, whereas cellulose IV can be obtained through diverse chemical treatments at elevated temperatures [16,17] such as treatment of cellulose III with glycerol at ca. 250 °C [18].

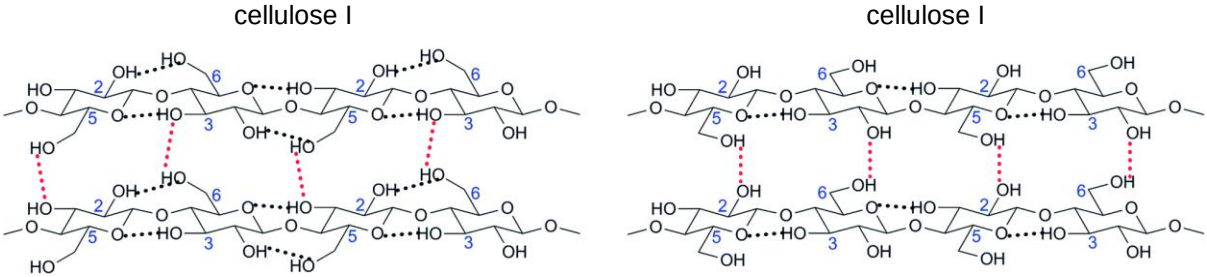


Figure 3. Inter (red) and intramolecular (black) hydrogen bondings in cellulose I and II [10]. Adapted with permission from the Royal Society of Chemistry.

Cellulose fibrils are located in a multilayered structure in the cell wall comprised of primary and secondary wall surrounding the lumen (Figure 4). The thin primary wall consists of cellulose microfibrils that are orientated randomly, whilst the secondary layer has 2-3 layers of cellulose microfibrils that are orientated in a specific direction. In wood, cellulose is typically accompanied by hemicelluloses, heteropolysaccharides believed to provide different regulatory functions and lignin, an aromatic macromolecule[19] playing a crucial role in providing mechanical strength, acting as a barrier against microbial attacks, and facilitating liquid transportation through hydrophobization [20–22]. The cell walls are glued together by a lignin-rich middle lamella. In addition, the presence of a small amounts of low molecular compounds,

known as extractives, with important physiological functions in the cell wall should also be considered. Unlike wood, cotton contains almost pure cellulose which constitutes approximately 90% of the total composition.

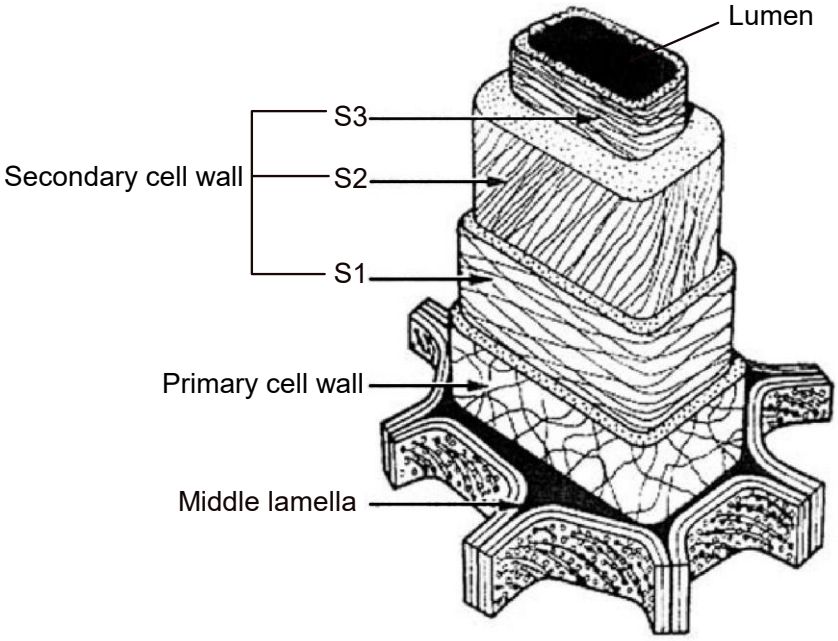


Figure 4. Structure of the cell wall of wood [23]. Adapted under the Creative Commons license (CC BY 4.0).

Various pulping processes are employed to isolate cellulose from e.g. wood, resulting in cellulose fibres of varying strengths and purity. During the pulping process, cellulose fibres are liberated by removing lignin and hemicellulose and pores are created in the cellulose fibre wall, which are critical to its accessibility. Also, the DP of cellulose is reduced to 300-1700 AGUs due to degrading side reactions during the rather harsh pulping processes [24].

Mechanical pulps, i.e. thermomechanical pulp (TMP) and chemo-thermomechanical pulp (CTMP), typically contain residual hemicellulose and around 20-25% residual lignin [25,26]. They are used for short term purposes (newsprint, toilet tissue, etc.) and middle layers of a paperboard since they turn yellow with age [25]. Dissolving pulps, on the other hand, exhibit a higher cellulose content, since the contents of lignin, hemicellulose and extractive is in total less than 10% [27]. Dissolving pulps are used to produce regenerated cellulose for applications such as textile fibres and films, as well as cellulose derivatives.

### 2.3 Cellulose reactivity and accessibility

The reactivity of cellulose relies primarily on the inherent chemical reactivity of its three hydroxyl groups present on each AGU: one primary hydroxyl on C6 and two secondary hydroxyls on C2 and C3 but is strongly dependent on their accessibility that plays a crucial role in chemical modification and dissolution processes. Various factors

influence the accessibility of cellulose, including pore sizes within the cellulose structure, the internal accessible surface (dependant on the size of fibril aggregates and degree of crystallinity), the sizes and types of reagent and solvent that are used [28]. The efficient chemical modification of cellulose therefore requires proper access to the hydroxyl groups. This can be achieved through complete dissolution, which is often not possible using conventional solvents, or by employing suitable pretreatments to enhance accessibility prior to performing heterogeneous modifications in a solid state or suspension. In order to promote the accessibility of cellulose, it is essential to keep the pores open, disrupt the fibrillar aggregates and the crystalline regions [29].

In recent decades, various pretreatment methods have been utilised to enhance the accessibility and reactivity of cellulose before further processing. These methods, which include mechanical, chemical, enzymatic and thermal pretreatments, have been extensively employed on both small laboratory and large industrial scales [30].

### 2.4 Cellulose solubility

Cellulose neither melts when heated nor dissolves in the most common organic solvents. It does not dissolve in water either, despite the potential for hydrogen bonding. Among the parameters contributing to the poor solubility of cellulose is its amphiphilicity that entails a combination of extensive intermolecular hydrogen bonding and association through hydrophobic effect stabilising a semi-crystalline supramolecular structure within a complex morphological organisation [31]. Moreover, compared to glucose monomer, high DP of cellulose and the chain stiffness (as a result of intramolecular hydrogen bonding) results in decreased entropy of dissolution [32].

It is noteworthy to mention that the different sources (cellulose biogenesis) and processes from which cellulose is extracted can affect its solubility due to the resulting differences in microstructure, chemical environment and chain length [33]. One prominent result of these differences in microstructure is "ballooning" that occurs during the dissolution of cellulose fibres, providing different levels of swelling and dissolution in different layers of the cell wall. This phenomenon is believed to be a consequence of the enhanced swelling and dissolution of cellulose within the inner parts of the fibres (primarily S2) compared to the more hard-to-dissolve outer layers. As the cellulose swells, the outer layers (likely the primary wall and the helically arranged S1 or parts of it) remain undissolved as a membrane, roll up and forms collars, rings or spirals, which restricts the uniform expansion of the fibre and gives rise to the formation of balloons [34] (Figure 5). This ballooning has been said to involve three primary areas: (i) fragments composed of the S2 layer that dissolve rapidly within the balloons, (ii) the balloon membrane, comprised of the swollen S1 layer, which dissolves gradually, and (iii) the helices and collars surrounding the balloons, composed probably of the primary wall and possibly parts of S1, which do not dissolve easily and eventually

rupture due to the expansion of the dissolving material [35–37]. The mechanism and the extent of ballooning depend strongly on the morphology of the fibre [33,37].

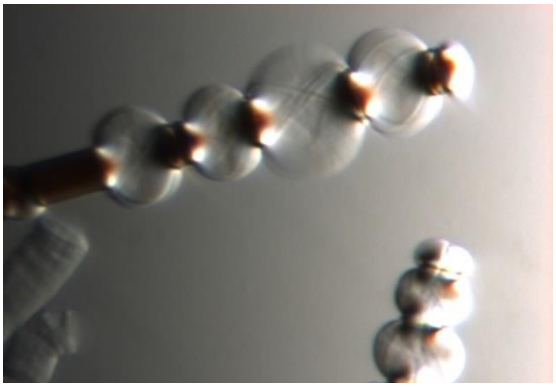

Figure 5. Image of the ballooning effect that occurs during the dissolution of 1 wt% dissolving pulp in 1.3 M *N,N*-dimethylmorpholinium hydroxide

For a long time, the insolubility of cellulose had been correlated mainly to the presence of extensive hydrogen bonding. However, today, the cellulose community has recognized the amphiphilic characteristic of cellulose and the resulting combination of different types of stabilizing interactions (e.g. hydrogen bonding combined with the van der Waals interactions in the hydrophobic areas) , along with poor entropy of dissolution as being decisive in this regard [38–41]. Using molecular dynamics simulations, Bergenstråhle *et al.* demonstrated that the impact of hydrogen bonding on cellulose insolubility in an aqueous environment was significantly smaller compared to the effects of hydrophobic contribution [42]. Similarly, it has been discussed that hydrogen bonding can hardly be the driving force behind the insolubility of cellulose because a polymer stabilised by hydrogen bonding ought to be soluble in water. Rather, it is the amphiphilic character of cellulose, and the resulting hydrophobic assembly, that need to be considered when discussing the insolubility of cellulose in aqueous media [32,43,44]. Among the other factors, in this media the amphiphilicity of cellulose leads, namely, to both poor enthalpy and entropy contributions from the aqueous solvent and can be explained briefly as follows: a robust hydrogen bonding network between water molecules would be disrupted in the presence of cellulose chains, particularly in the axial direction around the more hydrophobic regions of the pyranose rings, since these regions cannot participate in conventional hydrogen bonding. Consequently, water molecules in this region would experience both a reduction in the number of hydrogen bonds (not favoured in terms of enthalpy) and greater restrictions in their mobility (decrease in entropy). These disfavour solubilisation of the chains and, instead, favour the stacking of cellulose chains that would, in turn, enable water to be excluded from the hydrophobic surface. Yet, there is a debate whether the hydrophobic assembly is primarily influenced by enthalpy or entropy [45].

### 2.5 Cellulose solvent systems

Cellulose solvent systems can be classified into two main categories: derivatizing and non-derivatizing media. It is noteworthy to mention that certain agents have the ability to swell cellulose to a certain extent without fully dissolving it. These agents have the potential to be applied as functionalization media.

#### 2.5.1 Derivatizing solvents

In derivatizing solvents, cellulose undergoes a reaction to form a soluble cellulose derivative. These solvents serve multiple purposes namely for regenerating cellulose fibres used in textiles or further modifying the dissolved cellulose derivative, like carboxymethylation [46] to produce specific end products [47]. Typically, the solubilising substitution occurs at position 6 of the AGU, which can later act as a protecting group for subsequent derivatization. An inverse functionalization occurs during the workup process and the solubilising substitution is removed most typically in an aqueous solution [48].

A derivatizing solvent for cellulose, $CS_2$/NaOH(aq), has been employed on an industrial scale in the traditional viscose process, which is one of the oldest cellulose processing technologies. In this process, alkali cellulose reacts with carbon disulphide ($CS_2$) to form cellulose xanthate (Figure 6), a soluble derivative that can dissolve in dilute NaOH(aq). The resulting solution, known as viscose, is then extruded into a sulphuric acid bath, where the xanthate ester undergoes hydrolysis; this leads to regeneration of the cellulose, which then undergoes spinning into fibres for textile applications. Besides textile fibres, the viscose process is also utilised to create films (cellophane) and sponges [49]. The annual global demand for textile fibres is estimated to reach 133.5 million tons by 2030 [50–52].

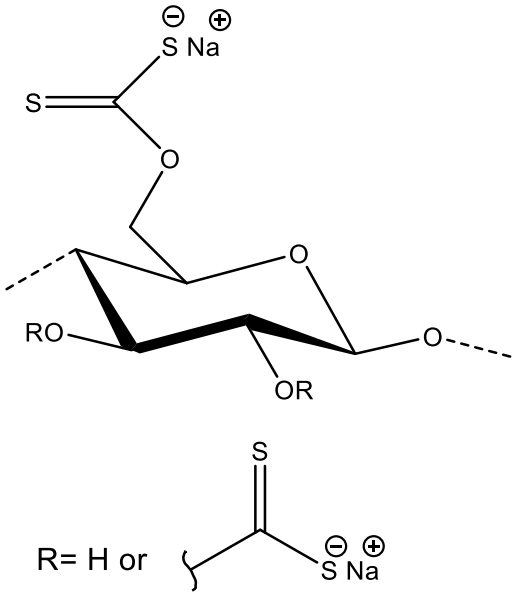


Figure 6. Structure of cellulose xanthate.

### 2.5.2 Non-derivatizing solvents

In non-derivatizing solvents, dissolution occurs via intermolecular interactions between the solvent and cellulose, hence no cellulose derivative is formed. An industrially used solvent which belongs to this category is *N*-methylmorpholine *N*-oxide (NMMO), which is used in the Lyocell process primarily for producing textile fibres. The potential of NMMO to dissolve cellulose was initially discovered and patented in 1970 [53]. Dilute solutions of NMMO(aq) induce cellulose swelling, whereas the monohydrate form (with a water content of 16% or less) [54] is capable of dissolving cellulose with high DP at temperatures above 80 °C [55]. The dissolution of cellulose in NMMO involves the breaking of cellulose hydrogen bonds particularly at C6-OH, the formation of new hydrogen bonds as well as ionic interactions between cellulose and NMMO [56–60] (Figure 7), and probably also stabilization of hydrophobic cellulose regions by van der Waals interactions with the solvent. Some challenges nevertheless remain to be overcome in this process, including the limited temperature range required for the dissolution and the instability of NMMO at high temperatures, especially when the water content is below the monohydrate composition in the presence of heavy metal ions, charcoal and polyelectrolytes [58–61]. The melting point of NMMO monohydrate is 78 °C and, at temperatures exceeding 120 °C, cellulose solutions are prone to strong exothermic reactions, leading to severe degradation [58].

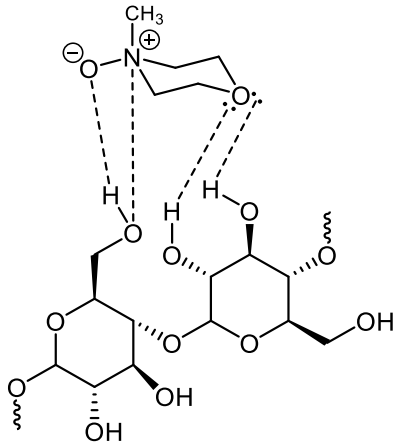


Figure 7. Interaction of NMMO and cellulose [62]. Adapted with the permission from Springer Nature B.V.

#### 2.5.2.1 Aqueous transition metal complexes

Since 1857, when $Cu(OH)_2/NH_3$ (Cuam, Schweizer reagent) was first reported as a cellulose solvent [63], a number of other aqueous metal complexes solvents have been investigated [64–66]. Dissolution mechanism of cellulose in Cuam involves the formation of a robust complex with the hydroxyl groups of cellulose at C2 and C3 (Figure 8). This reagent continues to be utilised widely for determining the DP of cellulose through viscometry.

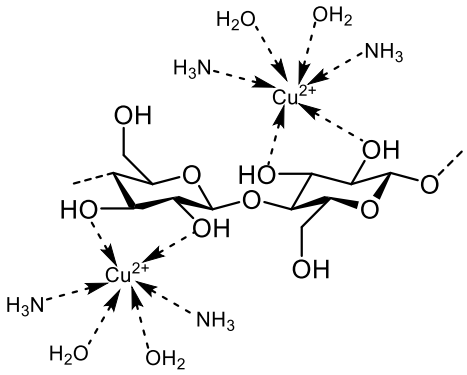


Figure 8. Structure of Cuam–cellulose complex [67]. Adapted under the Creative Commons licence (CC BY 4.0).

2.5.2.2 Ionic Liquids (ILs)

ILs constitute another category of solvents comprised of organic cations and inorganic or organic anions. As early as 1934, Graenacher investigated liquified salts of *N*-alkylpyridinium chloride as potential cellulose solvents [68], yet, active research on cellulose dissolution in ILs began since 2002 when Swatloski *et al.* reported cellulose dissolution in 1-butyl-3-methylimidazolium chloride (BMIMCl) [69]. Since then, several other ILs have been explored as cellulose solvents, including imidazolium-based ILs with various anions being able to dissolve cellulose efficiently at room temperature [70–73]. Many of the extensively studied ILs that are capable of dissolving cellulose have melting points below 100 °C possessing several advantages, such as low vapour pressure, low toxicity and high thermal stability. A number of commonly used ILs consist of pyridinium, imidazolium, ammonium and phosphonium as cations, and acetate ($OAc^-$), formate ($HCOO^-$), dimethyl phosphate ($(MeO)_2\ PO_2^-$) and chloride ($Cl^-$) as anions. Two well-known ILs, namely 1-allyl-3-methylimidazolium chloride (AMIMCl) and 1-ethyl-3-methylimidazolium acetate (EMIMAc), have been reported to dissolve up to 30 wt% cellulose with a relatively high DP of 650 in just 30 minutes [74]. Besides, less toxic morpholinium-based ILs such as 4-allyl-4-methylmorpholinium acetate (AMMorOAc) has been reported to dissolve cellulose with a DP of 789 to a 30 wt% concentration at 120 °C in 20 minutes [75].

Studies of the mechanism of dissolution in ILs have indicated that both the anion and cation contribute to the dissolution [76,77]. New hydrogen bonds formed between the anion and cellulose hydroxyl groups is suggested to disrupt cellulose hydrogen bonds, while the role of the cation is still a subject of debate even though a few studies have shown that the cation interacts with hydrophobic regions of cellulose via van der Waals interactions and consequently breaks the intersheet bonds of the supramolecular cellulose organization [78–81]. The structures of some cations in ILs are illustrated in Figure 9.

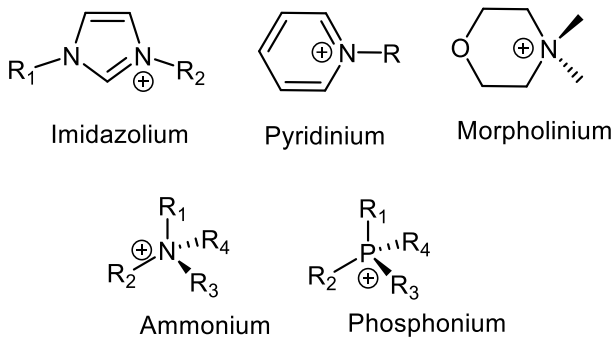


Figure 9. Structures of a few cations commonly used in ILs.

#### 2.5.2.3 Aqueous alkali hydroxides

Cellulose dissolution in NaOH(aq) can be traced back to 1920s, when Lilienfeld reported cellulose dissolution at low temperatures, specially below zero [82]. Soon later Davidson investigated cellulose dissolution in NaOH(aq) [83–85] after which extensive studies have been carried out to date. Except NaOH(aq), LiOH(aq), quaternary ammonium hydroxides (QAHs) and phosphonium hydroxides have demonstrated the ability to dissolve cellulose [86]. This group of solvents is attracting increasing attention due to their feasibility with large scale sustainable processing.

The ability of NaOH(aq) to either swell or dissolve cellulose depends on the temperature, the DP of cellulose and the concentration of NaOH(aq). In 1939, Sobue *et al.* demonstrated that NaOH(aq) could dissolve cellulose in a concentration range of 7-10 wt% and at temperatures between -5 to +1 °C [87]. In 1998, Isogai *et al.* reported that the optimal conditions, albeit mainly for the dissolution of cellulose with DP up to 190 (microcrystalline cellulose and its derived samples), were swelling in 8-9 wt% NaOH and freezing at -20 °C, followed by thawing and diluting the solution to the final concentration of 5 wt% NaOH(aq) [88].

The low temperature requirement for cellulose dissolution in NaOH(aq) still lacks a clear explanation. However, one possible explanation was suggested by Lindman *et al.* as follows: At lower temperatures, the conformation of the polymer chain favours more polar structure, which enhances attractive interactions with a polar solvent. This conformational change could potentially minimise the hydrophobic assembly effect and reduce cellulose chains reassociation at lower temperatures, thereby promoting cellulose dissolution [32,89]. Yet, this hypothesis remains uncertain and has been subject to further NMR studies to investigate the impact of temperature on conformational changes of cellulose mainly by studying model compounds in absence and presence of NaOH(aq) which could not detect any significant changes [90,91]. Another approach to explain the low temperature requirement for cellulose dissolution was taken by Yamashiki *et al.* [92] who correlated the temperature effect to the size of hydrated NaOH(aq) at different temperatures. He investigated hydration of ca. 5-14 wt%

NaOH(aq) at +4 °C and +20 °C and observed that the number of water molecules solvating NaOH(aq) at 4 °C is more than at 20 °C.

One significant challenge associated with cellulose dissolved in NaOH(aq) is the lack of stability of the dissolved state over time, often resulting in irreversible gelation [37]. To address this, additives such as ZnO [93], urea [94], thiourea [95] and polyethylene glycol (PEG) [96] have been used to aid in the dissolution process and delay gelation.

Overall, cellulose dissolution in NaOH(aq) involves several challenges; it cannot dissolve cellulose with a high DP, and the maximum cellulose dissolution is relatively low, while resulting in solutions that are not stable over time and are prone to the irreversible gelation.

#### 2.5.2.4 Quaternary ammonium hydroxides (QAHs)

Research on using QAHs as potential solvents for cellulose dates back to 1924 when Lilienfeld reported the dissolution of cellulose in 20-50 wt% solutions of tetraethylammonium hydroxide (TEAH), tetramethylammonium hydroxide (TMAH) and benzyltriemethylammonium hydroxide (Triton B) either at temperatures below 0 °C or at room temperature, depending on the type of cellulose employed [86]. Subsequent studies showed that benzyl-substituted QAHs were more effective cellulose solvents [97,98] particularly Triton B and dimethyldibenzylammonium hydroxide (Triton F ) [99,100]. This higher degree of efficiency that was observed for QAHs containing benzyl groups compared to alkyl groups (such as methyl, ethyl, propyl and butyl) is commonly related to the bulkiness of the cation which is believed to act as an effective wedge by disrupting cellulose-cellulose interactions and thereby separating the cellulose chains from each other [101]. Figure 10 shows the structure of a few QAHs.

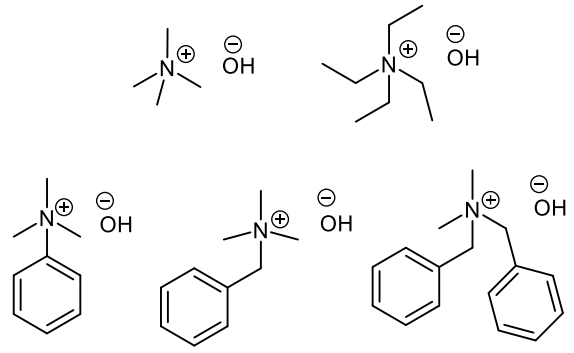


Figure 10. Structures of five quaternary ammonium hydroxides: Above, left to right: TMAH and TEAH. Below, left to right: trimethylphenylammonium hydroxide, Triton B and Triton F.

In a study by Brownsette *et al.* [99], the dissolution of cellulose in various concentrations of Triton B(aq) at 20 °C and 0 °C was investigated. This study revealed that the concentration required for maximum cellulose dissolution was lower in Triton B(aq) compared to other aqueous alkali namely NaOH(aq), LiOH(aq) and TMAH(aq).

Besides, decreasing the temperature to 0 °C resulted in a decrease in the solvent concentration required for maximum cellulose dissolution and an increase in the dissolution capacity. On the other hand, the same authors reported Triton F(aq) (containing an additional benzyl group compared to Triton B) as being a superior solvent in comparison to Triton B(aq), TMAH(aq), NaOH(aq) and LiOH(aq). When cellulose was dissolved in Triton F, it could be diluted to 0.5 N without any precipitation. In a more recent study conducted by Wang *et al.*, cellulose dissolution was investigated in a few aqueous QAHs containing alkyl and benzyl substituents [102]. Their results showed that freezing was required for all the solvents to dissolve cellulose successfully. The enhanced cellulose dissolution and stability of the dissolved samples were correlated to the increase in cation hydrophobicity of the studied QAHs. Since cellulose is amphiphilic, the increase in hydrophobicity is believed to stabilize the more hydrophobic regions of the pyranose ring and prevent cellulose aggregation caused by hydrophobic stacking.

In another study, Zhong *et al.* investigated cellulose dissolution in more concentrated solutions of alkyl-substituted QAHs with increasing alkyl chain length ranging from methyl to butyl [103]. In their study, dissolution took place at room or higher temperatures and tetrabutylammonium hydroxide with the most hydrophobic cation demonstrated the highest efficiency among the studied solvents. Efforts to study the mechanism of cellulose dissolution in these solvents by NMR pointed out the interactions between hydroxide and cellulose hydroxyl groups in addition to providing some evidence on the interaction between the cation of QAH and cellulose preventing the reassociation of cellulose chains.

### 2.6 Mechanism of cellulose dissolution in aqueous alkaline solvents

The dissolution mechanism of cellulose in aqueous alkaline media is not yet fully elucidated. However, studies, particularly those focusing on cellulose in NaOH(aq), propose that the dissolution is supported by the disruption of hydrogen bonding through competitive intermolecular interactions between the hydrated $OH^-$ ions and cellulose, probably supported by a certain partial deprotonation and charging of cellulose [38], even though this effect is probably limited due to the high ionic strength of the system (shielding the charges). Also, the cation probably plays a role in preventing the re-association of dissolved cellulose by being distributed between individual chains [104], most likely in the hydrophobic regions. In this context, as mentioned above, it has been observed that a higher hydrophobicity of the cation promotes the dissolution and stability of the solution [102]. Consequently, the influence of the hydrophobic assembly effect and the amphiphilic structure of cellulose on its dissolution and the stability of the dissolved state in aqueous systems [32] is highly prominent.

## 2.7 Cellulose modification

One way of modifying the properties of cellulose or enhancing its solubility is to use chemical functionalization which can be accomplished either heterogeneously or homogeneously. In heterogeneous functionalization, the primary determining factor is the accessibility of the cellulose hydroxyl groups since the fibre structure is preserved. Homogeneous functionalization, on the other hand, involves the complete dissolution of cellulose, making all cellulose hydroxyl groups equally available for modification. Solubility and properties of almost all cellulose derivatives rely on the degree of substitution (DS), i.e. the number of substituted hydroxyl groups per AGU, as well as the substitution pattern within the repeating unit and along the polymer chains. Another parameter used to characterise cellulose derivatives is molar substitution (MS) which is the average number of moles of substituents introduced per each glucose unit since sometimes the substituent might react further with the modifying reagent as the side reaction (cascade reaction). Currently, the most common cellulose derivatives, e.g. cellulose acetate (CA), methyl cellulose (MC), carboxymethyl cellulose (CMC) and nitrocellulose (NC) are predominantly synthesized heterogeneously on an industrial scale [105,106] due to the limited solubility of cellulose in conventional solvents. However, some drawbacks are associated with heterogeneous synthesis, such as poor control over the degree and pattern of substitution due to low accessibility of cellulose hydroxyl groups. For instance, two widely-produced cellulose derivatives, namely carboxymethyl cellulose (CMC) and cellulose acetate (CA) (Figure 11), are often used as blends from several batches to adjust their properties [105]. In contrast, homogeneous cellulose modification offers several advantages, including improved control over regioselectivity and substitution distribution and, consequently, product properties, along with increased control of cellulose degradation [105,107].

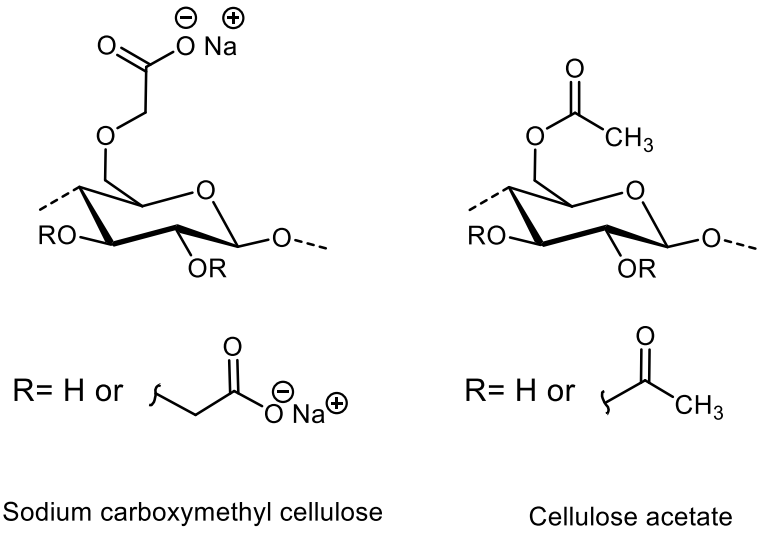


Figure 11. Structures of two of the most widely-produced cellulose derivatives.

### 2.7.1 Cellulose etherification in aqueous alkaline solvents

Cellulose ethers are non-toxic, most often, water soluble (affected by DS and its distribution pattern, as mentioned in Section 2.7), making them suitable for use as thickeners, suspending aids and flow-control agents alongside their extensive applications across various products such as food, paint, pharmaceuticals, adhesives and cosmetics. Aqueous alkaline solvents provide sufficient basicity to activate cellulose hydroxyl groups and promote their etherification. Cellulose modification in aqueous bases nevertheless poses challenges primarily due to the occurrence of competing reactions with water (e.g. hydrolysis of the etherification agents) and the generation of multiple by-products. These are non-commercialised processes being conducted on laboratory scale since further research ought to be undertaken to promote the scaling-up of homogeneous modification of cellulose. In this regard, NaOH(aq)/urea has been used frequently in cellulose etherification reactions mostly using alkyl halides and epoxides. Hu *et al.* [108] utilised NaOH(aq)/urea as the solvent to synthesise allyl cellulose (AC) using allyl chloride as the etherification agent. A DS of 0.98-1.65 was attained, and the obtained ACs were soluble in DMSO, DMAc and DMF. Higher DS could not be achieved because the introduction of substituent on cellulose resulted in the precipitation of AC which, in turn, decreased the accessibility of cellulose to the etherifying reagent. A similar effect was noticed when performing cellulose benzylation in an aqueous solution of NaOH(aq)/urea [109]. The obtained DS values varied between 0.29–0.54, being restricted due to high water content that caused precipitation of benzylated cellulose, thus lowered the accessibility of cellulose for further substitution. After cellulose is precipitated, it is most probable that the reaction can only progress at the surface, resulting in a low average DS [110]. The benzylated cellulose with a low DS of 0.51 was soluble in a number of organic solvents, namely DMSO, pyridine, DMF and DMAc. In addition to the mentioned studies, other examples of cellulose ethers have been produced in aqueous alkali/urea namely methyl cellulose (MC), hydroxypropyl cellulose (HPC) [111], carboxymethyl cellulose (CMC) [112], hydroxyethyl cellulose (HEC) [113] and cyanoethyl cellulose (CEC) [114,115]. Moreover, cross-linking reactions in this medium have been carried out by several research groups [116–118].

While dissolution in aqueous QAHs has been explored extensively, very little research has dealt with the chemical modification of cellulose in these media. In one study, Shi *et al.* attempted to create fluorescent cellulose films by etherifying cellulose in a solvent system composed of tetrabutylammonium hydroxide (TBAH)/$H_2O$/DMSO [119]. In another study, Sirviö *et al.* used aqueous tetraethylammonium hydroxide (TEAOH)/carbamide to carry out epoxide ring opening etherification of cellulose at room temperature [120]. During etherification, a new hydroxyl group was introduced onto the substituent (Figure 12, position marked with *), providing it with the possibility of further reaction (cascade reaction). It is notable that the cationic charge

densities obtained in this particular study were higher than when NaOH(aq)/ urea was used as the solvent.

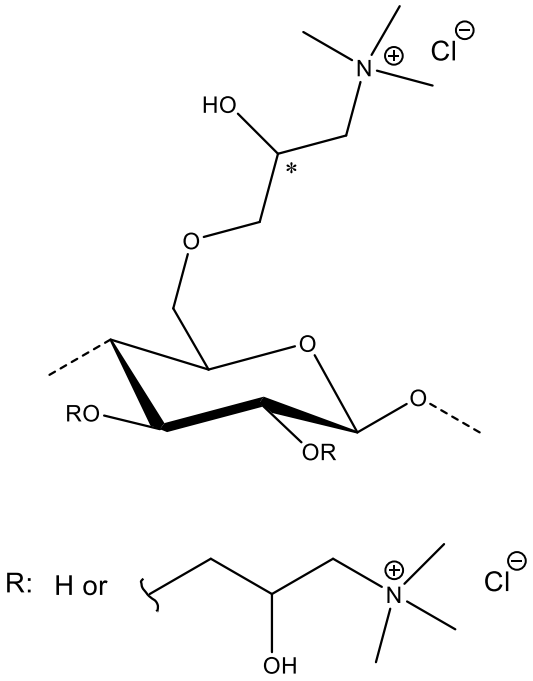


Figure 12. Etherified cellulose in (TEAOH)/carbamide solvent system with the possibility of cascade reaction on position marked with *.

### 2.8 Cellulose regeneration/coagulation

The regeneration/coagulation of cellulose is a process in which a cellulose solution comes into contact with an antisolvent leading to precipitation of the polymer from the dissolved state. When a derivatizing solvent is used, upon addition of an antisolvent a pure cellulose structure is regenerated as the substituents are removed. Typical antisolvents used to regenerate/coagulate cellulose include water, alcohols (usually ethanol) and acids such as HCl and $H_2SO_4$. A recent report by Kozlowski *et al.* cellulose coagulation in NaOH(aq) using $CO_2$(g) was investigated [121].

The kinetic of regeneration/coagulation is governed primarily by the relative velocities of the counter-diffusion process, which involves the diffusion of the solvent from the solution into the coagulation bath and the coagulant from the bath into the solution [122]. The exchange of solvent and non-solvent causes desolvation of the cellulose molecules, leading to the reformation of intra- and intermolecular hydrogen bonds in cellulose, albeit in a different pattern compared to the native structure [123,124]. The self-assembly of cellulose chains and the properties in regenerated/coagulated cellulose are highly influenced by the choice of cellulose solvent, coagulant and temperature [125,126].

When an aqueous cellulose solution comes into contact with antisolvent, the cellulose chains first tend to aggregate through glucopyranose rings stacking on top of each other, via van der Waals forces and hydrophobic pairing, creating a sheet-like structure. These sheet-like aggregates continue to stack together through hydrogen bonding, forming thin planar crystals that contain disordered regions. Subsequently, randomly dispersed structures make contact and adhere to each other, leading to the formation of regenerated/coagulated cellulose (three-dimensional structures) [127–129] (Figure 13).

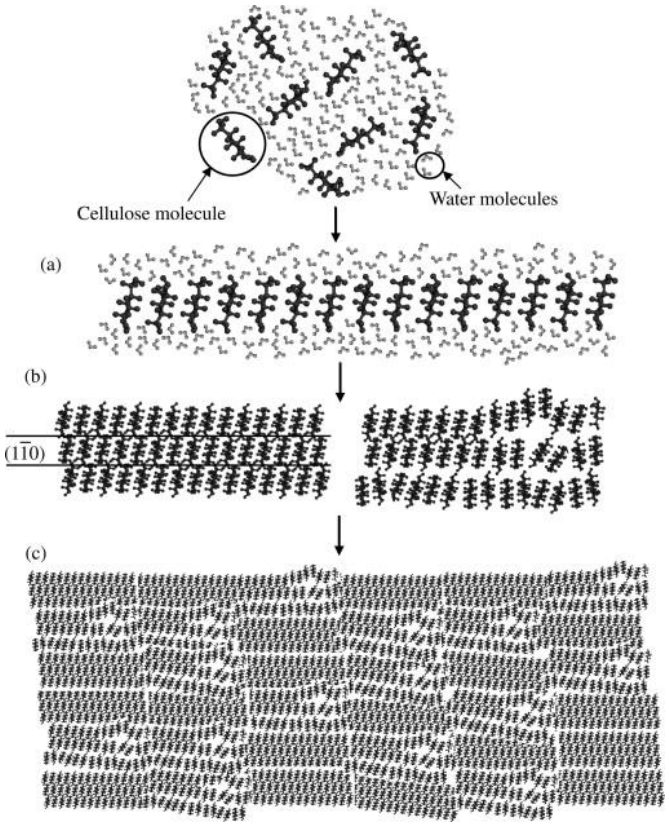


Figure 13. Schematic illustration of the model proposed for the formation of regenerated cellulose in an aqueous solution. (a) Molecular sheet formed by hydrophobic pairing and van der Waals forces; (b) Molecular sheets stacking by hydrogen bonding to form planar crystals containing amorphous regions; (c) Contact and adherence of the structural units to form regenerated cellulose [129]. Reprinted with permission from Elsevier.

# 3

# Materials and Methods

This chapter provides a brief explanation of the materials and methods employed throughout this thesis. More comprehensive and detailed descriptions can be found in the appended papers.

## 3.1 Materials

MCC (Avicel PH-101) was used in Papers I, II and IV, whilst acid-washed cellulose powder sourced from spruce was used in Paper III, to investigate the dissolution, etherification and coagulation of cellulose. Methyl-α-D-glucopyranoside was used as the model compound in Paper IV to investigate the deprotonation level of cellulose in the selected aqueous alkaline solvents. Triton B 40 wt% in $H_2O$ was used in Papers I and IV, and TMAH 25% in $H_2O$ and NaOH pellets were used in Paper I. Allyl glycidyl ether (AGE) and $CO_2$(g) 99% were used in Papers I and IV, respectively. Other morpholinium-based compounds were synthesised according to the procedures summarized in Papers II and III.

## 3.2 Experimental procedures

### 3.2.1 Synthesis of morpholinium-based compounds

General procedure included synthesis of morpholinium iodide/bromides, followed by an ion exchange to hydroxides, acetates or chlorides (details can be found in Papers II and III).

### 3.2.2 Cellulose dissolution

The desired amount of cellulose was added to a specific concentration of solvent (in some cases precooled solvents) in an ice bath or at room temperature depending on the solvent used. In the cases where the samples were required to be frozen, a freezer kept at -25 °C was used to store the solutions for 20 minutes, after which they were thawed at room temperature.

### 3.2.3 Cellulose etherification

Cellulose was dissolved in the studied solvents according to the general method explained above (details can be found in Paper I). The solution was heated to 50 °C before AGE was added with a molar ratio of 3:1 AGE to MCC. The reaction was carried out for 2 h for the purpose of further monitoring.

### 3.2.4 Cellulose coagulation

Ethanol was used as the coagulant in Papers I, II and III to promote the diffusion of cellulose out of the solutions. The coagulated cellulose was washed with ethanol to ensure complete removal of the remaining solutions. In Paper IV, cellulose was coagulated through addition of $CO_2$(g) after which ethanol was used for washing the precipitates.

## 3.3 Characterisation methods

### 3.3.1 Methods used for *in situ* monitoring of reactions

*In situ* FTIR monitoring was carried out using a Mettler Toledo ReactIR 15 DiComp probe recording spectra in an optical range of 650 $cm^{-1}$ –3000 $cm^{-1}$ excluding the diamond region as the blind spot (1950–2250 $cm^{-1}$). For etherification in Paper I, the probe was immersed in the solution prior to the addition of AGE; the equipment was configured to collect spectra at the resolution of 8 wavenumbers by averaging 159 scans in 1 min intervals for 2 h. In Paper IV, the probe was immersed in the solutions prior to the introduction of $CO_2$(g); the equipment was configured to collect spectra at the resolution of 8 wavenumbers by averaging 79 scans in 30 second intervals.

*In situ* time-sweep shear measurements were run using an Anton Paar MCR 702 Twin Drive rotational rheometer to investigate the stability and viscosity changes during cellulose etherification. The tests were performed in a single motor-transducer configuration using a double gap cylinder measuring system, and a solvent trap filled with water to prevent evaporation of the solvent. All experiments were performed for 1 h at 50 °C and a constant shear rate of 1500 $s^{-1}$ was used to provide extensive mixing. The measurements were started immediately, with no relaxation time.

### 3.3.2 Estimation of the molar substitution of 3-allyloxy-2-hydprhypropyl cellulose (AHP cellulose)

Quantitative $^{13}C$ NMR measurements were carried out using a single pulse experiment with $^{1}H$ decoupling during the acquisition, a 20° radiofrequency pulse, a repetition delay of 6 s and 12600 signal accumulations. The same experiment was carried out using a repetition delay of 12 s for comparison.

### 3.3.3 Methods used to investigate cellulose dissolution

Polarized light microscopy using a ZEISS SteREO Discovery.V12 microscope equipped with a camera was used to confirm the dissolution of cellulose when no particles could be detected (Papers II and III).

Turbidity measurements were made to assess cellulose dissolution (Paper II) by measuring the light transmitted by a solution. A double-beam spectrometer Specord 205, with a spectral bandwidth of 1.4 nm, was employed for this purpose to record UV-Vis measurements. In all of the measurements, plastic disposable cuvettes, with a light path length of 10 mm, were utilised and water was used as the background.

### 3.3.4 Estimation of maximum cellulose dissolution

Several solutions, containing increasing amounts of cellulose at specific solvent concentrations, were prepared and the maximum dissolution was investigated using polarized light microscopy and in some cases UV-Vis measurements as well.

### 3.3.5 Investigation of chemical stability of the dissolved cellulose by size exclusion chromatography and NMR

$^{13}C$ NMR experiments were carried out in order to detect the appearance of any shifts or extra peaks in cellulose solutions over time as a result of possible degradation processes. An 800 MHz ($^{1}H$) magnet, with a TXO probe and Bruker Avance HDIII console, was employed and a z-restored spin echo sequence to avoid a rolling baseline.

Size exclusion chromatography (SEC) was used to assess the molecular weight distribution of the coagulated cellulose. For this purpose, initially, cellulose was dissolved in the desired solvent and kept in the fridge overnight when alkaline solvents were used, and at room temperature when dissolved in morpholinium acetates/DMSO. Subsequently, the samples were coagulated and washed with ethanol to ensure the removal of residual solvents. Prior to running the SEC measurements, the samples underwent a series of solvent exchanges and were finally dissolved in LiCl/DMAc.

### 3.3.6 Methods used to measure the size and conformation of cellulose in the dissolved state

Dynamic light scattering (DLS) was used to measure the effective hydrodynamic radius (Rh), employing a Zetasizer Nano ZS from Malvern Panalytical with a 4 mW, 632.8 nm red laser and a scattering angle of 175° at a temperature of 20 °C. Measurements were run on both filtered (0.22 µm wwPTFE filter) and unfiltered samples. The viscosity of the solvent was determined at 20 °C using flow sweeps. The viscosity value of 1.7 mPa that was measured was utilised for data analysis, along with the refractive index value of 1.36.

Intrinsic viscosity measurements were made to estimate the extension of the cellulose chain in the solvents. Cellulose solutions, with concentrations of 0.15–0.55 wt%, were prepared and kept in a water bath at 25 °C for 30 min after dissolution. A capillary viscometer equipped with a circulating water bath to maintain a constant temperature of 25 °C was used and the time taken for the solutions to pass down the timing marks in the capillary was recorded. Each measurement was run in triplicate and the average measured time was used to calculate the relative viscosity. The intrinsic viscosity was obtained from linear regression, with a coefficient of determination of at least 0.97.

### 3.3.7 Methods used to investigate flow behaviour and viscoelastic properties

Flow sweep measurements were run to study the flow behaviour of cellulose solutions in different solvents and at different temperatures applying different shear rates (Papers III and IV). For these measurements, a TA Discovery Hybrid Rheometer (HR-3), with a sandblasted 40 mm plate–plate geometry with a gap of 400 or 500 µm, was used and the temperature was controlled by a Peltier plate with circulating cooling liquid. Solvent evaporation was avoided by using a solvent trap filled with water, and the rheometer was brought to the desired temperature without pre-shearing. Silicon oil was applied around the geometry border when morpholinium acetates/DMSO were used as the solvent to avoid the extra uptake of water from the air. The measurement started immediately on the prepared samples; temperature increases were made in series on the same sample in Paper III.

Oscillatory frequency tests were performed to study the viscoelastic properties of the cellulose solutions before and after gelation (Paper IV). Oscillatory strain sweep tests were conducted first, at constant angular frequencies in the range of 0.1 to 100% strain, to determine the viscoelastic region. Oscillatory frequency tests were then conducted, by measuring storage (G') and loss (G'') moduli at frequencies between 0.1-150 rad/s.

### 3.3.8 Assessment of cellulose crystalline structure after coagulation

Solid state NMR was carried out on coagulated cellulose using a Bruker Avance III 500 MHz spectrometer equipped with a 4 mm HX CP MAS probe. Experiments were recorded at a magic angle spinning (MAS) rate of 10 kHz and the temperature was set to 298 K. $^{1}$H decoupling with a ''spinal64'' decoupling scheme at 67 kHz was applied during the acquisitions. The cross-polarization (CP) contact time and the repetition time were set to 1.5 ms and 2 s, respectively. CP spectra were recorded with 4000 signal accumulations for the purpose of comparison.

Crystallinity was estimated according to the reported method by Sparrman *et al.*[130] with 128 signal accumulations using the integral of C1.

# 4

# Results and Discussion

The results obtained in this thesis are presented in the three following sections. The first summarises those acquired from cellulose etherification in QAHs(aq) and NaOH(a), along with different combinations of these solvents (Paper I). Next, the results obtained from the development of novel morpholinium-based solvents for cellulose (Papers II and III) are presented and, finally, cellulose gelation in QAHs(aq) is discussed (Paper IV).

## 4.1 Cellulose etherification in aqueous alkaline solutions: the impact of solvent composition

### 4.1.1 *In situ* monitoring of cellulose etherification using FTIR

Cellulose dissolution in Triton B(aq), TMAH(aq) and NaOH(aq), individually and in various combinations, has been studied by our group previously [131,132] which showed enhanced dissolution when QAHs(aq) were used. Given the importance of structural control of the product in cellulose modification, it was of great interest to investigate the impact of these solvents on the homogeneous modification of cellulose, especially etherification taking place in aqueous alkaline systems. With this objective in mind, the model reaction chosen for these investigations was etherification of microcrystalline cellulose using allyl glycidyl ether (AGE) (Figure 14). The primary goals of this study were to develop methods for monitoring cellulose etherification process while simultaneously attaining a deeper comprehension of how the composition of the solvent influences the reactivity and stability of the dissolved cellulose besides its impact on the cellulose ether obtained.

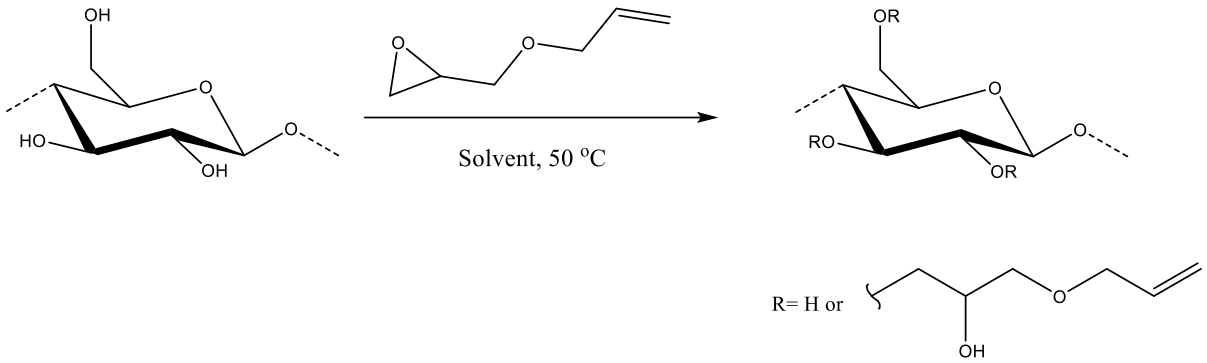


Figure 14. Model reaction for cellulose etherification.

*In situ* IR spectroscopy measurements offer the advantage of real-time monitoring of the occurrence and disappearance of IR absorption bands. These measurements are frequently employed to obtain a broader understanding of the reaction kinetics, enabling the assessment of conversions in a dynamic manner. There is currently a lack of knowledge regarding the applicability of this technique in assessing the information necessary for a thorough understanding of the cellulose etherification process, including reagent hydrolysis, solution stability and the completion of the etherification reaction itself. Therefore, the selection of this technique was motivated by the aim of highlighting both its advantages and limitations specifically in this reaction and acquiring a more profound understanding of the reaction kinetics.

Conducting kinetic investigations on cellulose etherification in aqueous media is not, however, straightforward: side reactions, including reagent hydrolysis and self-etherification (cascade reaction) give rise to multiple overlapping peaks. Figure 15 shows typical spectra obtained as a result of the *in situ* FTIR monitoring of cellulose etherification process with AGE. The main changes are detected in the region 900-1100 $cm^{-1}$, where absorption bands arising from both the formation of cellulose ether bonds (desired reaction) and the hydrolysis of the etherification agent (side reaction) occur. In addition, a small decrease in the water peak at 1640 $cm^{-1}$ and the carbonate peak at 1480 $cm^{-1}$ can be also observed: the former is due to a small water loss during the reaction and the latter is probably a result of the elimination of atmospheric $CO_2$(g) while performing the reaction under $N_2$(g). Despite the overlapping peaks related to the etherification and the associated side-reactions, valuable insights can nonetheless be gained that facilitate overall comparisons between the etherification processes carried out in different reaction media.

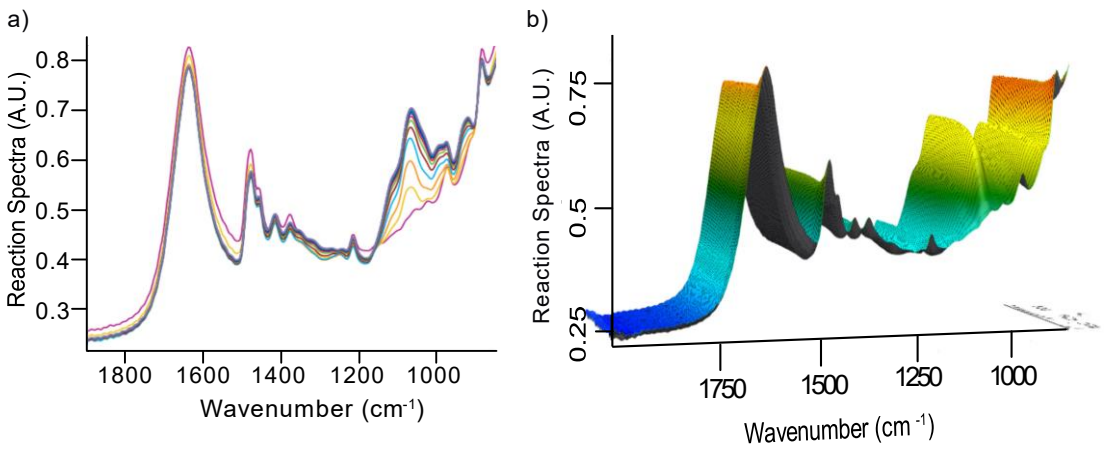


Figure 15. Spectra obtained from *in situ* FTIR monitoring of cellulose etherification with AGE over time. a) Overview of the spectra obtained for cellulose etherification in Triton B(aq) after 2 h and b) its corresponding 3D plot.

One approach is to examine the dissolution and consumption rate of the etherification agent (AGE) comparatively in model systems comprising only a solvent itself and AGE in order to relate the results obtained to the overall monitoring of the etherification reaction in the studied solvents. Upon adding AGE to the solvents, a biphasic solution is initially formed, which gradually transitions into a completely homogeneous solution. This transformation, which includes the dissolution of AGE and its subsequent hydrolysis (involving the oxirane ring opening and diol formation) in the alkaline reaction medium, could be monitored in each solvent. This process was tracked by following the absorption peak of the oxirane ring at 1253 $cm^{-1}$: an increase in the intensity of this peak indicates the gradual dissolution of AGE, whereas a following decrease indicates its consumption due to the hydrolytic ring opening (Figure 16).

According to this figure, all the solutions show the increase, followed by a decrease in the peak at 1253 $cm^{-1}$. Yet the dissolution rate was higher in solutions containing Triton B(aq), followed by TMAH(aq) and its mixtures, while the dissolution of AGE in NaOH(aq) seemed to be the slowest. Although the faster solubility of AGE in both Triton B(aq) and TMAH(aq) is expected to promote a more efficient etherification, its impact on the hydrolysis of the reagent must not be neglected.

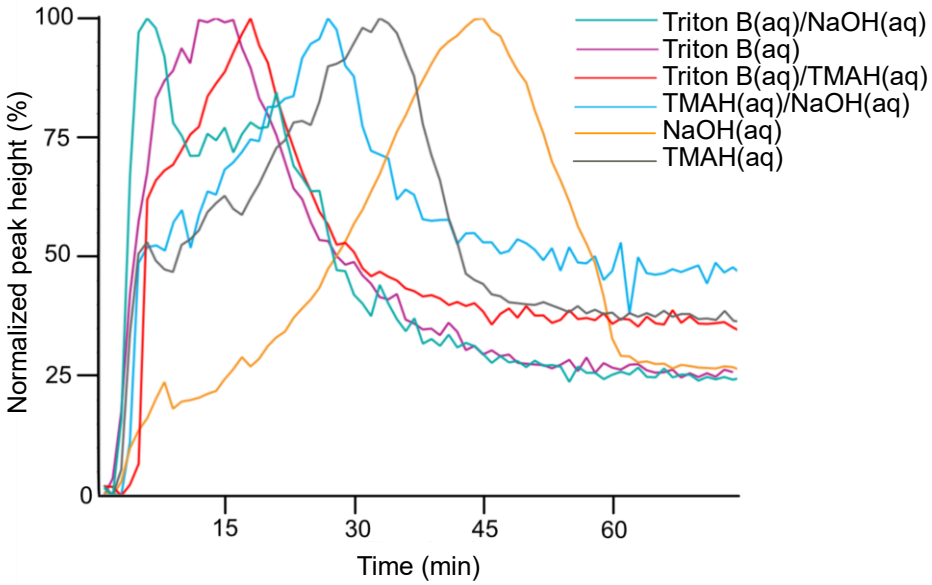


Figure 16. Trends of the AGE peak at 1253 $cm^{-1}$ during dissolution and subsequent hydrolysis in the studied solvents and solvent combinations.

Next, the region between 900 and 1100 $cm^{-1}$ containing the absorption bands arising from main chemical conversions which occurred during the studied processes -overlapping absorption bands arising both from etherification and hydrolysis reactions, i.e. different types of C-O bonds- was investigated. Figure 17 represents collected spectra recorded every one minute for 2 h in which each colour represents the spectrum at each minute. Spectra corresponding to all solvent media can be found in Paper I. During etherification, the height of the peaks in this region in most of the solutions increased up to a certain point, after which no changes in the intensity could be detected (Figure 17a). However, in NaOH(aq) (Figure 17b) a drop in the peak intensity was observed after its maximum height was reached. It should be noted that the IR probe used in this study is capable of detecting species only in the dissolved state: a decrease in the intensity of the peaks can, therefore, be attributed to either the consumption of a specific compound or its precipitation. Here, the decrease observed is most likely a consequence of the reduced stability of cellulose solution in NaOH(aq) under the conditions applied (50 °C), leading to the precipitation of cellulose. Lower stability of cellulose solution in NaOH(aq) was also observed visually: the solution turned cloudy and turbid soon after the temperature was raised to 50 °C and the etherification reaction started. A similar interpretation is valid for cellulose etherification in TMAH(aq)/NaOH(aq) (Figure 17c) but to a much lesser extent. In contrast, cellulose in other solvents proved to be stable since no signs of precipitation (decrease in the absorption peak) or visual turbidity could be noted. Observations of changes in the stability of the reaction mixtures, therefore, make it highly relevant for a complementary rheology monitoring of the reaction systems, which is discussed later.

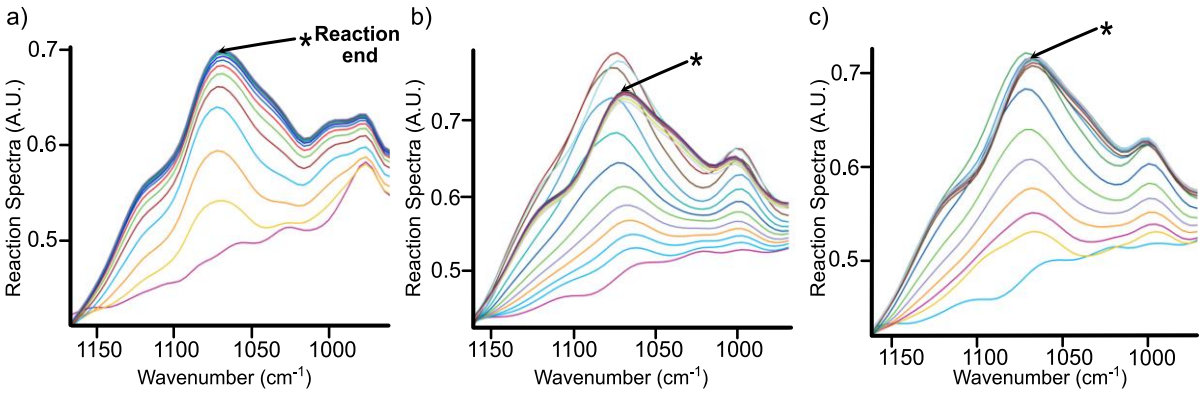


Figure 17. Overview of the spectral region between 900–1100 $cm^{-1}$ for each minute during cellulose etherification over 2 h in (a) Triton B(aq), (b) NaOH(aq) and (c) TMAH(aq)/NaOH(aq).

Further analysis in this region involved considerable challenges due to the presence of various C-O moieties resulting from, as mentioned above, both etherification and hydrolysis, with a significant overlap. Reference spectra of dissolved cellulose, the desired product (etherified cellulose) and the hydrolysis product were therefore collected and superimposed in Figure 18a not only to simplify spectral analysis but also to enable identification of the absorption bands associated with the formation of 3-allyloxy-2-hydroxypropyl-cellulose (AHP-cellulose, i.e. the desired product) and the hydrolysis product (diol). In addition, an experiment was carried out in which cellulose etherification was monitored while AGE was added gradually in several aliquots (Figure 18c), to aid the distinction between the absorption bands arising from cellulose etherification from those arising from reagent hydrolysis. Additionally, the experiment in which the hydrolysis of AGE was monitored in absence of MCC (Figure 18d) was used for purposes of comparison.

As shown in Figure 18a, two distinct peaks can be distinguished at 996 $cm^{-1}$ and 1028 $cm^{-1}$, indicative of hydrolysis and etherification, respectively. The peak at 996 $cm^{-1}$ was only detected in the hydrolysis spectra of the reagent: it showed a gradual increase, followed by a plateau, when monitoring the changes that occurred after AGE was added to Triton B(aq) (Figure 18b). Following the peak at 1028 $cm^{-1}$, on the other hand, was more challenging as it was present in both the reference cellulose as well as the cellulose ether obtained (AHP-cellulose). This peak is indicative of C-O groups originating from various compounds such as hemiacetals and acetals from the cellulose structure and ether bonds from the substituents introduced in AHP-cellulose. In addition, this peak showed a continuous increase during etherification (Figure 18c) as well as during the AGE hydrolysis in the absence of cellulose (Figure 18d): this made it impossible to distinguish whether the signals were from the desired etherification or hydrolysis of the reagent. Since no other distinct peaks corresponding to etherification (with no contribution of hydrolysis) could be isolated, it was only possible to follow the peak at 996 $cm^{-1}$ (corresponding to C-O in primary alcohols formed during the

oxirane ring hydrolysis) to compare the hydrolysis rate in different reaction media (Figure 19).

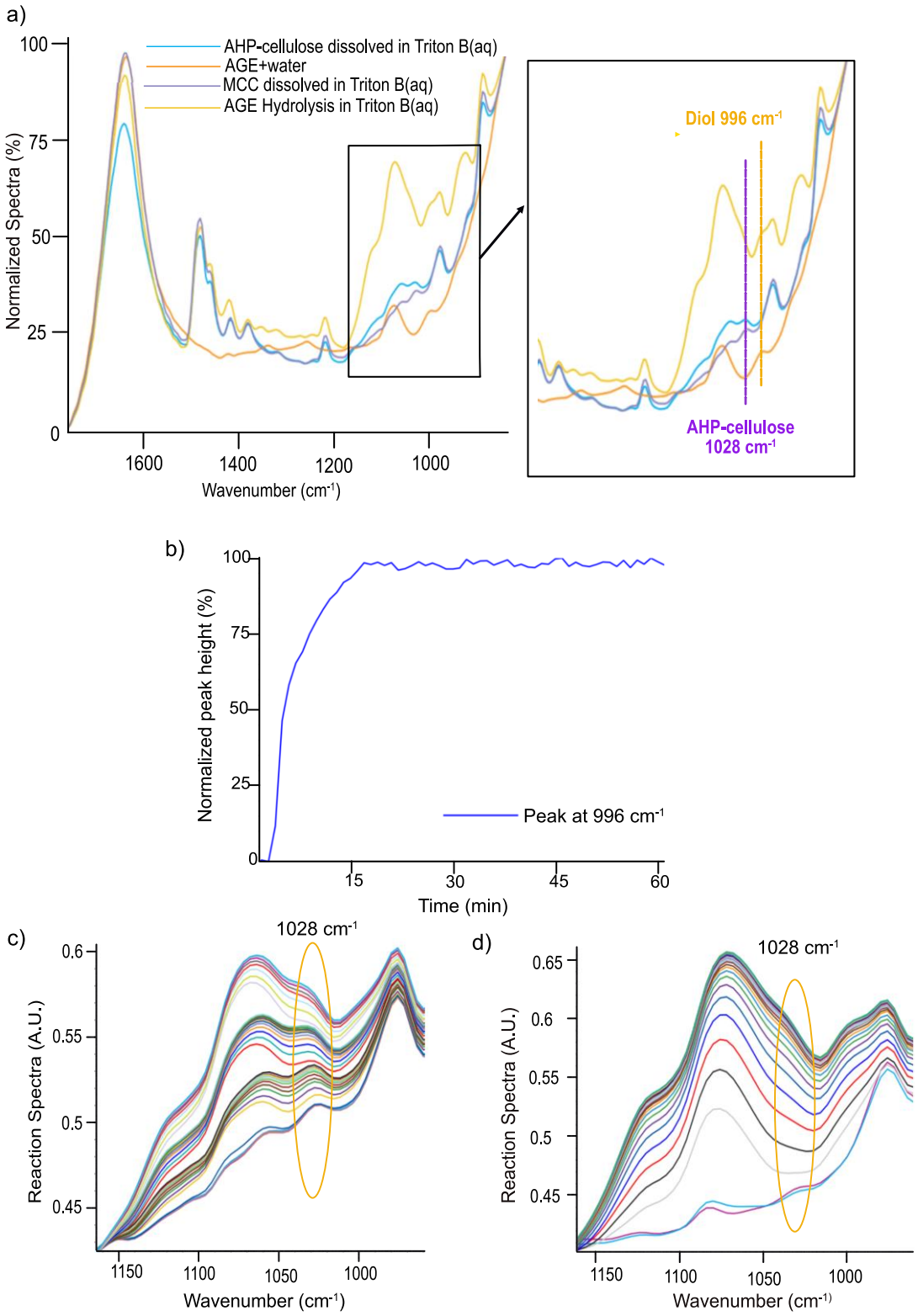


Figure 18. a) Stacked spectra of the individual reactants and reaction products for identification and assignment of distinct peaks, b) Trend in the peak at 996 $cm^{-1}$ arising from AGE hydrolysis in Triton B(aq) in absence of MCC, c) MCC etherification by adding AGE in aliquots in Triton B(aq) and d) AGE hydrolysis in Triton B(aq).

The trends of the 996 $cm^{-1}$ peak shown in Figure 19 indicate a comparable behaviour of the etherification reagent during hydrolysis in different solvents. The combination of Triton B(aq)/TMAH(aq) exhibits the shortest time to reach its maximum hydrolysis, while NaOH(aq) demonstrates the slowest hydrolysis rate. It is likely that the faster hydrolysis of AGE is attributed to its more rapid dissolution, as discussed previously.

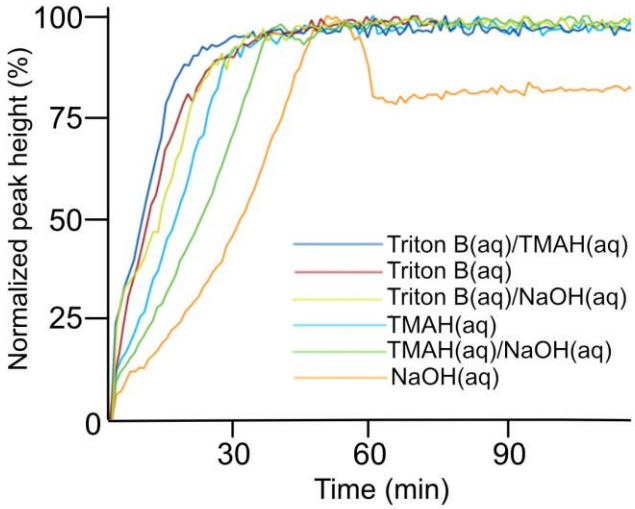


Figure 19. Trend of the peak at 996 $cm^{-1}$ in the studied solvents during etherification.

A valuable result obtained from the *in situ* IR monitoring of cellulose etherification is the possibility to estimate the endpoint of the process: this is determined as the time point after which no changes in the C-O region is detected, i.e. there is no further etherification or hydrolysis (Table 1). The results obtained indicate that the overall process is the fastest in Triton B(aq) or TMAH(aq)/Triton B(aq). The addition of TMAH(aq) to Triton B(aq) did not appear to have any effect on the overall kinetics of the reaction. In contrast, the reactions conducted in other solvents took longer time to reach completion, with cellulose in NaOH(aq) starting to precipitate after 46 minutes.

Table. 1. Estimated time required for completion of cellulose etherification reaction.

| **Solvent** | **Estimated reaction completion time (min)** |
|---|---|
| Triton B(aq)/TMAH(aq) | 27 |
| Triton B(aq) | 28 |
| TMAH(aq) | 35 |
| Triton B(aq)/NaOH(aq) | 46 |
| TMAH(aq)/NaOH(aq) | 47 |
| NaOH(aq) | 46 (precipitation time) |

In summary, based on the analysis of the necessary reference spectra, *in situ* FTIR made it possible to follow the dissolution and consumption of the etherification reagent and one of the side reactions i.e. the hydrolysis of the oxirane ring providing the peak at 996 $cm^{-1}$ representative of a primary alcohol C-O, which differed from the contributions of the etherified and non-etherified cellulose. Moreover, the method provided information on the completion of the process, insight into the stability of the reaction mixtures and emphasized the importance of the complementary monitoring using rheometry.

### 4.1.2 Complementary *in situ* monitoring using rheometry

As implied above, the etherification studied proceeded under stability changes (aggregation) that affected reaction efficiency, making it important to examine these changes via complementary *in situ* time-sweep shear measurements. According to Figure 20, an initial decrease was observed in the viscosity of all the solutions upon the addition of AGE (due to dilution of the system) followed by an increase as the reaction progressed, most likely due to the formation of AHP-cellulose with a higher molecular weight. Smoother trends were obtained when Triton B(aq) was used alone, or in combination (Figure 20d), which is indicative of homogeneous solutions, however, Noticeable fluctuations were detected when TMAH(aq) and NaOH(aq) were used (Figures 20 b and 20c). A double gap cylinder was used in these experiments and, although a high shear rate of 1500 $s^{-1}$ was selected to mimic the extensive mixing during IR measurements, less optimal mixing caused inhomogeneities to be formed. As these cellulose aggregates travelled up the cylinder, they interrupted the measurements and appeared as "jumps" in the resulting curves. Another consequence of a less optimal mixing rate was that, with the exception of Triton B(aq), other solutions did not reach their maximum viscosity corresponding to reaction completion. These findings highlight the critical role of uniform mixing when homogeneous modification is being carried out in alkaline solutions specifically at high temperatures, since these solutions are prone to aggregation. Furthermore, the curves indicate that Triton B(aq) alone, or in combination with other bases promotes a higher stability of cellulose solutions and a faster increase in viscosity, whereas NaOH(aq) causes a slower viscosity increase and the formation of an inhomogeneous system as observed previously by IR spectroscopy.

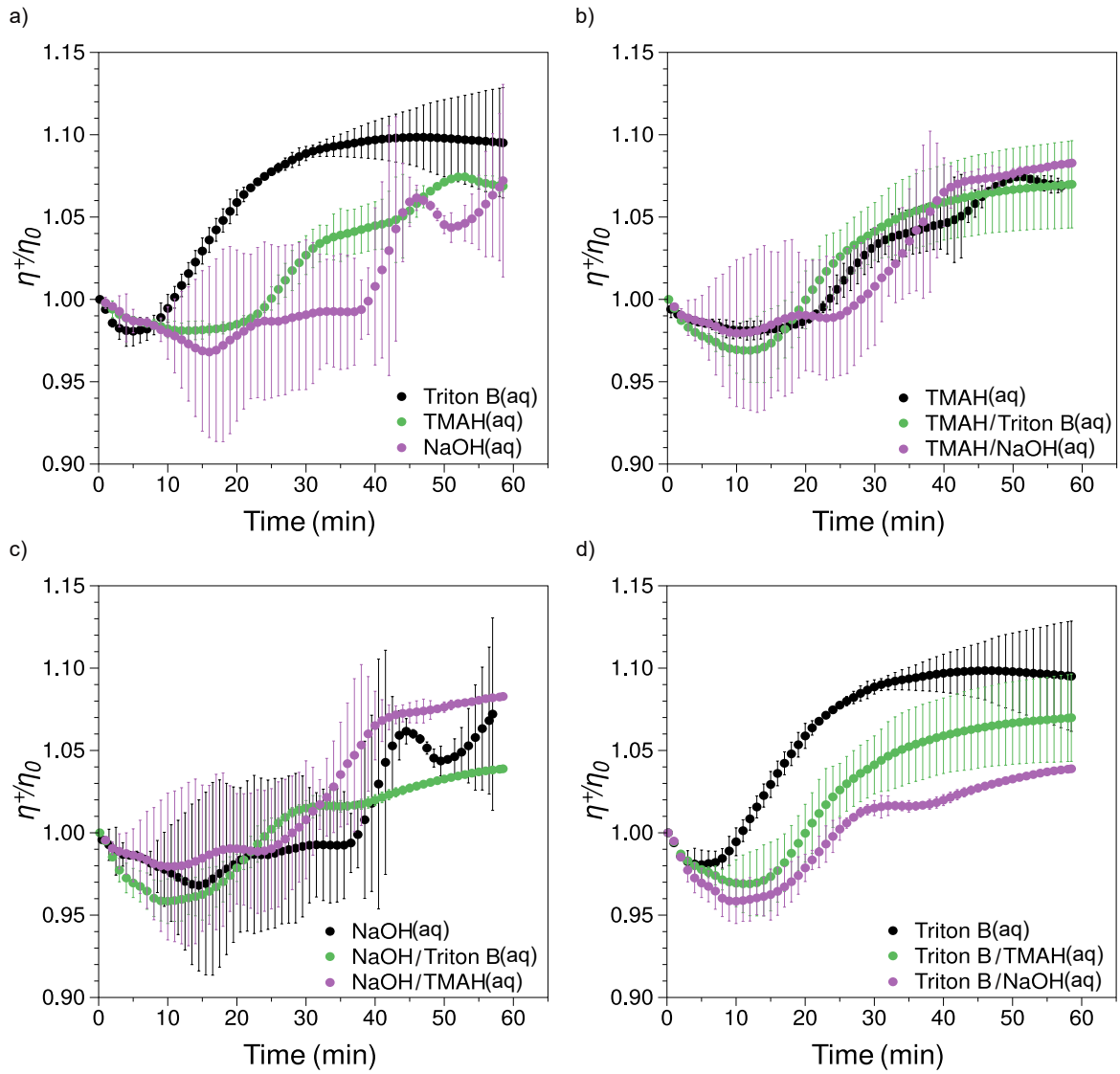


Figure 20. Reduced transient viscosity, $\eta^+/\eta_0$, vs. time at constant shear rate $\dot{\gamma} = 1500$ 1/s at 50 °C.for: a) individual solvents, b) TMAH(aq) and its combinations with other solvents, c) NaOH(aq) and its combinations with other solvents and d) Triton B(aq) and its combinations with other solvents. The error bars represent the standard deviation based on averaging 2 individual measurements. $\eta^+(t)$ is the instantaneous transient viscosity and $\eta_0$ is the viscosity at t=0.

### 4.1.3 Impact of the solvent composition on the molar substitution

Figure 21 shows the $^{13}$C NMR spectrum of the AHP-cellulose synthesised in TMAH(aq), with partial substitution on all hydroxyl groups of cellulose at 70.5, 82.25 and 82.89 ppm assigned to substituted C6, C2 and C3 (denoted as C6s, C2s and C3s). Moreover, an additional peak for C1 (labelled as C1s) at 102 ppm is detected as a result of the substitution on the adjacent carbon (C2). Both $^1$H NMR and HSQC were measured for further confirmation which can be found in Paper I.

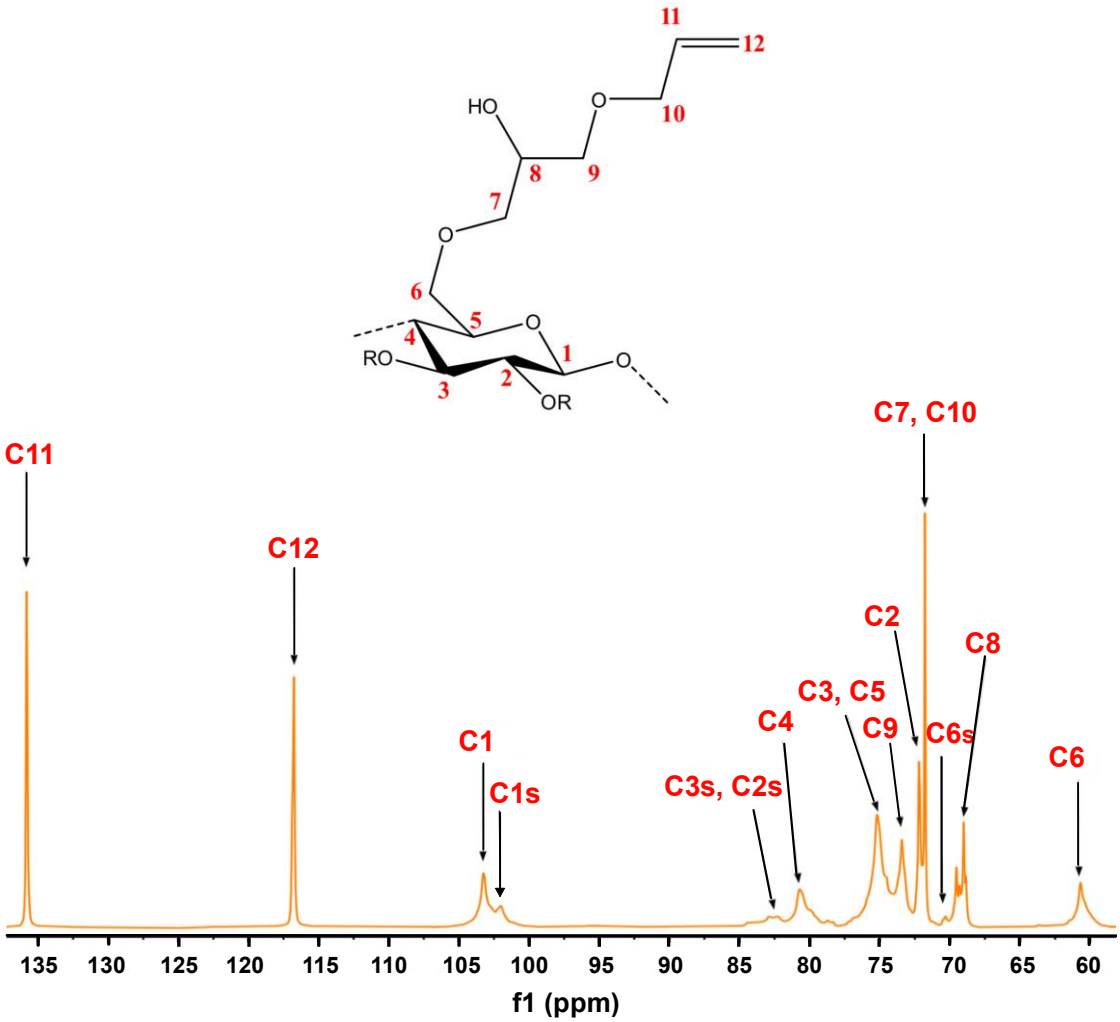


Figure 21. $^{13}$C NMR spectrum of AHP-cellulose synthesised in TMAH(aq).

Quantitative $^{13}$C NMR was used to estimate the degree of substitution by calculating the ratio between the integral values of C11 (substituent) and C1 (cellulose). However, since every newly-introduced substituent on cellulose bears one OH as a result of the AGE oxirane ring opening in position 8 (Figure 21), a further side-reaction with another AGE (cascade reaction) is possible (Figure 22). Thus, rather than using the degree of substitution (DS), it is more feasible to estimate the molar substitution (MS, Eq. 1), which corresponds to the average number of moles of substituents introduced per each glucose unit (Table 2).

$$MS = \frac{C_{11}}{C_1} \quad Eq.\ 1$$

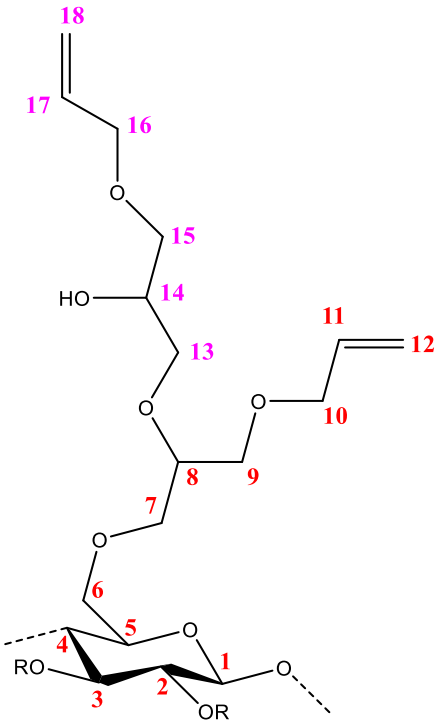


Figure 22. Product resulting from one cascade reaction occurring on OH group of C8. A further cascade reaction is possible on OH group of C14.

Surprisingly enough, the highest MS (1.49) was observed for AHP-cellulose formed in NaOH(aq), while the values obtained in other solvents were lower and actually quite similar, ranging from 0.79 to 0.88. These results were unexpected, considering the fact that cellulose in NaOH(aq) exhibited the poorest solution stability during the reaction (Figures 17b, 20a, 20c) and AGE showed the slowest dissolution rate in this solvent (Figure 16). Several observations were taken into consideration to further clarify the implications of the MS values obtained.

Table 2. Molar substitution of AHP-cellulose obtained in different solvents.

| **Solvent** | **MS** |
|---|---|
| NaOH(aq) | 1.49± 0.10 |
| TMAH(aq) | 0.88± 0.06 |
| TMAH(aq)/Triton B(aq) | 0.81± 0.06 |
| Triton B(aq) | 0.79± 0.06 |
| Triton B/NaOH(aq) | 0.79± 0.06 |
| TMAH/NaOH(aq) | 0.79± 0.06 |

It was observed that, when attempting to dissolve AHP-cellulose in DMSo-$d_6$ for NMR measurements, AHP-cellulose formed in NaOH(aq) exhibited a lower solubility compared to the products obtained from other solvents. This would commonly indicate a lower DS of the cellulose hydroxyl groups when NaOH(aq) was used as the solvent, yet here we deal with a comparably higher molar substitution (MS) that does not

necessary reflect the degree of cellulose substitution, but rather the total amount of substituent introduced. Furthermore, as mentioned earlier, all cellulose hydroxyl groups were partially substituted (confirmed by $^{1}$H NMR and HSQC, see Paper I). A more detailed examination of the $^{13}$C NMR of AHP-cellulose formed in NaOH(aq) vs. that formed in other solvents revealed a different intensity of the peaks (corresponding to substituted and unsubstituted positions) but similar width allowing comparison between the spectra. Figure 23 shows $^{13}$C NMR spectra of AHP-cellulose obtained in NaOH(aq) and TMAH(aq); the spectra of the product obtained in other solvents can be found in Paper I Supporting Information. The $^{13}$C NMR spectrum of the AHP-cellulose obtained in NaOH(aq) was similar to other $^{13}$C NMR spectra (corresponding to AHP-cellulose obtained in other solvents) except for the higher peak intensity of C1 (adjacent to unsubstituted C2) and the lower intensity of C1s (adjacent to substituted C2) compared to the other solvents. This indicates a lower DS of cellulose hydroxyls, which is in line with the lower solubility observed for these products [133]. In combination with the high molar substitution, these results indicate a higher extent of cascade reactions as a result of AGE reacting preferably with the newly formed hydroxyl groups on the introduced substituents over the cellulose hydroxyl groups (Figure 22). The precipitation of cellulose observed in NaOH(aq) during the etherification process is indeed likely to reduce the accessibility of cellulose hydroxyl groups to AGE. However, the newly formed hydroxyl group on the substituent (positions 8 and 14 in Figure 22) exhibit likely a higher accessibility to react with another AGE molecule, thereby promoting the cascade reaction and leading to a higher MS value. Further investigations are, however, necessary to confirm this hypothesis.

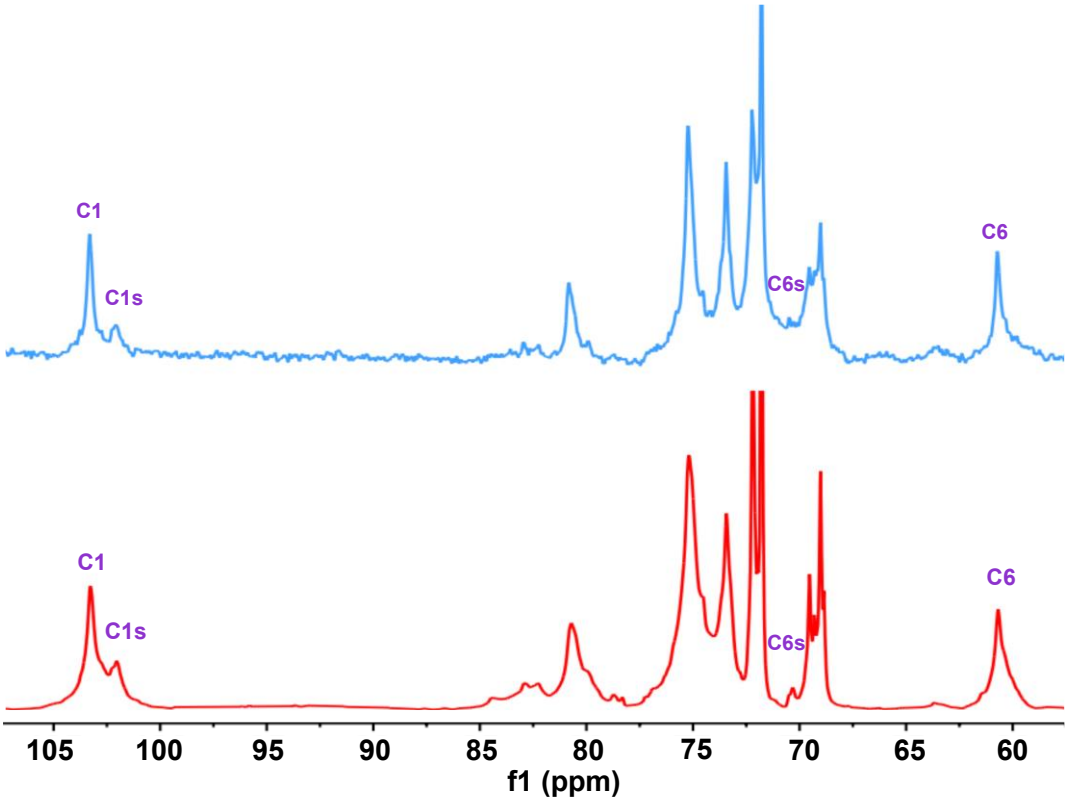


Figure 23. $^{13}C$ NMR spectra of AHP-cellulose yielded in NaOH(aq) (blue) and TMAH(aq) (red).

To summarize, detailed NMR investigations, supported by the information obtained during *in situ* studies (reagent solubility, stability of the reaction mixtures, etc.), provided deeper insight into the etherification process and possible identification of the cascade reaction.

### 4.2 Development of morpholinium-based solvents for cellulose

Following on our study on cellulose etherification that highlighted the significance of stable cellulose solutions for controlled modification as well as our previous work pointing out the favourable interaction of cellulose with QAHs [131,132], the objective of the continuation of the work was set to develop new quaternary ammonium salts as cellulose solvents based on morpholinium cations. This work was inspired by *N*-methylmorpholine *N*-oxide (NMMO), a commercially-employed solvent for the direct dissolution of cellulose in the Lyocell process, and the good stability of ionic liquids based on morpholinium cations [134]. In order to gain a deeper insight into the structural requirement of efficient cellulose solvents, the objectives of the following studies were set to synthesize several morpholinium cations and combine them not only with $OH^-$ but also $OAc^-$ and $Cl^-$, which have previously been reported as effective counter ions in a number of cellulose solvents [135–142] to investigate their potential for cellulose dissolution.

Figure 24 shows general procedures employed to synthesise different morpholinium salts. In the first step, *N*-methyl morpholinium iodides and bromides with varying *N*-alkyl chains were synthesized. Normally yields higher than 89% were achieved for bromide/iodide salts except for *N*-heptyl substituent in which the yield decreased to ca. 70%. This was not surprising as halides with longer alkyl chains usually show a lower reactivity. These salts were not extensively hygroscopic since they absorbed water relatively slowly when in contact with air and were, thus, convenient to work with. When synthesis of morpholinium chlorides (MorCl) was attempted, lower yields, around 50%, were obtained, along with a highly hygroscopic nature of the salts making them challenging to handle. To synthesize morpholinium acetates (MorOAc), an ion exchange resin was used to convert the bromides to hydroxides followed by an additional exchange step converting the obtained hydroxides to acetates. These were very viscose and highly hygroscopic liquids containing residual water even after prolonged vacuum drying. For the preparation of morpholinium hydroxides (MorOH) either bromide or iodide salts were ion exchanged using $Ag_2O$. Since the aim was to prepare aqueous MorOH(aq) for further dissolution investigation and as quaternary ammonium hydroxides are well-known to be hygroscopic, their water solutions with desired concentration were directly prepared to eliminate the need for concentrating the solutions (causing possible Hoffman elimination). Detailed synthesis procedures and characterization of each salt can be found in Paper II and III.

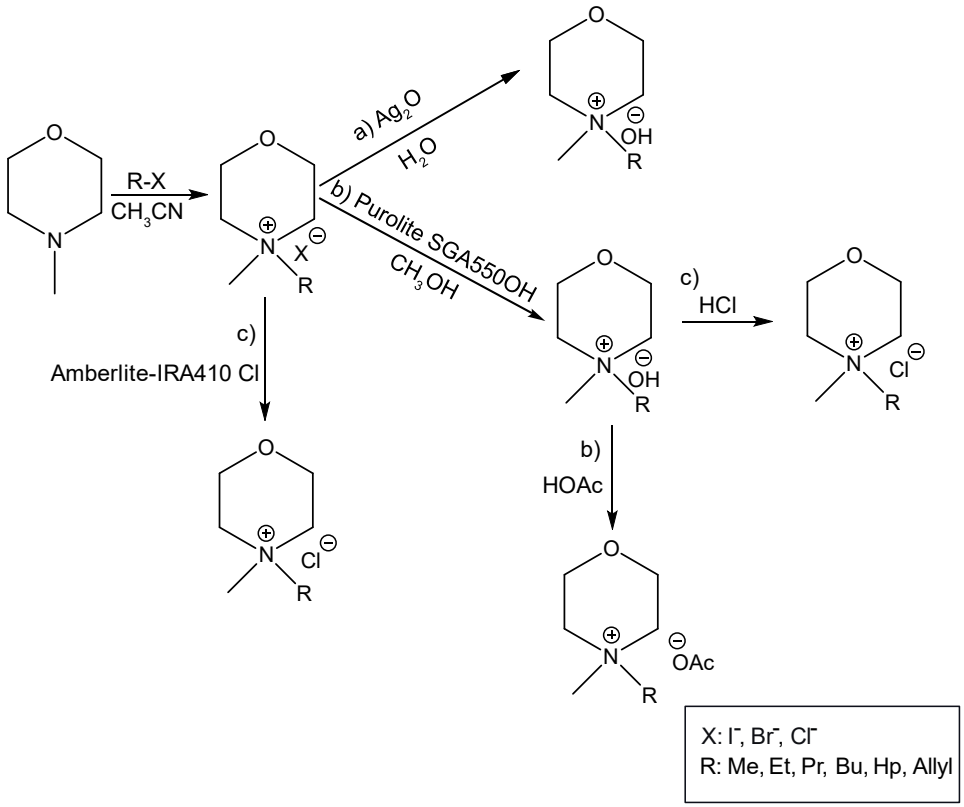


Figure 24. Overview of the general procedures used for the synthesis of (a MorOH(aq) (b MorOAc and (c MorCl.

### 4.2.1 Potential of morpholinium salts as cellulose solvents

The synthesized MorCl shown in Table 3 were solids with melting points above 180 °C (Paper III). These salts were either insoluble or poorly soluble in common organic solvents (e.g. DMSO, DMAc and acetone) even at elevated temperatures. This might indicate that a strong interaction exists between morpholinium cation and chloride ion, hindering their dissociation in these solvents. Previously, Köhler *et al.* observed a correlation between the dissolution of quaternary ammonium fluorides (QAFs) in a polar aprotic solvent (DMSO) and their ability to dissolve cellulose [143]. They emphasized that the dissociation of the salt ions in DMSO was essential for achieving effective interactions with cellulose. On the other hand, aqueous solutions of MorCl did not dissolve cellulose either. In order for aqueous solutions to be able to dissolve cellulose, it is usually, among the other requirements, necessary to have components capable of deprotonating cellulose or making a strong complex with its hydroxyls. In other halide salt systems, such as ionic liquids (e.g. BMIMCl) and salts in aprotic organic solvents (e.g. LiCl/DMAc, TBAF/DMSO), even traces of water have been observed to impede cellulose dissolution [144,145]. Thus, in a non-deprotonating chloride salt solution, the hydration and size of the ions and their hydration (hindering interactions with cellulose hydroxyls) in addition to inaccessibility of cellulose in the absence of charging species that would trigger swelling are likely the reason behind cellulose insolubility in aqueous MorCl.

Table 3. Synthesized MorCl and their melting points.

| **Compound** | 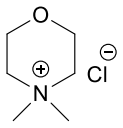 (NDMMCl) | 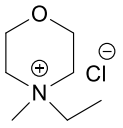 (EMMorCl) | 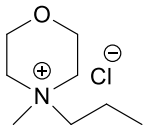 (MPMorCl) | 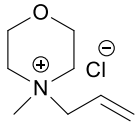 (AMMorCl) |
|---|---|---|---|---|
| **Melting point (°C)** | > 300 | 217 | 244.5 | 182.5 |

Moving on to hydroxides, the synthesized MorOH(aq) with varying alkyl chain lengths were assessed for their ability to dissolve cellulose mainly by polarized light microscopy and turbidity measurements (Papers II and III). As summarised in Table 4, all the synthesized compounds were able to dissolve cellulose when the freeze-thaw method commonly used for aqueous alkaline solvents was applied. As mentioned previously in section 2.5.2.3, the exact reason behind the low temperature requirement for cellulose dissolution in aqueous hydroxides is not yet completely comprehended. It is, however, likely to be linked to the amphiphilic nature of cellulose and the necessity to stabilise both its hydrophilic and hydrophobic regions through interactions with the solvent while avoiding unfavourable entropy loss of water upon dissolution. Lindman *et al.*

proposed that, at low temperatures, the polymer chain conformation minimises the exposure of cellulose hydrophobic regions: this reduces the tendency of cellulose-cellulose interactions occurring through hydrophobic pairing, and minimises restrictions in water mobility, thus facilitating dissolution [89,146]. In addition, temperature dependency of the hydration and, thus, the size of the hydrated ions in these systems should probably also be considered.

In this context, an intriguing finding emerged while studying cellulose dissolution in MorOH(aq) was that chain lengths longer than ethyl in MorOH(aq) resulted in the ability to dissolve cellulose at room temperature (Table 4). Moreover, the concentration of the solvent required for cellulose dissolution at room temperature decreased slightly as the alkyl chain length increased. This finding concurs with previous work by Wang *et al.*, who reported that an increase in cationic hydrophobicity enhances cellulose dissolution in aqueous alkaline solutions [102]. The advantage observed of longer alkyl chain lengths in promoting cellulose dissolution in the present study can probably be attributed to the strong interactions between the morpholinium cations and the hydrophobic regions of cellulose, which prevent the reassociation of cellulose chains even at room temperature (where stabilisation by hydrogen bonding is reduced and the amphiphilicity might be even more pronounced due to potential conformational reasons). Consequently, this interaction might contribute towards preventing the reassociation of cellulose chains through hydrophobic pairing.

The solvent concentration required for cellulose dissolution ranged between 1-2.3 M except for the methyl substituted salt (NDMMOH(aq)), where concentrations higher than 2 M resulted in undissolved cellulose. It is interesting that the longest alkyl chain studied (i.e. heptyl in HMMorOH(aq)) promoted dissolution at an even lower concentration of 0.8 M, emphasising further the advantage of the longer alkyl chain. In order to gain insight into whether cellulose is dissolved molecularly in MorOH(aq), and also to detect the presence of aggregates, dynamic light scattering (DLS) measurements were conducted on dilute cellulose solutions in NDMMOH(aq), as described in Paper II. The results disclosed a minor population of larger structures representative of either aggregates or dust, while the majority of the sample consisted of structures 10 nm in size (based on the volume and number distributions), which aligns with the anticipated size of the molecularly dissolved cellulose [147].

In order to investigate the maximum solubility of cellulose in these solvents, varying amounts of cellulose were added to 1.3 M solvent solutions. Interestingly, the length of the alkyl chains did not appear to have an impact on the maximum dissolution capacity of cellulose. In all of the solvents, it was found that a maximum concentration of 7 wt% cellulose could be dissolved.

Table 4. Cellulose dissolution in MorOH(aq).

| **Solvent** | **Freeze-thaw dissolution** | **Solvent concentration limit for freeze-thaw dissolution** | **r.t. dissolution** | **Solvent concentration required for r.t. dissolution** |
|---|---|---|---|---|
| 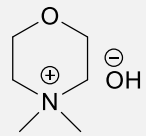 (NDMMOH) | ✓ | 1-2 M | ✖ | - |
| 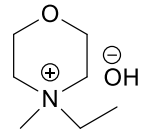 (EMMorOH) | ✓ | 1-2.3 M | ✖ | - |
| 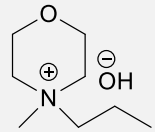 (MPMorOH) | ✓ | 1-2.3 M | ✓ | 2.1 M |
| 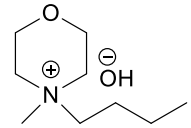 (BMMorOH) | ✓ | 1-2.3 M | ✓ | 2 M |
| 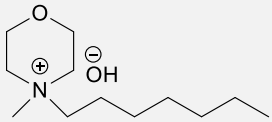 (HMMorOH) | ✓ | 0.8-2.3 M | ✓ | 1.9 M |

Subsequently, MorOAc containing cations similar to those in MorOH(aq) were studied (Table 5, Paper III). These compounds are highly viscose liquids at room temperature, containing traces of water despite undergoing extensive vacuum drying for several days as mentioned before. The presence of residual water appears to be almost unavoidable due to its strong interaction with ILs or since extensive drying can cause degradation [148–150]. However, it was noted that the amount of water decreased as the alkyl chain length increased, which is consistent with previous reports on the relationship between cationic hydrophobicity and water content [151–153]. In Table 5, it can be seen that MPMorOAc deviated from this trend: it contained the highest amount of water (2.06 wt%) even though efforts were made to extend the vacuum drying time. This

suggests that the remaining water may be in the form of bound water, which is impossible to remove completely with used method.

Due to the high viscosity of the synthesized MorOAc, attempts were made to dissolve cellulose at elevated temperatures, as high as 120 °C, but successful dissolution was not achieved. However, the addition of DMSO, a polar aprotic cosolvent, in a mole ratio of 1:4.6 (MorOAc:DMSO) aided the dissolution process by swelling cellulose [154] and enhancing mass transport by reducing the viscosity of the system [155,156]. This combination proved to be successful in dissolving cellulose within 15 minutes at a temperature of 120 °C. The high temperature required for cellulose dissolution in ILs has been attributed mainly to promotion of mass transport as well as ion pair dissociation, thus enhancing their interactions with cellulose hydroxyl groups [157,158]. It is, though, apparent that further investigations are necessary to elucidate the role played by temperature on the dissolution of cellulose in this study.

In contrast to the behaviour of MorOH(aq), an increase in the alkyl chain length in MorOAc had a negative effect leading to decrease in cellulose dissolution (Table 5). The highest cellulose dissolution capacity (14 wt%) was obtained when EMMorOAc with the shortest alkyl chain length (ethyl) was used; this amount decreased to 10 wt% in BMMorOAc/DMSO and HMMorOAc/DMSO containing butyl and heptyl chains respectively. Comparable findings were reported in previous studies involving the use of imidazolium ILs [144,159,160], where it was speculated that the steric hindrance caused by the larger cation hampered the interactions between cellulose and the anion [69], and also potentially restricted the number of anions accessing cellulose [144]. Interestingly, the water content, also possibly correlating with the alkyl chain length, decreased with the increasing chain length (MPMorOAc being an outlier) but did not seem to enhance the dissolution capacity.

Table 5. Cellulose dissolution capacity in MorOAc(aq) and the water content of these solvents.

| **Solvent** | **Maximum amount of cellulose dissolved (wt%)** | **Water content in MorOAc (wt%)** |
|---|---|---|
| 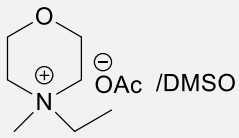 (EMMorOAc) | 14 | 1.28 |
| 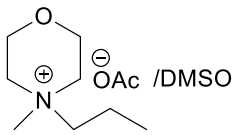 (MPMorOAc) | 3 | 2.06 |
| 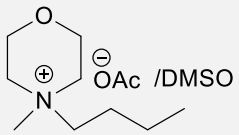 (BMMorOAc) | 10 | 0.86 |
| 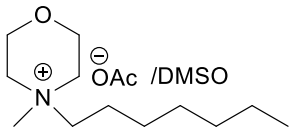 (HMMorOAc) | 10 | 0.76 |

In summary, the results obtained highlight the importance of the accessibility of cellulose, mass transport, ion dissociation and ability to form stabilizing cellulose-solvent interactions when attempting to dissolve cellulose. Only aqueous solutions of MorOH and DMSO-solutions of MorOAc were able to dissolve cellulose. In contrast, cellulose could not be dissolved in MorCl based systems, as these salts were insoluble in the common cellulose swelling agents (e.g. DMSO, DMAc) and showed very high melting points, failing thus, probably, to accomplish ions pair dissociation necessary for interactions with cellulose. Besides, water solutions of MorCl did not show any swelling or dissolution ability, likely due to inability of the hydrated ions to establish strong interactions with cellulose. These findings underlined the importance of the accessibility of cellulose and mass transport. With the MorOH(aq) the accessibility was not an issue as these strong bases could efficiently swell cellulose and most likely accomplish a partial charging supporting the dissolution. In DMSO/MorOAc, on the other hand the strong swelling agent DMSO promoted both swelling and the necessary mass transport of the ions. The length of the alkyl chain, interestingly enough, showed different effects in water and DMSO systems. In aqueous MorOH, where stabilising hydrophobic regions in cellulose is crucial, increasing the alkyl chain length not only

enables dissolution in a broader concentration range but also promotes cellulose solubility at room temperature (for alkyl chains longer than ethyl). In the case of DMSO/MorOAc solvents, cellulose dissolution seemed to decrease despite the fact that longer alkyl chains (butyl and heptyl) lead to a reduction in the amount of residual water: this is probably as a result of steric hindrance, caused by a larger cation, limiting cellulose-anion interactions. In general, MorOAc/DMSO showed a higher dissolution capacity for cellulose compared to MorOH(aq).

### 4.2.2 Investigating the dissolution of pulp in MorOH(aq) and MorOAc/DMSO

The dissolution of 0.5 wt% pulp in 1.3 M NDMMOH(aq) (Paper II) and 1 wt% pulp in 2 M EMMorOH(aq) (Paper III) at room temperature resulted in swollen fibres showing ballooning effect (Figures 25a and 25b). This is a precursor to the dissolution step, comprising heterogeneous swelling and the partial dissolution of the differently orientated cellulose microfibrils layers in the fibre walls. After applying the freeze-thaw procedure, complete dissolution was achieved in EMMorOH(aq) while in NDMMOH(aq), traces of remaining ballooning structures were detected despite the high transmittance and transparent solution that was obtained. The majority of the pulp was dissolved when EMMorOAc/DMSO was used as the solvent; a few undissolved particles could be detected by optical microscopy (Figure 25c).

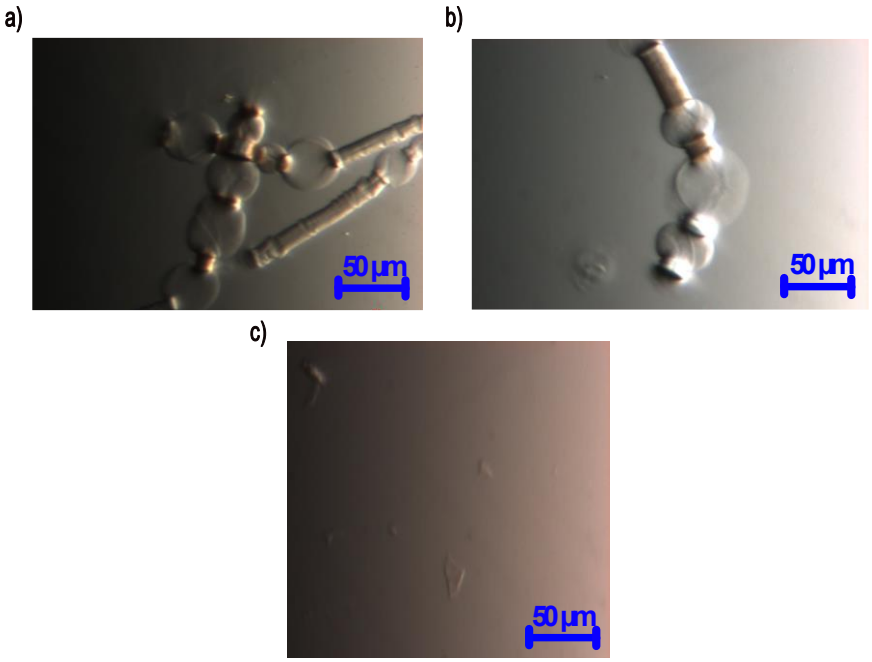


Figure 25. Microscopy images of a) 1 wt% pulp in 2 M EMMorOH(aq) at r.t., b) 0.5 wt% pulp in 1.3 M NDMMOH(aq) at r.t. and c) 0.5 wt% pulp in EMMorOAc/DMSO at 120 °C.

### 4.2.3 Chemical stability of cellulose solutions in MorOH(aq)

Upon the dissolution of cellulose in MorOH(aq), a yellow colour appeared that darkened over time (Figure 26). In order to assess whether this colour change was caused by any form of degradation, fresh and aged cellulose solutions in NDMMOH(aq) and MPMorOH(aq) were subjected to $^{13}C$ NMR analysis.

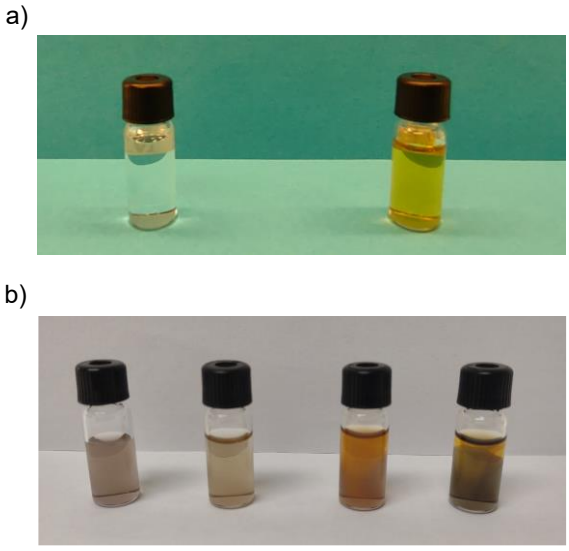


Figure 26. a) 1.3 M NDMMOH(aq) (left) and 3 wt% cellulose dissolved in it (right). b) 3 wt% cellulose dissolved in: left to right: 1 M, 1.3 M, 1.8 M and 2.1 M MPMorOH(aq) after storage in the fridge overnight.

As shown in Figure 27, no shifts or extra peaks could be observed indicating that cellulose solutions in MorOH(aq) are chemically stable over the time investigated. It is, though, possible that the colour observed in cellulose solutions possibly originates from beta-elimination reaction that occurs on the reducing end of cellulose chains, which are highly accessible in the dissolved state as well as oxidation caused by atmospheric oxygen which might form small amounts of strong chromophores.

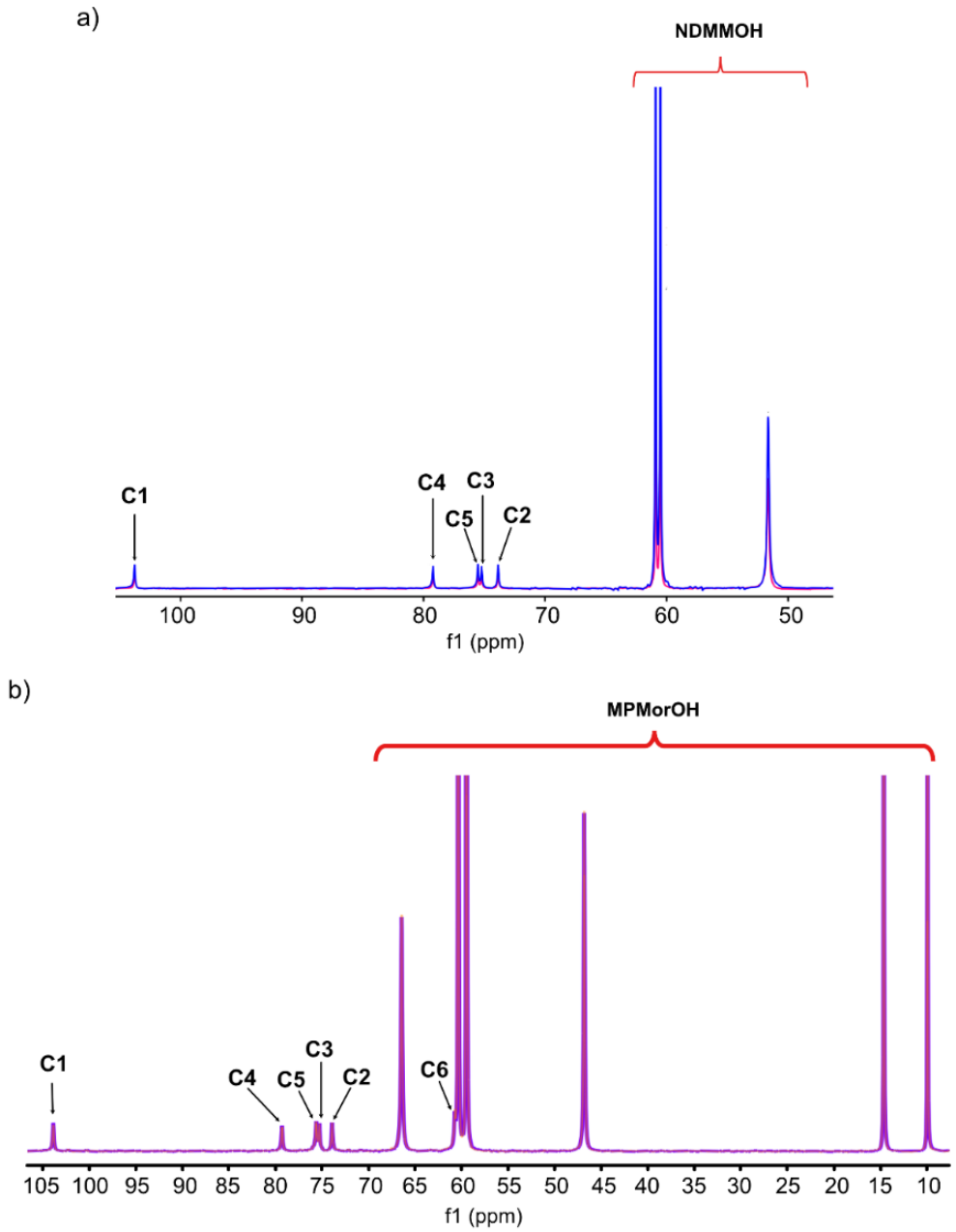


Figure 27. a) Overlayed $^{13}$C NMR spectra of freshly dissolved 3 wt% cellulose in 1.3 M NDMMOH(aq) (pink) and an aged solution kept refrigerated for 16 h post dissolution (blue); b) overlayed $^{13}$C NMR spectra of freshly dissolved 4 wt% cellulose in 1.3 M MPMorOH(aq) (orange) and an aged solution refrigerated for 22 h post dissolution (purple). The pink spectrum in a) and the orange spectrum in b) are not visible due to the perfect overlap of the spectra.

The chemical stability of cellulose dissolved in both MorOH(aq) and MorOAc/DMSO was further confirmed by size exclusion chromatography (SEC) analysis on the cellulose coagulated from these solvents after being stored overnight. In Figure 28 it appears that the chromatograms of the reference samples and those coagulated from the studied solutions are almost identical, with no significant deviation in molecular weight distribution. The minor decrease in $M_w$ could be attributed to beta-elimination, as mentioned earlier. Detailed SEC analysis data can be found in Paper III Supporting Information.

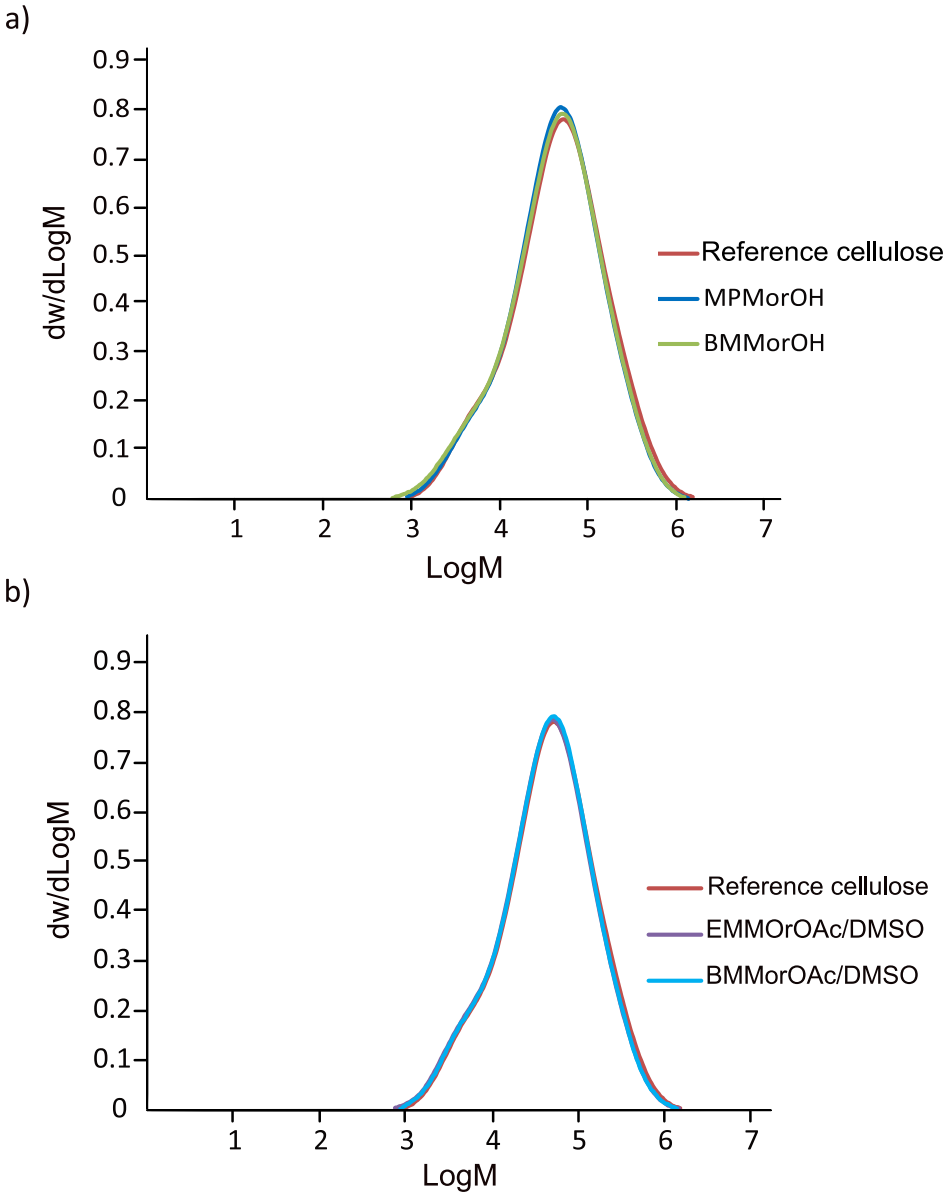


Figure 28. Molecular weight distribution (determined by SEC in DMAc/ LiCl) for cellulose as the reference (red) and a) cellulose dissolved and precipitated, from MPMorOH(aq) (blue) and BMMorOH(aq) (green) after 24 h storage in the fridge; b) cellulose dissolved and precipitated, from EMMorOAc/DMSO (purple) and BMMorOAc/DMSO (blue) (1:4.6 mole ratio) after 24 h storage at room temperature.

### 4.2.4 Characterisation of cellulose solutions by rheometry and NMR

The stability of the solutions at different temperatures was investigated by running a series of flow sweep measurements on cellulose dissolved in MorOH(aq) and MorOAc/DMSO (Figure 29). As expected, cellulose solutions in MorOAc/DMSO have higher viscosity than in MorOH(aq). When shear rates of 1-500 $s^{-1}$ and temperatures between 0-55 °C were applied, all of the solutions showed Newtonian behaviour, and the viscosity of the solutions decreased as the temperature increased. No aggregates could therefore be detected thus the enhanced stability of cellulose in these solvents

could be confirmed when compared to TMAH(aq) and NaOH(aq) solutions investigated previously [132].

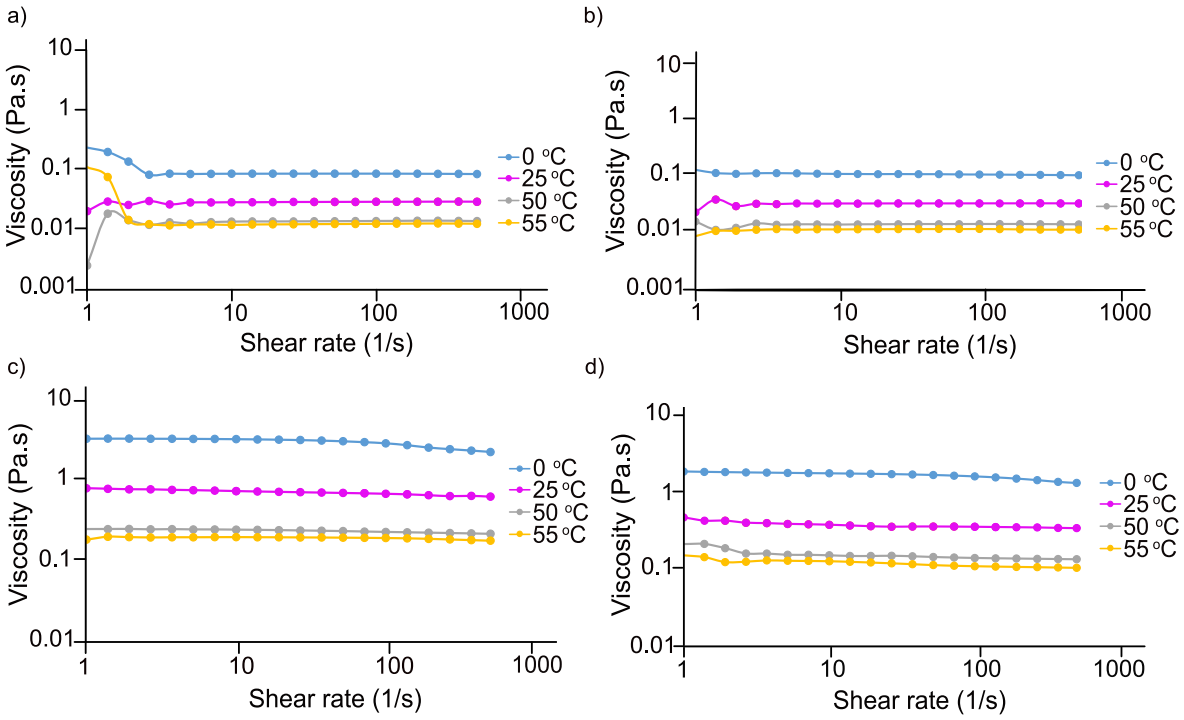


Figure 29. Flow sweep curves of 3 wt% cellulose dissolved in (a) 1.3 M MPMorOH(aq), (b) 1.3 M BMMorOH(aq), (c) EMMorOAc/DMSO and (d) MPMorOAc/DMSO.

In another study (Paper IV) flow behaviour of cellulose solutions in NDMMOH(aq), BMMorOH(aq) and Triton B(aq) were compared (Figure 30). The pure solvents exhibited very low viscosities, similar to that of water and behaved in a Newtonian manner within the shear rate range of 10-100 $s^{-1}$: BMMorOH(aq) showed the highest viscosity, followed by Triton B(aq) and, finally, NDMMOH(aq). After the addition of cellulose (Figure 30b), the viscosity increased as anticipated, and the solutions maintained their Newtonian behaviour. The viscosity of cellulose solutions in NDMMOH(aq) remained the lowest, although higher and, somewhat surprisingly, similar viscosities were observed for cellulose solutions in BMMorOH(aq) and Triton B(aq). This disparity in viscosity suggested the presence of distinct conformations of cellulose chains in different solvents, thus prompted the need for making intrinsic viscosity measurements.

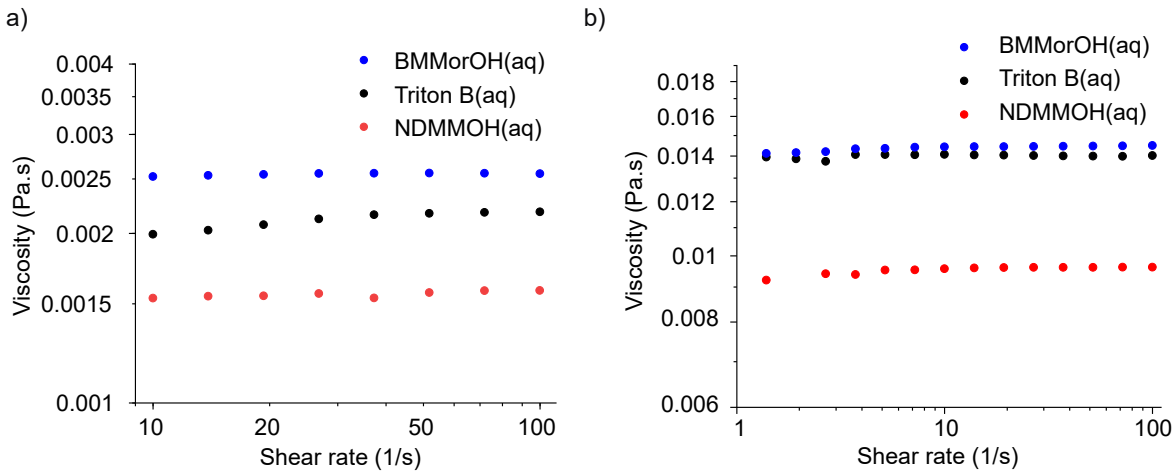


Figure 30. Flow sweep measurements of a) 1.5 M solvents b) 2 wt% cellulose dissolved in each solvent.

It is interesting that the intrinsic viscosity results (Figure 31) revealed that cellulose chains were extended the most in Triton B(aq), slightly less in BMMorOH(aq) and the least in NDMMOH(aq). The estimated intrinsic viscosity values were 1.12, 0.9, and 0.78 dL/g, respectively.

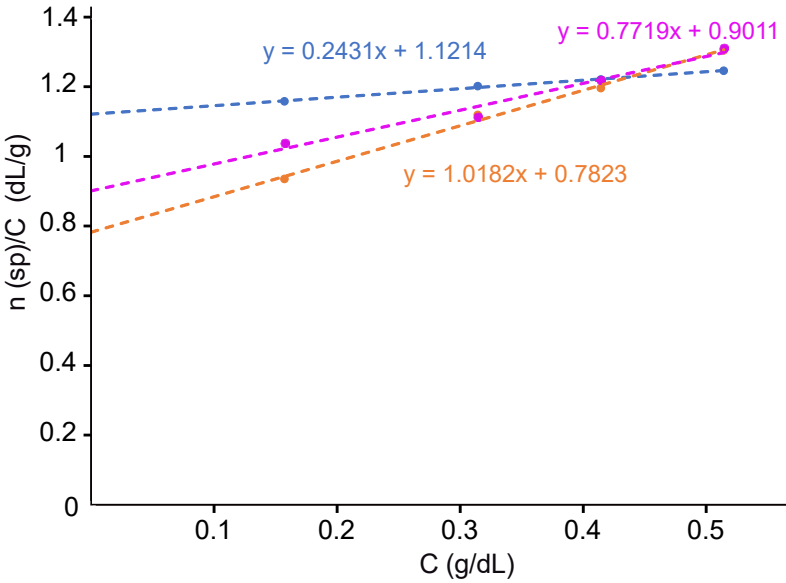


Figure 31. Intrinsic viscosity extrapolated from $\eta_{sp}$ /C plotted vs. C for cellulose dissolved in 1.5 M Triton B(aq) (blue), BMMorOH(aq) (pink) and NDMMOH(aq) (orange).

Further NMR analysis of the solutions, using methyl-α-D-glucopyranoside as a model compound, did not reveal any significant differences in the deprotonation or extent of H-bonding that could be detected as shielding or deshielding effects on the $^{1}$H or $^{13}$C chemical shifts [161] (Figure 32). A very minor shielding detected by lower chemical shift (approx. 0.05 ppm) of the $^{1}$H peaks in Triton B(aq) might be indicative of slightly higher deprotonation of cellulose in this solvent, although identical chemical shifts were

obtained in $^{13}C$ NMR spectra (see Paper IV). Altogether, these findings highlight the fact that there are similar deprotonation levels in all of the solvents.

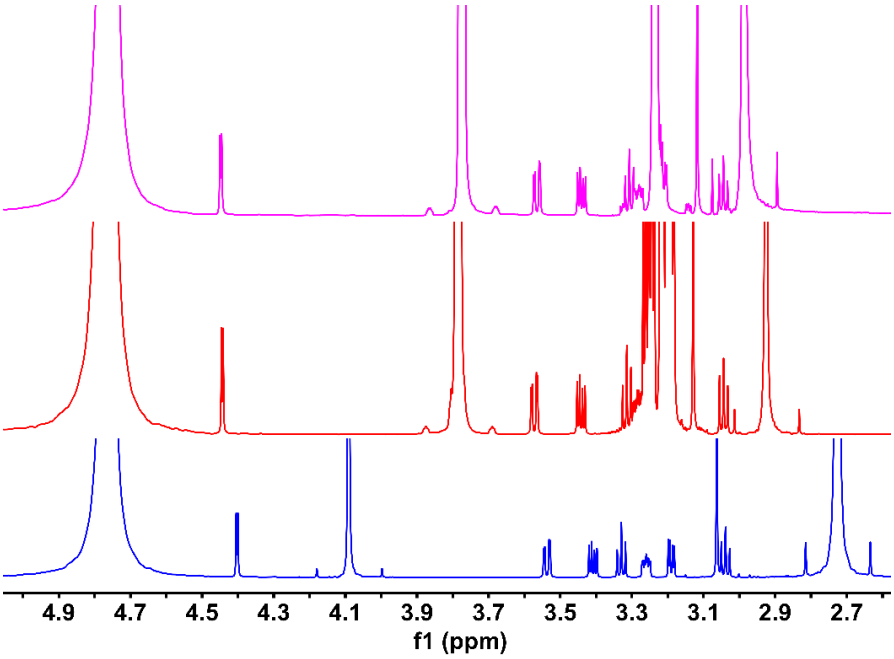


Figure 32. $^{1}H$ NMR spectra of 3 wt% methyl-α-D-glucopyranoside used as the model compound dissolved in 1.5 M Triton B(aq) (blue), 1.5 M BMMorOH(aq) (red) and 1.5 M NDMMOH(aq) (pink) in $D_2O$.

Continuing the investigation, a particular interest arose to examine how the similarities and differences observed in cellulose solutions in NDMMOH(aq), BMMorOH(aq) and Triton B(aq) would be manifested in cellulose coagulation. Based on a previous work in our group [121], $CO_2$(g) was chosen as the coagulant for the purpose of monitoring this process *in situ* with FTIR. In this study, $CO_2$(g) with a flow rate of 200 ml/min, was bubbled through each cellulose solution, after which immediate formation of gel was observed (Figure 33).

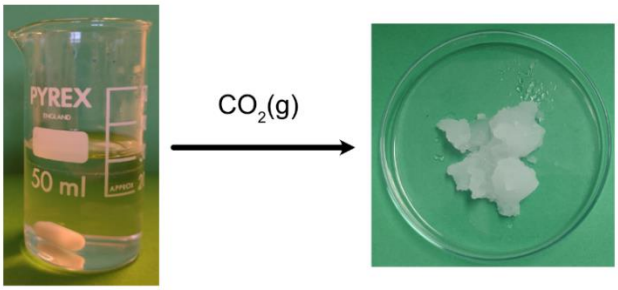


Figure 33. Cellulose solution in Triton B before (left) and after (right) $CO_2$(g) introduction.

### 4.3 *In situ* monitoring of cellulose gelation

Figure 34 shows an overview of the *in situ* monitoring of cellulose gelation in NDMMOH(aq) upon the introduction of $CO_2$(g). Attempts to follow the coagulation

of cellulose using FTIR encountered problems similar to those described in Section 4.1.1: the characteristic peaks of cellulose which overlapped with those of the organic solvents turned out to be problematic in assessing the completion of coagulation because both of these peaks showed decreases during coagulation. The decrease of cellulose peaks was due to its precipitation and the decrease of the solvent peaks due to the formation of water in the system via a reaction between $CO_2$(g) and hydroxides, which resulted in dilution of the system and thus a decrease in peak absorption. Consequently, making a quantitative assessment of the precipitation was not possible. Attempts to subtract the solvent spectra from the corresponding spectra of the cellulose-containing systems were not successful either, since baseline shifts were observed due to small deviations in probe alignments (angles), which could not be avoided.

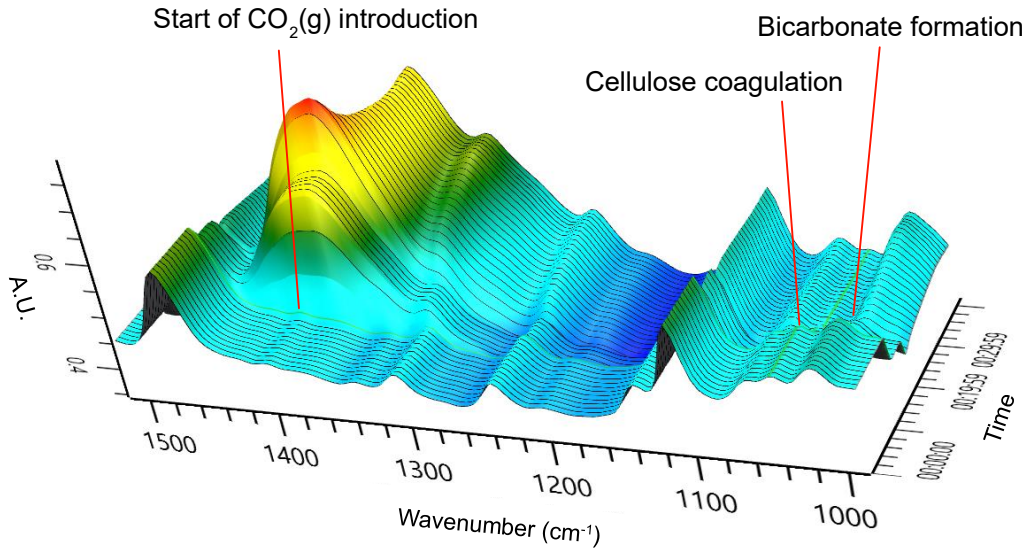


Figure 34. 3D spectra of the *in line* monitoring of cellulose gelation in 1.5 M NDMMOH(aq) upon the introduction of $CO_2$(g) with the flow rate of 200 ml/min.

A qualitative analysis of the formations of carbonate and bicarbonate as well as pH and temperature profiles during the coagulation was nevertheless possible, (Figure 35); figures related to other solvents can be found in Paper IV. It is interesting to note that, in the systems studied, almost identical responses were detected during coagulation with $CO_2$(g) as no significant differences could be observed in pH and temperature profiles or trends in carbonate and bicarbonate species throughout the precipitation process. Typically, upon the introduction of $CO_2$(g) into these highly alkaline solutions and subsequent carbonate formation, there is a noticeable rapid and sharp decrease in pH and an increase in temperature. As the carbonates reach their maximum concentration and bicarbonates start to form, the pH continues to decrease at a slower rate, accompanied by a steady decline in temperature. Precipitation of cellulose takes place immediately after initial introduction of the $CO_2$(g), in the high pH region and its completion is manifested as a plateau in the carbonate trend. The fluctuations observed in carbonate absorption in cellulose solutions might arise from

gelation hindering accurate quantification by the FTIR probe which requires further investigations.

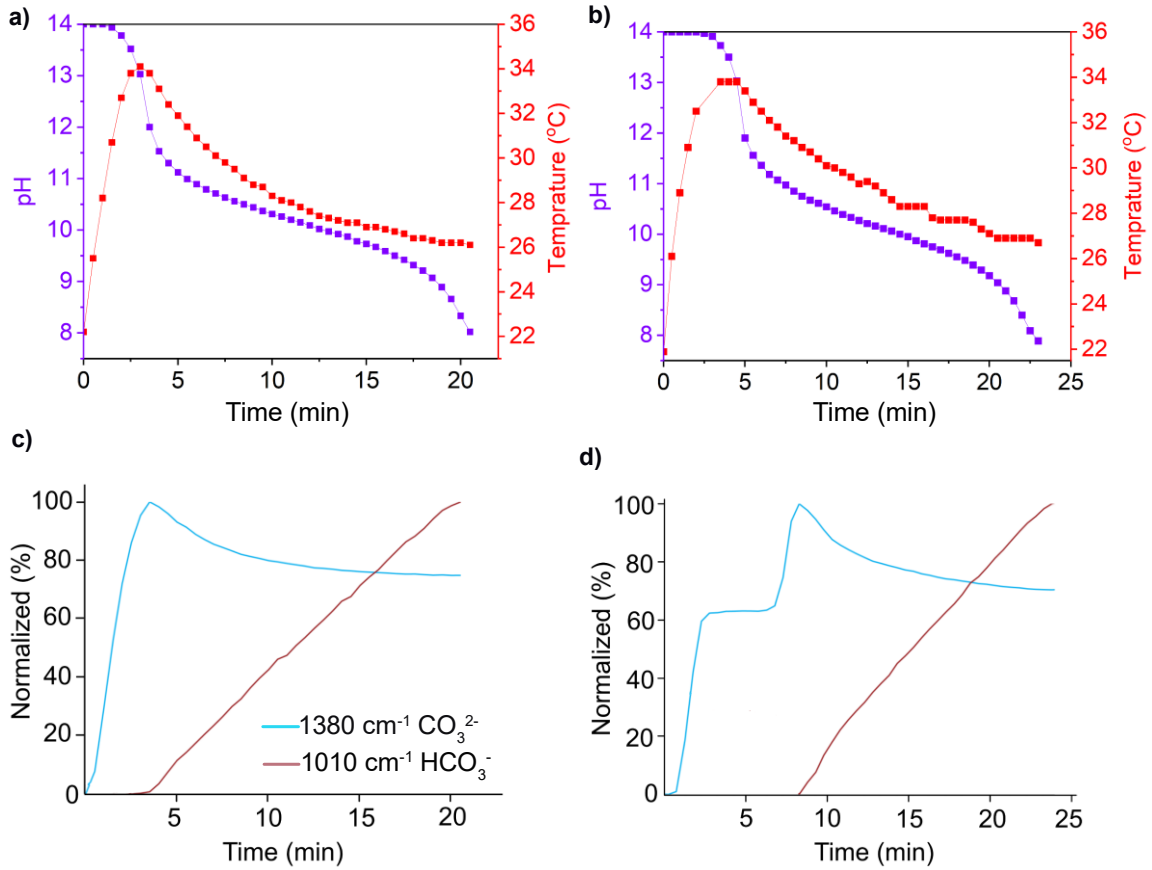


Figure 35. pH, temperature and carbonate/bicarbonate trends (based on FTIR absorption) while introducing $CO_2$(g) (200 ml/min, room temperature) to the following solutions: a) & c) 1.5 M NDMMOH(aq); b) & d) 2 wt% MCC dissolved in 1.5 M NDMMOH(aq).

Complementary characterisation was necessary to determine whether any differences could be detected in these systems after gelation which is discussed in more detail below.

### 4.4 Rheological properties of the systems after gelation

While no significant differences in response to $CO_2$(g) coagulation could be detected by FTIR (Figure 5 in Paper IV), the gels obtained from the different solutions appeared to be very different. It was visually obvious that the gel formed in Triton B(aq) was more compact than the (loose) gel obtained in NDMMOH(aq) after the addition of $CO_2$(g). When BMMorOH(aq) was used, it could be seen that the gel formed was neither as loose as in NDMMOH(aq) nor as compact as in Triton B(aq). These visual findings called for rheological characterisation of the systems after gelation to shed light on any potential differences.

The flow sweep curves in Figure 36 show shear thinning behaviour in all the samples, which is typically observed in most of the gels. The highest viscosity was obtained in Triton B(aq) followed by BMMorOH(aq) and NDMMOH(aq), respectively, being in line with what was observed visually. It is interesting that these results which show a significant difference in the viscosities obtained did not reflect the differences observed in the dissolved state prior to $CO_2$(g) introduction in Figure 30b (where Triton B and BMMorOH solutions show very similar viscosities).

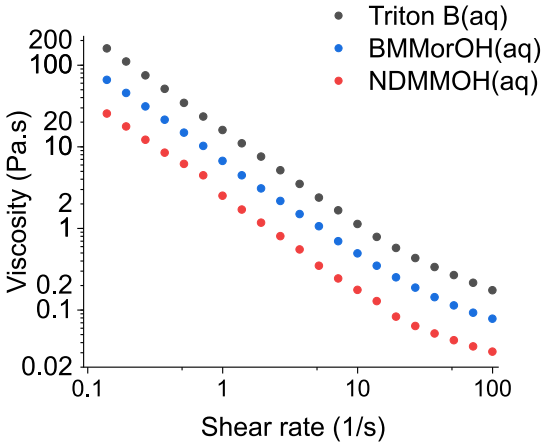


Figure 36. Flow sweep curves of cellulose solutions after gelation.

The frequency sweep measurements (Figure 37) comparing the solid contribution of the materials (G', storage modulus) in different solvents before and after gelation concurred with these results. Indeed, G' after gelation appeared in the following order: Triton B(aq) > BMMorOH(aq) > NDMMOH(aq), reflecting the order of the gel strength. The observed differences in the gel strength despite the similar viscosities of the initial Triton B(aq) and BMMorOH(aq) solutions and the similar coagulation procedure called for further investigation using molecular dynamics (MD) simulations, which are discussed below.

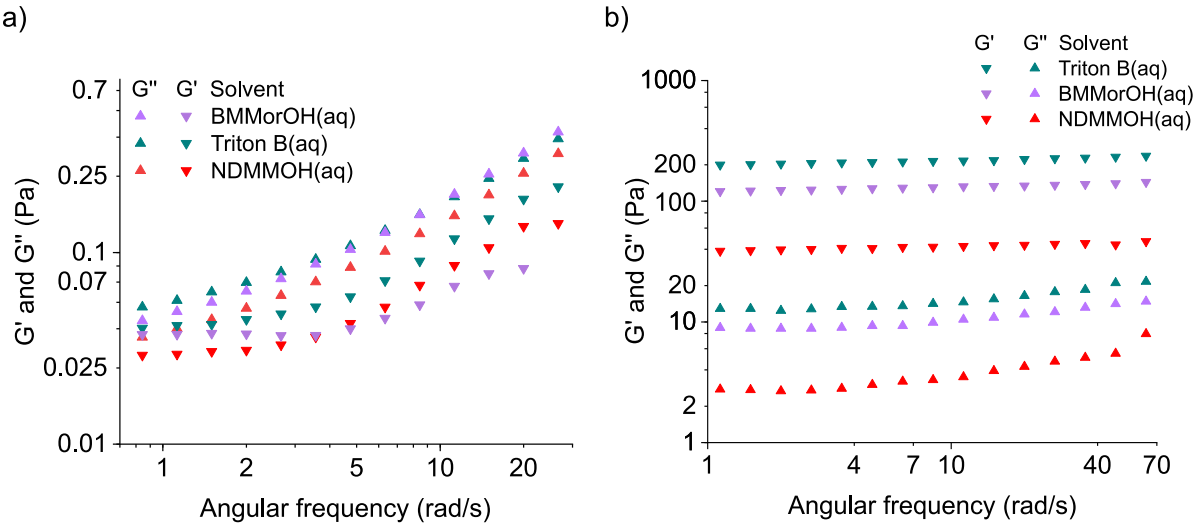


Figure 37. Frequency sweep measurements of cellulose solutions a) before and b) after gelation.

### 4.5 MD simulations of cellulose solutions before and after coagulation

MD simulations aimed at gaining a deeper insight into the differences observed in the studied cellulose solutions upon $CO_2$(g) introduction by examining the interactions between two cellulose chains (considering both hydrophilic and hydrophobic faces) in Triton B(aq), NDMMOH(aq) and BMMorOH(aq) before and after $CO_2$(g) introduction. To explore the impact of $CO_2$(g) on cellulose solutions, hydroxide ions were substituted with carbonate ions. To quantify the interaction between the cellulose chains, calculations of the free energy profile between cellulose centres of masses were conducted along a specific direction before and after CO2(g) introduction. Details on the methodology can be found in Paper IV Supporting Information. It is noteworthy to mention that Triton B cation is referred to as $BTMA^+$ (abbreviation corresponding to benzyltrimethylammonium) in the figures.

Figure 38 depicts the free energy profiles of the interactions between the hydrophilic (110 plane) and hydrophobic cellulose faces (100 plane) in the solvents studied. X axis represents the distance between the center of masses of cellulose chains and the y axis represents potential of mean force (PMF) (attraction or repulsion) observed in the simulations.

A system exhibits a tendency to reside in the region of minimum energy (ROME). Hence, it is evident from Figure 38a (considering hydrophilic sides of cellulose prior to $CO_2$(g) introduction) that the chains tend to shift to the right-hand side (RHS), where the secondary energy minimum has considerably lower energy barriers (in the region between 1.47 to 1.62 nm). The specific depths and positions of these secondary minima depend on the solvents employed, as shown in Figure 38a. If cellulose chains are to be pulled apart, they must surpass the energy maxima on the right-hand side, consequently the viscosity of a system is influenced by the amount of energy required to surpass the energy maxima (i.e. the difference between the energy minima and maxima): the greater the energy needed to overcome the energy maxima, the greater the viscosity.

Such secondary minima can also be observed in the region between 1.0 and 1.62 nm when the hydrophobic faces of the cellulose chains are considered in the absence of carbonate ions (Figure 38b). Comparing Figures 38a and 38b reveals that the aforementioned energy barriers are more pronounced during interactions between the hydrophobic segments of the cellulose chains, indicating that hydrophobic contributions play a more significant role in determining the viscosity of cellulose solutions. A quantitative estimation of the energy barrier in Figure 38b representing the interactions between the hydrophobic faces of cellulose chains is as follows: 2.5 kJ/mol for Triton B, 2.4 kJ/mol for BMMorOH and 1.2 kJ/mol for NDMMOH. This indicates that cellulose in Triton B(aq) and BMMorOH(aq) tend to have similar

viscosities, higher than that in NDMMOH(aq), in line with the measured viscosities of the systems (Figure 30).

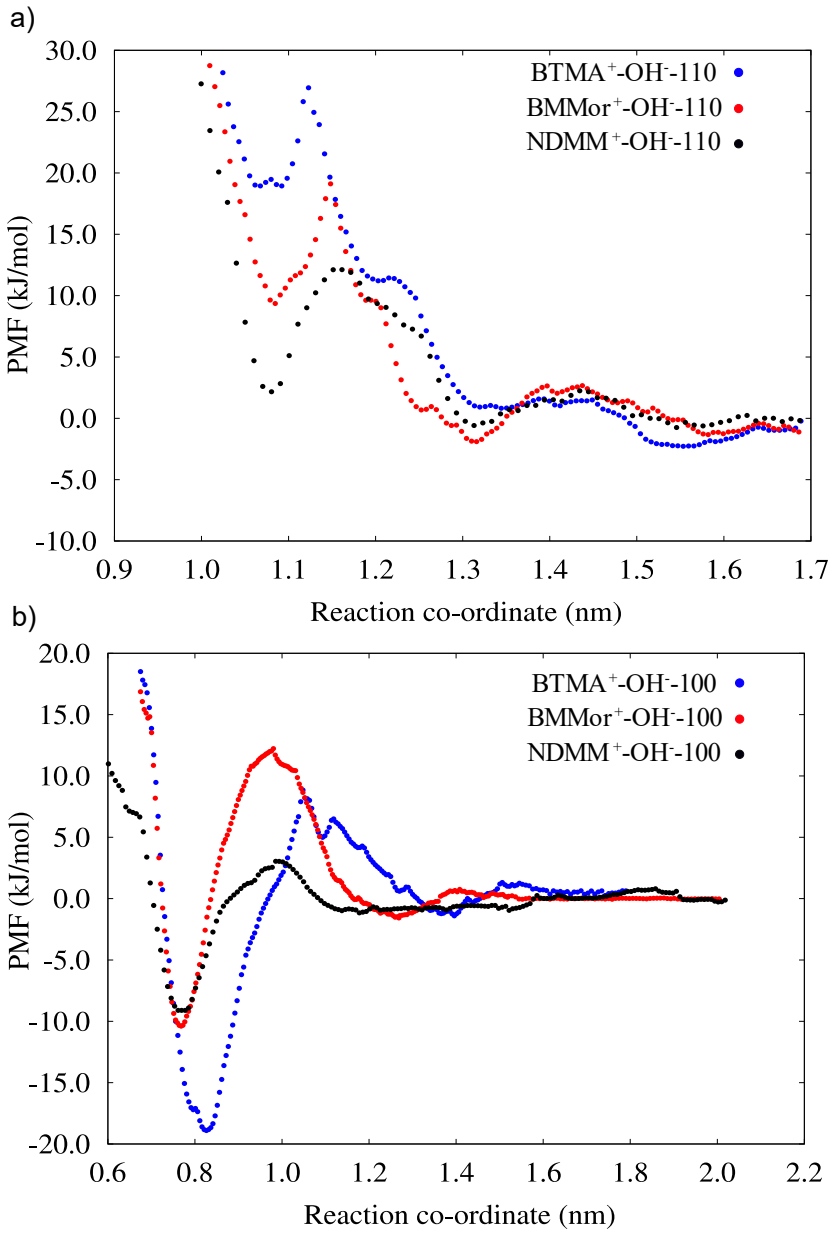


Figure 38. Free energy profiles of interaction between a) hydrophilic and b) hydrophobic faces of cellulose in absence of carbonate ions. $BTMA^+$ refers to cation in Triton B(aq).

Upon the introduction of carbonate ions, according to Figures 39a and 39b, deep energy valleys are created that are more pronounced when the hydrophobic regions of cellulose interact. Figure 39b shows that, in Triton B(aq), a deeper ROME (in the region between 1.0 and 1.8 nm) is created which shifted slightly towards the left hand side compared to Figure 38b in the absence of carbonate ions pointing out to cellulose aggregation. This observation indicates the instantaneous formation of the gel in which the cellulose chains containing the solvents are trapped in a valley with little possibility of movement, causing higher viscosity of the resulting gel. A similar behaviour is

observed in solutions containing $BMMor^+$ and carbonate ions. However, in the case of the $NDMM^+$ containing solvent, the ROME shifts further towards the RHS, promoting the expulsion of solvent molecules from between the cellulose chains and the formation of a loosely connected aggregate. Since the values of the energy barrier created when carbonate ions are introduced appear in the order Triton B(aq) > BMMorOH(aq) > NDMMOH(aq), these findings suggest that the viscosity of the resulting gel is higher in the case of the Triton B(aq) solutions and slightly lower in BMMorOH(aq). Conversely, very loose aggregates are formed in the solution containing NDMMOH(aq), leading to the suspension with the lowest viscosity.

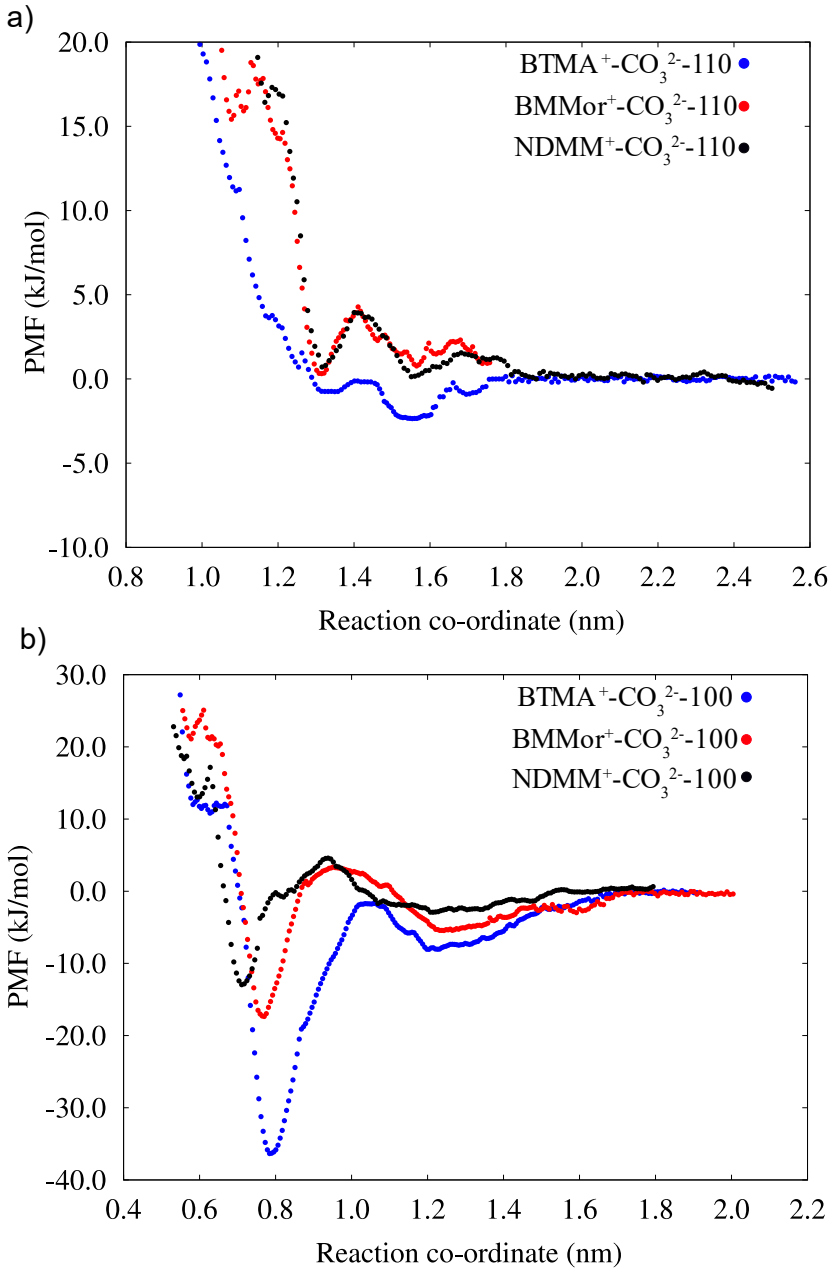


Figure 39. Free energy profiles of interaction between a) hydrophilic and b) hydrophobic faces of cellulose in presence of carbonate ions. $BTMA^+$ refers to cation in Triton B(aq).

### 4.6 Impact of solvent and coagulant on the crystallinity of the coagulated cellulose

In order to assess the impact of both the solvent and antisolvent on the crystallinity of the coagulated cellulose, the following comparisons were made:

a) Ethanol coagulation of cellulose from MorOH(aq) vs. MorOAc/DMSO (Paper III) to see the effect of the solvents
b) Coagulation of cellulose dissolved in QAHs (MorOH(aq) and Triton B(aq)) using $CO_2$(g) vs. ethanol as the antisolvents (Paper IV) to study the effect of antisolvent

Figure 40 demonstrates the CP/MAS $^{13}$C NMR spectra obtained from cellulose coagulated from MorOH(aq) and MorOAc/DMSO. It can be seen that the two spectra corresponding to cellulose coagulated from MorOH(aq) are identical, and that those from MorOAc/DMSO overlap. However, spectra of cellulose coagulated from MorOH(aq) differ from the corresponding ones obtained from MorOAc/DMSO. The formation of cellulose II gives rise to two characteristic peaks at ca. 107 and 87.5 ppm [162–166]. These are evident in the samples coagulated from MorOH(aq) through the appearance of a shoulder at 107.1 and a peak at 87.7 ppm, however none of these peaks appeared in the samples coagulated from MorOAc/DMSO, yet an increase in the peak intensity indicative of amorphous cellulose at 84 ppm could be observed. Similar results were obtained where ethanol or water were used for coagulation of cellulose from EMIMAc in which more amorphous cellulose was obtained using ethanol, while higher degree of cellulose II was formed as a result of using water as an antisolvent [167,168]. Östlund *et al.* correlated the lower crystallinity of ethanol coagulated cellulose to slower diffusion of EMIMAc in ethanol than in water. On the other hand, Tan *et al.* suggested that ethanol caused cellulose chains aggregation into a relatively disorganized state while water promoted realignment of molecular chains and the rebuilding of an ordered cellulose structure. In the present study, it is probable that these factors likely contribute to the differences observed in the crystallinity of cellulose coagulated from MorOH(aq) vs. MorOAc/DMSO, yet more profound investigations are necessary to shed light on the underlying reasons.

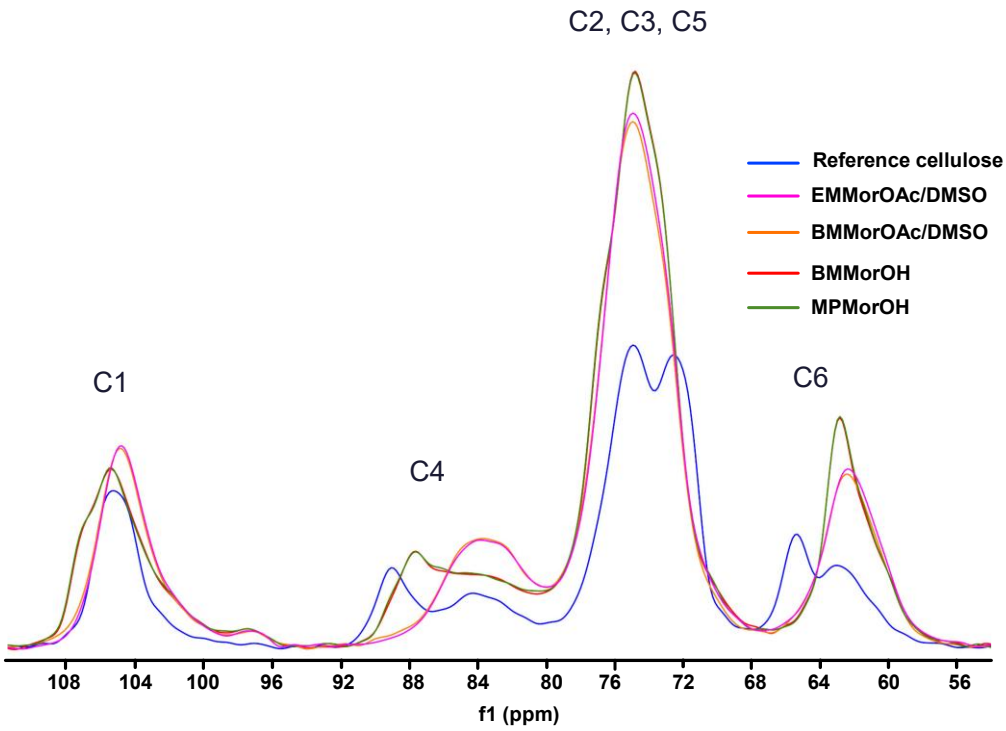


Figure 40. CP/MAS $^{13}C$ NMR of reference cellulose and cellulose coagulated in different solvents.

Qualitative analysis of the crystallinity was also confirmed by a method developed previously assessing the integrals obtained from two different pulse sequences in which the difference in T1 for crystalline and amorphous cellulose was used [130]. Due to overlap of C4 and C2,3,5 peaks, C1 integral was used. The results are summarized in Table 6 below confirming higher crystallinity of cellulose coagulated from MorOH(aq) than when MorOAc/DMSO was used as the solvent.

Table 6. Estimated crystallinity of cellulose coagulated from MorOH(aq) vs. MorOAc/DMSO

| **Sample** | **Estimated crystallinity** |
|---|---|
| Reference cellulose | 0.44 |
| Cellulose coagulated from MPMorOH(aq) | 0.36 |
| Cellulose coagulated from BMMorOH(aq) | 0.36 |
| Cellulose coagulated from EMMorOAc/DMSO | 0.23 |
| Cellulose coagulated from BMMorOAc/DMSO | 0.29 |

The impact that the antisolvent has on the crystallinity of the coagulated cellulose was investigated further by studying coagulation with $CO_2$(g) as well as ethanol. Solid state NMR spectra (Figure 41) show that, when $CO_2$(g) was used as the coagulant, cellulose

I showed a clear transformed into cellulose II. This was validated by the appearance of peaks at 107.2 and 87.8 ppm, whereas the signal at 65.3 ppm representing cellulose I in the reference cellulose disappeared in all the samples. Nevertheless, crystallinity differed between the cellulose coagulated from the solvents studied here using ethanol. While cellulose coagulated from NDMMOH(aq) appeared mostly in the form of cellulose II (confirmed by the peak at 87.8 ppm and a very minor shoulder at 107.2 ppm), none of the aforementioned peaks could be seen in the case of Triton B(aq). Thus, a more amorphous cellulose was obtained using Triton B(aq) as the solvent and ethanol as the coagulant.

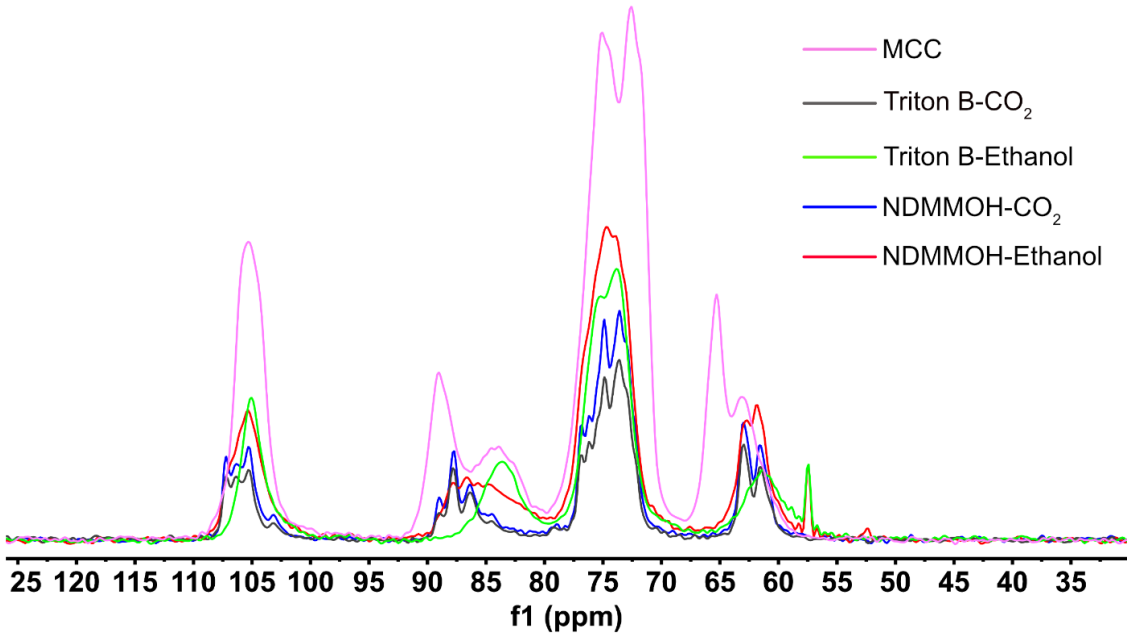


Figure 41. CP/MAS $^{13}C$ NMR of reference cellulose and cellulose coagulated from different solvents, using ethanol or $CO_2$(g) as the coagulant.

In summary, both the solvent and the coagulant affect the crystallinity of the cellulose coagulated. Coagulation from MorOH(aq), using ethanol or $CO_2$(g) as the coagulant, leads to the formation of cellulose II. Coagulation from MorOAc/DMSO using ethanol as the coagulant, on the other hand, results in more amorphous structure. Different coagulants show different effect on cellulose coagulated from Triton B(aq); while $CO_2$(g) yields mostly coagulated cellulose II, more amorphous cellulose is obtained when ethanol is used.

# 5

# Concluding Remarks

The overall goal of this thesis was to investigate the dissolution, modification and coagulation of cellulose in quaternary ammonium-based solvents (mainly QAHs(aq)) to shed light on the impact of the solvent structural features on these processes. Based on the results obtained, several concluding remarks can be made as follows:

- *In situ* monitoring of cellulose etherification in aqueous alkaline solutions is challenging due to the occurrence of several side reactions, such as hydrolysis and cascade reactions, instability of the solution and multiple overlapping signals. Valuable insights can nonetheless be gained into reagent hydrolysis, reaction endpoints and solution stability during the process, which may be complemented by *in situ* viscosity measurements.

- The significant role of the solvent structure (e.g. its ability to provide good solubility of cellulose and the modification agent in the reaction solution) for the outcome of modification has been highlighted. Specifically, the two studied QAHs (Triton B(aq) and TMAH(aq)), which are hydroxide bases with relatively hydrophobic organic cations, contributed to the stability of cellulose solutions at higher temperatures, improved the dissolution of etherifying reagent (AGE) and accelerated the overall reaction rates when compared to NaOH(aq). Cascade reactions (i.e. self-etherification of the substituent introduced) were significantly promoted in NaOH(aq) most likely as a result of the reduced temperature stability of the cellulose solution and, consequently, lower accessibility of cellulose OH groups in the partly-gelled reaction mixture.

- *N*-methyl morpholinium hydroxides with varying *N*-alkyl chain lengths proved to be capable of dissolving cellulose (up to 7 wt%) when combined with water;

their acetate counterparts could also dissolve cellulose when combined with DMSO. MorOH(aq) dissolve cellulose when subjected to the freeze-thaw method commonly applied to aqueous alkali solvents in a range of concentrations, whereas dissolution in MorOAc/DMSO took place at elevated temperature (120 °C). The length of the alkyl chain in the morpholinium cation has a different impact on the dissolution ability of the two solvent categories mentioned: while chains longer than ethyl enabled dissolution at room-temperature in MorOH(aq), increasing the alkyl chain length was observed to lead to a decrease in the dissolution ability of MorOAc in DMSO solutions. In MorOH(aq), it is most likely that a more hydrophobic cation prevents cellulose chains from reassociation through improved stabilisation of the hydrophobic cellulose regions, while increased hydrophobicity causes steric hindrance that probably hampers effective interaction between cellulose and the anion in MorOAc. The presence of strong swelling agent e.g. DMSO promotes the accessibility of cellulose and effective cellulose-solvent interactions. In contrast, the synthesized MorCl (solids with high melting points) did not have the potential to dissolve cellulose. Apart from their high melting points, they were either not soluble or poorly soluble in common cosolvents. It is likely due to the strong interaction between the morpholinium cation and chloride ions preventing their dissociation in these solvents. In addition, the inability of aqueous solutions of MorCl to dissolve cellulose might be attributed to the size of hydrated ions (being extensively hydrated) possibly hindering complexation or interaction with cellulose.

- The intriguing differences observed in the consistency of the gels obtained in different QAHs(aq) after coagulation using $CO_2$(g) might present opportunities for creating gels with properties that can be fine-tuned using various solvents. The cation in the solvent proved to impact the properties of the gel, most likely as a result of different cellulose-solvent interactions and, consequently, different conformations of cellulose chains. This leads to variations in the viscosity of the solutions as well as to specific interconnected networks within the gels.

# 6

# Future Work

In the present work, several morpholinium-based salts have been developed and their potential to dissolve cellulose was investigated. Considering the results obtained in Paper I on the enhanced cellulose modification in QAHs(aq), it would be of interest to study cellulose modification in these new solvents and investigate their impact on the stability of cellulose solutions during the course of reaction as well as on the product obtained.

When MorOAc/DMSO were studied for cellulose dissolution, only one molar ratio of the cosolvent: solvent was considered. A question that remains open, and is worth more examination, is how different molar ratios impact the dissolution conditions and the maximum cellulose dissolution. In-depth studies on molecular levels would be of interest to obtain detailed insight on the state of dissolved cellulose in MorOH(aq) and MorOAc/DMSO. It would be advantageous if more theoretical studies are carried out to understand the mechanism of cellulose dissolution in the solvents developed and, in particular, to assess the enthalpy and entropy contributions in the different solvents as a function of the *N*-alkyl chain length and the cation structure in general. This would shed further light on the features required when designing new cellulose solvents. In addition, further efforts could be made with regard to the recyclability of the solvents obtained and developing strategies for this purpose, as well as improving the synthesis procedures of the salts studied.

This work has used mainly low molecular weight cellulose to investigate the dissolution of cellulose. More detailed studies on dissolution using dried/never dried pulp, spinning and coagulating the solutions, as well as on the mechanical properties of the fibres, would be of great interest, especially for industrial applications.

Considering the preliminary results obtained on the gelation of cellulose in QAHs(aq), it would be interesting to study the coagulation of cellulose using $CO_2$(g) in different solvents and to fully characterise the gels obtained to assess their potential use in further applications.

# 7

# Acknowledgements

I would like to start by thanking the Knut and Alice Wallenberg Foundation within Wallenberg Wood Science Center for funding this Ph.D. project. Erasmus+, Bo Rydin and Åforsk foundations are also gratefully acknowledged for providing the financial support necessary to make a research exchange in Germany and participation in international conferences.

Completing my Ph.D. would not be possible without the support of the following people with whom I have shared a memorable chapter of my life.

- First of all, I would like to thank my main supervisor, Assoc. Prof. Merima Hasani, for providing me the opportunity to make my dream true of moving abroad to study Ph.D. I am so grateful to you not only for your scientific support but also for treating me as a friend. You always told me, "We will make it work together, Shirin!" and you were right: we did!
- My co-supervisor, Assoc. Prof. Diana Bernin: I was so privileged to have you during this journey. Your support and encouragement have always given me motivation to move forward. You are an amazing friend!
- My examiner, Prof. Hans Theliander, for encouragement and making sure that everything was on the right track.
- Prof. Thomas Heinze for providing the opportunity for me to do a research exchange in your group in Jena, Germany, and our scientific discussions.
- Dr. Andreas Koschella for invaluable supervision during my stay in Germany, and support whenever I needed help there. I learnt so much from you during my three months stay. I am so grateful to you!
- Dr. Paul Kujpers from Metler-Toledo for invaluable guidance and support during *in line* FTIR studies, Dr. Nabin Kumar Karna for conducting MD simulations and Dr. Beatrice Swensson for DLS measurements.
- Prof. Roland Kádár, Ms. Sylwia Wojno, Prof. Anna Ström and Mr. Jakob Karlsson for rheology measurements, discussions and help with the equipment. Mr. Michael

Andersson-Sarning and Ms. Ximena Rozo Sevilla for all their help with lab associated works and solving technical issues. I am so grateful to you Michael for your excellent expertise and help in the lab. You are an excellent problem solver!

- Dr. Ulrika Brath for valuable discussions on NMR results and the Swedish NMR centre for providing spectrometer time.
- Ms. Maureen Sondell for excellent linguistic review.
- Ms. Johanna Spång for all the help with administrative work. You are so kind and helpful!
- Ms. Malin Larsson for kind support and help all the time, above and beyond administrative work, and especially so when I was new in Sweden. I never felt alone when you were around.
- My previous and current officemates, Dr. Maria Gunnarsson, Ms. Anna Hjorth and Mr. Linus Kron, for all the chit chat, help and exchange of knowledge during working hours.
- All my previous and current colleagues at SIKT and Wallenberg wood science center, for all the fun times we had together. You have always helped me through hardships. I am so grateful to you all!
- My dear friend who is becoming a doctor soon: Sylwia Wojno for all the support you have given me and the memorable times we had together. I am so happy that we have become close friends and look forward to creating more memories together.
- Dr. Anders Ahlbom for all the support, help and motivation you gave me when I needed it. They all have become wonderful memories which I will always remember. So happy to have you as a friend!

- خانواده عزیزم: پدرم باسم،مادرم سوهاد، خواهرم یاسمن و برادرم احسان. بدون حمایت شما آغاز این سفر برایم ممکن نبود. عشق و حمایت شما همیشه چراغ راه من بوده و هست. مادر عزیزم با نگاه های پر مهرت همیشه به من انرژی بخشیدی و همچنین شما پدر عزیزم، همیشه به یاد دارم که در آغاز این سفر به من گفتی: "قوی باش دخترم!" و من همیشه با یاداوری آن برای رسیدن به اهدافم انگیزه گرفتم .

- Last but not least, my dear husband Soheil. You have always believed in me, supported me and helped me whenever I needed it. You are my dearest and closest friend in life! You are unique!

Thank you all, indeed!

# 8

# References


[1] D. Majumdar, A. Bhanarkar, C. Rao, D. Gouda, Carbon disulphide and hydrogen sulphide emissions from viscose fibre manufacturing industry: A case study in India, Atmos. Environ. X. 13 (2022) 100157.

[2] T. Rosenau, A.D. French, N-Methylmorpholine-N-oxide (NMMO): hazards in practice and pitfalls in theory, Cellulose. 28 (2021) 5985–5990.

[3] A. Payen, C.R. Hebd, Sur un moyen d'isoler le tissue élémentaire des bois, Seances Acad. Sci. 7 (1838) 1125.

[4] A. Payen, C.R. Hebd, Mémoire sur la composition du tissu propre des plantes e du ligneux, Seances Acad. Sci. 7 (1838) 1052.

[5] A. Brogniart, A. Pelonze, R. Dumas, Report on a Memoir of M. Payen, on the Composition of the Woody Nature, Comptes Rendus. 8 (1839) 51 – 53.

[6] H. Staudinger, Über Polymerisation, Ber. Dtsch. Chem. Ges. 53 (1920) 1073–1085.

[7] B. Medronho, B. Lindman, Brief overview on cellulose dissolution / regeneration interactions and mechanisms, Adv. Colloid Interface Sci. 222 (2015) 502–508.

[8] C. Olsson, G. Westman, Direct Dissolution of Cellulose: Background, Means and Applications, in: Cellul. - Fundam. Asp., Intech, 2013: pp. 2–37.

[9] J.W.S. Hearl, A Fringed Fibril Theory of Structure in Crystalline Polymers, J. Polym. Sci. XXVIII (1958) 432–435.

[10] J. Credou, T. Berthelot, Cellulose: from biocompatible to bioactive material, J. Mater. Chem. B. 2 (2014) 4767–4788.

[11] P. Zugenmaier, Morphology, in: Crystalline Cellululose and Derivatives Characterization and Structure, Springer Berlin Heidelberg, Berlin, Heidelberg, 2008: pp. 207–221.

[12] A. Chami Khazraji, S. Robert, Interaction effects between cellulose and water in nanocrystalline and amorphous regions: A novel approach using molecular modeling, J. Nanomater. 2013 (2013) 1–10.

[13] Y. Nishiyama, J. Sugiyama, H. Chanzy, P. Langan, Crystal Structure and Hydrogen Bonding System in Cellulose Iα from Synchrotron X-ray and Neutron Fiber Diffraction, J. Am. Chem. Soc. 125 (2003) 14300–14306.

[14] K.H. Gardner, J. Blackwell, The structure of native cellulose, Biopolymers. 13 (1974) 1975–2001.

[15] P. Langan, Y. Nishiyama, H. Chanzy, X-ray structure of mercerized cellulose II at 1 Å resolution, Biomacromolecules. 2 (2001) 410–416.

[16] E.S. Gardiner, A. Sarko, Packing analysis of carbohydrates and polysaccharides. 16. The crystal structures of celluloses IV I and IV II , Can. J. Chem. 63 (1985) 173–180.

[17] J. Hayashi, A. Sufoka, J. Ohkita, S. Watanabe, The conformation of existences of cellulose $III_I$, $IIII_I$, $IV_I$ and $IV_{II}$ by the X-ray method, Polym Sci Polym Lett. 13 (1975) 23–27.

[18] L. Loeb, L. Segal, Preparation of cotton cellulose IV from cotton cellulose III, J. Polym. Sci. 14 (1954) 121–123.

[19] K. Jedvert, T. Heinze, Cellulose modification and shaping - A review, J. Polym. Eng. 37 (2017) 845–860.

[20] D. Fengel, G. Wegener, Wood: Chemistry, Ultrastructure, Reactions., De Gruyter, Inc., Berlin/Boston, Germany, 1983.

[21] A.M. Boudet, Lignins and lignification: Selected issues, Plant Physiol. Biochem. 38 (2000) 81–96.

[22] J. Ruwoldt, F.H. Blindheim, G. Chinga-Carrasco, Functional surfaces, films, and coatings with lignin – a critical review, RSC Adv. 13 (2023) 12529–12553.

[23] X. Zhang, L. Li, F. Xu, Chemical Characteristics of Wood Cell Wall with an Emphasis on Ultrastructure: A Mini-Review, Forests. 13 (2022).

[24] D. Klemm, B. Heublein, H.P. Fink, A. Bohn, Cellulose: Fascinating biopolymer and sustainable raw material, Angew. Chemie - Int. Ed. 44 (2005) 3358–3393.

[25] H. Sixta, Pulp Properties and Applications, in: Handb. Pulp, Wiley-VCH Verlag GmbH & Co., 2006: p. 1010.

[26] P. Lahtinen, S. Liukkonen, J. Pere, A. Sneck, H. Kangas, A Comparative Study of Fibrillated Fibers from Different Mechanical and Chemical Pulps, Bioresources. 9 (2014) 2115–2127.

[27] D. Li, D. Ibarra, V. Köpcke, M. Ek, Production of Dissolving Grade Pulps from

Wood and Non-Wood Paper-Grade Pulps by Enzymatic and Chemical Pretreatments, in: Funct. Mater. from Renew. Sources, American Chemical Society, 2012: pp. 167–189.

[28] V. Köpcke, Improvement on cellulose accessibility and reactivity of different wood pulps, KTH Royal Institute of Technology, 2008.

[29] H.A. Krässig, Cellulose, Structure, Accessibility and Reactivity, Gordon and Breach Publishers, Amsterdam, 1993.

[30] F.R. Amin, H. Khalid, H. Zhang, S. Rahman, R. Zhang, G. Liu, C. Chen, Pretreatment methods of lignocellulosic biomass for anaerobic digestion, AMB Express. 7 (2017) 1–12.

[31] S. Acharya, S. Liyanage, P. Parajuli, S.S. Rumi, J.L. Shamshina, N. Abidi, Utilization of Cellulose to Its Full Potential: A Review on Cellulose Dissolution, Regeneration, and Applications., Polymers (Basel). 13 (2021).

[32] B. Lindman, G. Karlström, L. Stigsson, On the mechanism of dissolution of cellulose, J. Mol. Liq. 156 (2010) 76–81.

[33] N. Le Moigne, P. Navard, Dissolution mechanisms of wood cellulose fibres in NaOH–water, Cellulose. 17 (2010) 31–45.

[34] P. Navard, C. Cuissinat, Cellulose swelling and dissolution as a tool to study the fiber structure, OAI. (2006).

[35] N. Le Moigne, E. Montes, C. Pannetier, H. Höfte, P. Navard, Gradient in Dissolution Capacity of Successively Deposited Cell Wall Layers in Cotton Fibres, Macromol. Symp. 262 (2008) 65–71.

[36] N. Le Moigne, J. Bikard, P. Navard, Rotation and contraction of native and regenerated cellulose fibers upon swelling and dissolution: the role of morphological and stress unbalances, Cellulose. 17 (2010) 507–519.

[37] T. Budtova, P. Navard, Cellulose in NaOH–water based solvents: a review, Cellulose. 23 (2016) 5–55.

[38] B. Lindman, B. Medronho, L. Alves, C. Costa, H. Edlund, M. Norgren, The relevance of structural features of cellulose and its interactions to dissolution, regeneration, gelation and plasticization phenomena, Phys. Chem. Chem. Phys. 19 (2017) 23704–23718.

[39] B. Medronho, B. Lindman, Brief overview on cellulose dissolution/regeneration interactions and mechanisms, Adv. Colloid Interface Sci. 222 (2015) 502–508.

[40] B. Medronho, H. Duarte, L. Alves, F. Antunes, A. Romano, B. Lindman, Probing cellulose amphiphilicity, Nord. Pulp Pap. Res. J. 30 (2015) 58–66.

[41] B. Medronho, B. Lindman, Competing forces during cellulose dissolution: From solvents to mechanisms, Curr. Opin. Colloid Interface Sci. 19 (2014) 32–40.

[42] M. Bergenstråhle, J. Wohlert, M.E. Himmel, J.W. Brady, Simulation studies of the insolubility of cellulose, Carbohydr. Res. 345 (2010) 2060–2066.

[43] B. Medronho, A. Romano, M.G. Miguel, L. Stigsson, B. Lindman, Rationalizing cellulose (in)solubility: reviewing basic physicochemical aspects and role of hydrophobic interactions, Cellulose. 19 (2012) 581–587.

[44] B. Lindman, B. Medronho, L. Alves, M. Norgren, L. Nordenskiöld, Hydrophobic interactions control the self-assembly of DNA and cellulose, Q. Rev. Biophys. 54 (2021) e3.

[45] D. Chandler, Interfaces and the driving force of hydrophobic assembly, Nature. 437 (2005) 640–647.

[46] T. Liebert, D. Klemm, T. Heinze, Synthesis and Carboxymethylation of Organo-Soluble Trifluoroacetates and Formates of Cellulose, J. Macromol. Sci. Part A Pure Appl. Chem. 33 (1996) 613–626.

[47] B. Volkert, W. Wagenknecht, M. Mai, Structure-Property Relationship of Cellulose Ethers – Influence of the Synthetic Pathway on Cyanoethylation, ACS Symp. Ser. 1033 (2010) 319–341.

[48] D. Klemm, T. Heinze, B. Philipp, W. Wagenknecht, New approaches to advanced polymers by selective cellulose functionalization, Acta Polym. 48 (1997) 277–297.

[49] G. Askew, H. Bahia, C. Foxall, S. Law, H. Street, Cellulose sponges, WO 98/28360, 1998.

[50] F.M. Haemmerle, The cellulose gap (the future of cellulose fibres), Lenzinger Berichte. 89 (2011) 12–21.

[51] D. Eichinger, A vision of the world of cellulosic fibers in 2020, 2012.

[52] M. Hummel, A. Michud, M. Tanttu, S. Asaadi, Y. Ma, L.K.J. Hauru, A. Parviainen, A.W.T. King, I. Kilpeläinen, H. Sixta, Ionic liquids for the production of man-made cellulosic fibers: opportunities and challenges, Cellul. Chem. Prop. Fibers, Nanocelluloses Adv. Mater. (2016) 133–168.

[53] D.L. Johnson, Method of Prefaring Polymers From a Mixture of Cyclic amine oxides and polymers, 3,508,941, 1970.

[54] H. Chanzy, S. Nawrot, A. Peguy, P. Smith, Phase Behavior of the Quasiternary System N - Methylmorpholine-N-Oxide , Water , and Cellulose, J. Polym. Sci. 20 (1982) 1909–1924.

[55] T. Rosenau, A. Potthast, H. Hettegger, M. Bacher, M. Opietnik, T. Röder, I. Adorjan, On the role of N-methylmorpholine-N-oxide (NMMO) in the generation of elemental transition metal precipitates in cellulosic materials, Cellulose. 28 (2021) 10143–10161.

[56] M. Michael, R.N. Ibbett, O.W. Howarth, Interaction of cellulose with amine oxide solvents, Cellulose. 7 (2000) 21–33.

[57] E.R. Maia, S. Perez, Organic solvents for cellulose. IV. Modeling of the interaction between N-methylmorpholine N-oxide (MMNO) molecules and a cellulose chain, Nov J Chim. 7 (1983) 89–100.

[58] T. Rosenau, A. Potthast, H. Sixta, P. Kosma, The chemistry of side reactions and byproduct formation in the system NMMO/cellulose (Lyocell process), Prog. Polym. Sci. 26 (2001) 1763–1837.

[59] F. Wendler, G. Graneß, T. Heinze, Characterization of autocatalytic reactions in modified cellulose/NMMO solutions by hermal analysis and UV/VIS spectroscopy, Cellulose. 12 (2005) 411–422.

[60] F. Wendler, A. Kolbe, F. Meister, T. Heinze, Thermostability of Lyocell dopes modified with surface-active additives, Macromol. Mater. Eng. 290 (2005) 826–832.

[61] F. Wendler, G. Graneß, R. Büttner, F. Meister, T. Heinze, A Novel Polymeric Stabilizing System for Modified Lyocell Solutions, J Polym Sci, Part B Polym Phys. 44 (2006) 1702–1713.

[62] A.J. Sayyed, N.A. Deshmukh, D. V. Pinjari, A critical review of manufacturing processes used in regenerated cellulosic fibres: viscose, cellulose acetate, cuprammonium, LiCl/DMAc, ionic liquids, and NMMO based lyocell, Cellulose. 26 (2019) 2913–2940.

[63] E. Schweizer, Das Kupferoxyd-Ammoniak, ein Auflösungsmittel für die Pflanzenfaser, J. Für Prakt. Chemie. 72 (1857) 109–111.

[64] W. Traube, Behavior of metallic hydroxides to alkylenediamino solutions, Ber Dtsch Chem Ges. 44 (1912) 3319–3324.

[65] A.D. Bain, An NMR-study of the interactions between cadoxen and saccharides, Carbohydr Res. 84 (1980) 1–12.

[66] J. Burger, G. Kettenbach, P. Klüfers, Coordination equilibria in transition-metal based cellulose solvents, Macromol Symp. 95 (1995) 113–126.

[67] F. Wurm, B. Rietzler, T. Pham, T. Bechtold, Multivalent ions as reactive crosslinkers for biopolymers—A review, Molecules. 25 (2020).

[68] C. Graenacher, Cellulose solution, US1943176A, 1934.

[69] R.P. Swatloski, S.K. Spear, J.D. Holbrey, R.D. Rogers, Dissolution of Cellose with Ionic Liquids, J. Am. Chem. Soc. 124 (2002) 4974–4975.

[70] A. Xu, J. Wang, H. Wang, Effects of anionic structure and lithium salts addition on the dissolution of cellulose in 1-butyl-3-methylimidazolium-based ionic liquid solvent systems, Green Chem. 12 (2010) 268–27.

[71] Y. Fukaya, A. Sugimoto, H. Ohno, Superior solubility of polysaccharides in low viscosity, polar and halogen-free 1,3-dialkylimidazolium formates, Biomacromolecules. 7 (2006) 3295–3297.

[72] A. Brandt, M.J. Ray, T.Q. To, D.J. Leak, R.J. Murphy, T. Welton, Ionic liquid pretreatment of lignocellulosic biomass with ionic liquid–water mixtures, Green Chem. 13 (2011) 2489–2499.

[73] B. Zhao, L. Greiner, W. Leitner, Cellulose solubilities in carboxylate-based ionic liquids, RSC Adv. 2 (2012) 2476–2479.

[74] J. Zhang, Q. Ren, J.S. He, No Title, ZL02155945, 2002.

[75] D.G. Raut, O. Sundman, W. Su, P. Virtanen, Y. Sugano, K. Kordas, J. Mikkola, A morpholinium ionic liquid for cellulose dissolution, Carbohydr. Polym. 130 (2015) 18–25.

[76] R.S. Payal, R. Bharath, G. Periyasamy, S. Balasubramanian, Density functional theory investigations on the structure and dissolution mechanisms for cellobiose and xylan in an ionic liquid: Gas phase and cluster calculations, J. Phys. Chem. B. 116 (2012) 833–840.

[77] G. Bentivoglio, R. Thomas, M. Fasching, M. Buchberger, H. Schottenberger, H. Sixta, Cellulose processing with chloride-based ionic liquids, Lenzinger Berichte. 86 (2006) 154–161.

[78] H. Liu, K.L. Sale, B.A. Simmons, S. Singh, Molecular Dynamics Study of Polysaccharides in Binary Solvent Mixtures of an Ionic Liquid and Water, J. Phys. Chem. B. 115 (2011) 10251–10258.

[79] A.S. Gross, J.-W. Chu, On the Molecular Origins of Biomass Recalcitrance: The Interaction Network and Solvation Structures of Cellulose Microfibrils, J. Phys. Chem. B. 114 (2010) 13333–13341.

[80] H.M. Cho, A.S. Gross, J.-W. Chu, Dissecting Force Interactions in Cellulose Deconstruction Reveals the Required Solvent Versatility for Overcoming Biomass Recalcitrance, J. Am. Chem. Soc. 133 (2011) 14033–14041.

[81] B.D. Rabideau, A. Agarwal, A.E. Ismail, The Role of the Cation in the Solvation of Cellulose by Imidazolium-Based Ionic Liquids, J. Phys. Chem. B. 118 (2014) 1621–1629.

[82] L. Lilienfeld, Cellulose solution and process for making same, US1658606A, 1928.

[83] G.F. Davidson, The dissolution of chemically modified cotton cellulose in alkaline solutions: Part I—In solutions of sodium hydroxide, particularly at temperatures below the normal, J. Text. Inst. Trans. 25 (1934) T174–T196.

[84] G.F. Davidson, The dissolution of chemically modified cotton cellulose in alkaline solutions. Part II.—a comparison of the solvent action of solutions of lithium,

sodium, potassium, and tetramethylammonium hydroxides, J. Text. Inst. Trans. 27 (1936) T112–T130.

[85] G.F. Davidson, 4.—The dissolution of chemically modified cotton cellulose in alkaline solutions. part 3—in solutions of sodium and potassium hydroxide containing dissolved zinc, beryllium and aluminium oxides., J. Text. Inst. Trans. 28 (1937) T27–T44.

[86] L. Lilienfeld, Cellulose solutions and process for their production, US1771462A, 1930.

[87] H. Sobue, H. Kiessig, K. Hess, The cellulose–sodium hydroxide–water system as a function of the temperature., Z Phys Chem B. (1939) 309–328.

[88] A. Isogai, R.H. Atalla, Dissolution of cellulose in aqueous NaOH solutions, Cellulose. 5 (1998) 309–319.

[89] B. Lindman, G. Karlström, Nonionic polymers and surfactants: Temperature anomalies revisited, Comptes Rendus Chim. 12 (2009) 121–128.

[90] M. Bergenstråhle-Wohlert, T. Angles d'Ortoli, N.A. Sjöberg, G. Widmalm, J. Wohlert, On the anomalous temperature dependence of cellulose aqueous solubility, Cellulose. 23 (2016) 2375–2387.

[91] M. Gunnarsson, M. Hasani, D. Bernin, Influence of urea on methyl β-D-glucopyranoside in alkali at different temperatures, Cellulose. 26 (2019) 9413–9422.

[92] T. Yamashiki, K. Kamide, K. Okajima, K. Kowsaka, T. Matsui, H. Fukase, Some Characteristic Features of Dilute Aqueous Alkali Solutions of Specific Alkali Concentration (2.5 mol l−1) Which Possess Maximum Solubility Power against Cellulose, Polym. J. 20 (1988) 447–457.

[93] M. Kihlman, B. Medronho, A. Romano, U. Germgård, B. Lindman, Cellulose dissolution in an alkali based solvent: influence of additives and pretreatments., J Braz Chem Soc. 24 (2013) 295–303.

[94] B. Xiong, P. Zhao, K. Hu, L. Zhang, G. Cheng, Dissolution of cellulose in aqueous NaOH/urea solution: Role of urea, Cellulose. 21 (2014) 1183–1192.

[95] H. Jin, C. Zha, L. Gu, Direct dissolution of cellulose in NaOH/thiourea/urea aqueous solution, Carbohydr. Res. 342 (2007) 851–858.

[96] L. Yan, Z. Gao, Dissolving of cellulose in PEG/NaOH aqueous solution, Cellulose. 15 (2008) 789–796.

[97] D.H. Powers, L.H. Bock, Cellulose Solutions, US2009015A, 1935.

[98] R. Ehert, V.T. Lieser, Zur Eenntnis der Kohlenhydrate. X, Viscositiitsuntersuchungen an Cellul. 532 (1937) 94–103.

[99] T. Brownsett, D.A. Clibbens, 4— The dissolution of chemically modified cotton cellulose in alklaline solutions. Part VII. The solevnt action of solutions of triemethylbenzyl-and dimethyldibenzyl- ammonium hydroxides (Tritons B and F)., J. Text. Inst. Trans. 32 (1941) T32–T44.

[100] T. Brownsett, D.A. Clibbens, A comparison of the rates of flow of modified cotton celluloses dissolved in solutions of trimethylbenzylammonium hydroxide (triton b), dimethyldibenzylammonium hydroxide (triton F), sodium hydroxide, cuprammonium and cupri-ethylenediamine, J. Text. Inst. Trans. 32 (1941) T57–T70.

[101] S.M. Hudson, J.A. Cuculo, The Solubility of Unmodified Cellulose : A Critique of the Literature The Solubility of Unmodified Cellulose : A Critique of the Literature, J. Macromol. Sci. 18 (1980) 1–82.

[102] Y. Wang, L. Liu, P. Chen, L. Zhang, A. Lu, Cationic hydrophobicity promotes dissolution freezing – thawing, Phys. Chem. Chem. Phys. 20 (2018) 14223–14233.

[103] C. Zhong, F. Cheng, Y. Zhu, Z. Gao, H. Jia, P. Wei, Dissolution mechanism of cellulose in quaternary ammonium hydroxide: Revisiting through molecular interactions, Carbohydr. Polym. 174 (2017) 400–408.

[104] A. Tsurumaki, M. Tajima, M. Abe, D. Sato, H. Ohno, Effect of the cation structure on cellulose dissolution in aqueous solutions of organic onium hydroxides, Phys. Chem. Chem. Phys. 22 (2020) 22602–22608.

[105] O.A. El Seoud, H. Nawaz, E.P.G. Arêas, Chemistry and Applications of Polysaccharide Solutions in Strong Electrolytes/Dipolar Aprotic Solvents: An Overview, 18 (2013) 1270–1313.

[106] M. Oprea, S.I. Voicu, Recent advances in composites based on cellulose derivatives for biomedical applications, Carbohydr. Polym. 247 (2020) 116683.

[107] H. Nawaz, R. Casarano, O.A. El Seoud, First report on the kinetics of the uncatalyzed esterification of cellulose under homogeneous reaction conditions : a rationale for the effect of carboxylic acid anhydride chain-length on the degree of biopolymer substitution, Cellulose. 19 (2012) 199–207.

[108] H. Hu, J. You, W. Gan, J. Zhou, L. Zhang, Synthesis of allyl cellulose in NaOH/urea aqueous solutions and its thiol–ene click reactions†, Polym. Chem. 6 (2015) 3543–3548.

[109] M.-F. Li, S.-N. Sun, F. Xu, R.-C. Sun, Cold NaOH/urea aqueous dissolved cellulose for benzylation: Synthesis and characterization, Eur. Polym. J. 47 (2011) 1817–1826.

[110] O. Sundman, T. Gillgren, M. Boström, Homogenous benzylation of cellulose: impact of different methods on product properties, Cellul. Chem. Technol. 49 (2015) 745–755.

[111] J. Zhou, L. Zhang, Q. Deng, X. Wu, Synthesis and Characterization of Cellulose Derivatives Prepared in NaOH / Urea Aqueous Solutions, J. Polym. Sci. Part A Polym. Chem. 42 (2004) 5911–5920.

[112] H. Qi, T. Liebert, F. Meister, T. Heinze, Homogenous carboxymethylation of cellulose in the NaOH/urea aqueous solution, React. Funct. Polym. 69 (2009) 779–784.

[113] J. Zhou, Y. Qin, S. Liu, L. Zhang, Homogenous Synthesis of Hydroxyethylcellulose in NaOH / Urea Aqueous Solution, (2006) 84–89.

[114] J. Zhou, Q. Li, Y. Song, L. Zhang, X. Lin, A facile method for the homogeneous synthesis of cyanoethyl cellulose in NaOH/urea aqueous solutions, Polym. Chem. 1 (2010) 1662–1668.

[115] Q. Li, P. Wu, J. Zhou, L. Zhang, Structure and solution properties of cyanoethyl celluloses synthesized in LiOH/urea aqueous solution, Cellulose. 19 (2012) 161–169.

[116] J. Zhou, C. Chang, R. Zhang, L. Zhang, Hydrogels Prepared from Unsubstituted Cellulose in NaOH / Urea Aqueous Solution, Macromol. Biosci. 7 (2007) 804–809.

[117] C. Chang, L. Zhang, J. Zhou, L. Zhang, J.F. Kennedy, Structure and properties of hydrogels prepared from cellulose in NaOH / urea aqueous solutions, Carbohydr. Polym. 82 (2010) 122–127.

[118] X. Qin, A. Lu, L. Zhang, Gelation behavior of cellulose in NaOH / urea aqueous system via cross-linking, Cellulose. 20 (2013) 1669–1677.

[119] T. Shi, Y. Lu, Fluorescent cellulose films with pH response and polarized emission, Polymer (Guildf). 189 (2020) 122167.

[120] J.A. Sirviö, J.P. Heiskanen, Room-temperature dissolution and chemical modification of cellulose in aqueous tetraethylammonium hydroxide–carbamide solutions, Cellulose. 27 (2020) 1933–1950.

[121] A.M. Kozlowski, M. Hasani, Cellulose interactions with CO2 in NaOH(aq): The (un)expected coagulation creates potential in cellulose technology, Carbohydr. Polym. 294 (2022) 119771.

[122] P. Singh, H. Duarte, L. Alves, F. Antunes, N. Le Moigne, J. Dormanns, B. Duchemin, M.P.S. and B. Medronho, From Cellulose Dissolution and Regeneration to Added Value Applications — Synergism Between Molecular Understanding and Material Development, in: M. Poletto, H.L.O. Junior (Eds.), IntechOpen, Rijeka, 2015: p. Ch. 1.

[123] S. Zhang, F. Li, J.Y. Yu, Kinetics of cellulose regeneration from cellulose-NaOH/thiourea/urea/H2O system, Cellul. Chem. Technol. 45 (2011) 593–604.

[124] R. Li, L. Zhang, M. Xu, Novel regenerated cellulose films prepared by coagulating with water: Structure and properties, Carbohydr. Polym. 87 (2012) 95–100.

[125] N. Isobe, S. Kimura, M. Wada, S. Kuga, Mechanism of cellulose gelation from aqueous alkali-urea solution, Carbohydr. Polym. 89 (2012) 1298–1300.

[126] Y. Hata, T. Serizawa, Self-assembly of cellulose for creating green materials with tailor-made nanostructures, J. Mater. Chem. B. 9 (2021) 3944–3966.

[127] C. Yamane, T. Aoyagi, M. Ago, K. Sato, K. Okajima, T. Takahashi, Two different surface properties of regenerated cellulose due to structural anisotropy, Polym. J. 38 (2006) 819–826.

[128] M. Kiyose, E. Yamamoto, C. Yamane, T. Midorikawa, T. Takahashi, Structure and properties of low-substituted hydroxypropylcellulose films and fibers regenerated from aqueous sodium hydroxide solution, Polym. J. 39 (2007) 703–711.

[129] H. Miyamoto, M. Umemura, T. Aoyagi, C. Yamane, K. Ueda, K. Takahashi, Structural reorganization of molecular sheets derived from cellulose II by molecular dynamics simulations, Carbohydr. Res. 344 (2009) 1085–1094.

[130] T. Sparrman, L. Svenningsson, K. Sahlin-Sjövold, L. Nordstierna, G. Westman, D. Bernin, A revised solid-state NMR method to assess the crystallinity of cellulose, Cellulose. 26 (2019) 8993–9003.

[131] B. Swensson, A. Larsson, M. Hasani, Dissolution of cellulose using a combination of hydroxide bases in aqueous solution, Cellulose. 27 (2020) 101–112.

[132] B. Swensson, A. Larsson, M. Hasani, Probing interactions in combined hydroxide base solvents for improving dissolution of cellulose, Polymers (Basel). 12 (2020) 1310.

[133] T. Miyamoto, Y. Sato, T. Shibata, H. Inagaki, 13C Nuclear Magnetic Resonance Studies of Cellulose Acetate, J. Polym. Sci. 22 (1984) 2363–2370.

[134] D.G. Raut, O. Sundman, W. Su, P. Virtanen, Y. Sugano, K. Kordas, J.P. Mikkola, A morpholinium ionic liquid for cellulose dissolution, Carbohydr. Polym. 130 (2015) 18–25.

[135] M. Kostag, T. Liebert, O.A. El Seoud, T. Heinze, Efficient Cellulose Solvent : Quaternary Ammonium Chlorides, Macromol. Rapid Commun. 34 (2013) 1580–1584.

[136] J. Miao, H. Sun, Y. Yu, X. Song, L. Zhang, Quaternary ammonium acetate: an efficient ionic liquid for the dissolution and regeneration of cellulose, RSC Adv. 4 (2014) 36721–36724.

[137] X. Meng, J. Devemy, V. Verney, A. Gautier, P. Husson, J.-M. Andanson,

Improving Cellulose Dissolution in Ionic Liquids by Tuning the Size of the Ions: Impact of the Length of the Alkyl Chains in Tetraalkylammonium Carboxylate, ChemSusChem. 10 (2017) 1749–1760.

[138] A. Idström, L. Gentile, M. Gubitosi, C. Olsson, B. Stenqvist, M. Lund, K.-E. Bergquist, U. Olsson, T. Köhnke, E. Bialik, On the dissolution of cellulose in tetrabutylammonium acetate/dimethyl sulfoxide: a frustrated solvent, Cellulose. 24 (2017) 3645–3657.

[139] Y. Tseng, Y. Lee, S. Chen, Synthesis of Quaternary Ammonium Room-Temperature Ionic Liquids and their Application in the Dissolution of Cellulose, Appl. Sci. 9 (2019) 1750.

[140] M. Kostag, P.A.R. Pires, O.A. El Seoud, Dependence of cellulose dissolution in quaternary ammonium acetates/DMSO on the molecular structure of the electrolyte: use of solvatochromism, micro-calorimetry, and molecular dynamics simulations, Cellulose. 27 (2020) 3565–3580.

[141] J.-O. Müller, B. Oschmann, K. Holger, T. Witt, Solution of cellulose in a quaternary ammonium compound and a co-solvent, WO2021073961A1, 2021.

[142] V. Diez, A. DeWeese, R.S. Kalb, D.N. Blauch, A.M. Socha, Cellulose Dissolution and Biomass Pretreatment Using Quaternary Ammonium Ionic Liquids Prepared from H-, G-, and S-Type Lignin-Derived Benzaldehydes and Dimethyl Carbonate, Ind. Eng. Chem. Res. 58 (2019) 16009–16017.

[143] S. Köhler, T. Heinze, New Solvents for Cellulose: Dimethyl Sulfoxide/Ammonium Fluorides, Macromol. Biosci. 7 (2007) 307–314.

[144] R.P. Swatloski, S.K. Spear, J.D. Holbrey, R.D. Rogers, Dissolution of Cellose with Ionic Liquids, JACS. 124 (2002) 4974–4975.

[145] Å. Östlund, D. Lundberg, L. Nordstierna, K. Holmberg, M. Nydén, Dissolution and Gelation of Cellulose in TBAF/DMSO Solutions: The Roles of Fluoride Ions and Water, Biomacromolecules. 10 (2009) 2401–2407.

[146] B. Lindman, G. Karlström, L. Stigsson, On the mechanism of dissolution of cellulose, J. Mol. Liq. 156 (2010) 76–81.

[147] K. Saalwächter, W. Burchard, P. Klüfers, G. Kettenbach, P. Mayer, D. Klemm, S. Dugarmaa, Cellulose solutions in water containing metal complexes, Macromolecules. 33 (2000) 4094–4107.

[148] R.S. Anaredy, A.J. Lucio, S.K. Shaw, Adventitious Water Sorption in a Hydrophilic and a Hydrophobic Ionic Liquid: Analysis and Implications, ACS Omega. 1 (2016) 407–416.

[149] C. Ma, A. Laaksonen, C. Liu, X. Lu, X. Ji, The peculiar effect of water on ionic liquids and deep eutectic solvents, Chem. Soc. Rev. 47 (2018) 8685–8720.

[150] P. Migowski, P. Lozano, J. Dupont, Imidazolium based ionic liquid-phase green catalytic reactions, Green Chem. 25 (2023) 1237–1260.

[151] Y. Cao, Y. Chen, X. Sun, Z. Zhang, T. Mu, Water sorption in ionic liquids: kinetics, mechanisms and hydrophilicity, Phys. Chem. Chem. Phys. 14 (2012) 12252–12262.

[152] M.G. Freire, C.M.S.S. Neves, P.J. Carvalho, R.L. Gardas, A.M. Fernandes, I.M. Marrucho, L.M.N.B.F. Santos, J.A.P. Coutinho, Mutual Solubilities of Water and Hydrophobic Ionic Liquids, J. Phys. Chem. B. 111 (2007) 13082–13089.

[153] A.C. MacMillan, T.M. McIntire, S.A. Epstein, S.A. Nizkorodov, Effect of Alkyl Chain Length on Hygroscopicity of Nanoparticles and Thin Films of Imidazolium-Based Ionic Liquids, J. Phys. Chem. C. 118 (2014) 29458–29466.

[154] L.C. Fidale, N. Ruiz, T. Heinze, O.A. El Seoud, Cellulose Swelling by Aprotic and Protic Solvents: What are the Similarities and Differences?, Macromol. Chem. Phys. 209 (2008) 1240–1254.

[155] J.-M. Andanson, E. Bordes, J. Devémy, F. Leroux, A.A.H. Pádua, M.F.C. Gomes, Understanding the role of co-solvents in the dissolution of cellulose in ionic liquids, Green Chem. 16 (2014) 2528–2538.

[156] C. Zhang, H. Kang, P. Li, Z. Liu, Y. Zhang, R. Liu, J. Xiang, Y. Huang, Dual effects of dimethylsulfoxide on cellulose solvating ability of 1-allyl-3-methylimidazolium chloride, Cellulose. 23 (2016) 1165–1175.

[157] H. Zhang, J. Wu, J. Zhang, J. He, 1-Allyl-3-methylimidazolium Chloride Room Temperature Ionic Liquid: A New and Powerful Nonderivatizing Solvent for Cellulose, Macromolecules. 38 (2005) 8272–8277.

[158] Y. Li, J. Wang, X. Liu, S. Zhang, Towards a molecular understanding of cellulose dissolution in ionic liquids: Anion/cation effect, synergistic mechanism and physicochemical aspects, Chem. Sci. 9 (2018) 4027–4043.

[159] S. Tang, G.A. Baker, S. Ravula, J.E. Jones, H. Zhao, PEG-functionalized ionic liquids for cellulose dissolution and saccharification, Green Chem. 14 (2012) 2922–2932.

[160] J. Zhang, J. Wu, J. Yu, X. Zhang, J. He, J. Zhang, Application of ionic liquids for dissolving cellulose and fabricating cellulose-based materials: state of the art and future trends, Mater. Chem. Front. 1 (2017) 1273–1290.

[161] A. Isogai, NMR analysis of cellulose dissolved in aqueous NaOH solutions, Cellulose. 4 (1997) 99–107.

[162] R.H. Atalla, J.C. Gast, D.W. Sindorf, V.J. Bartuska, G.E. Maciel, Carbon-13 NMR spectra of cellulose polymorphs, J. Am. Chem. Soc. 102 (1980) 3249–3251.

[163] G.E. Maciel, W.L. Kolodziejski, M.S. Bertran, B.E. Dale, Carbon-13 NMR and

order in cellulose, Macromolecules. 15 (1982) 686–687.

[164] H. Lennholm, T. Iversen, Estimation of Cellulose I and II in Cellulosic Samples by Principal Component Analysis of $^{13}$C-CP/MAS-NMR-Spectra, 49 (1995) 119–126.

[165] G. Zuckerstätter, G. Schild, P. Wollboldt, T. Röder, K. Hedda, H. Sixta, The elucidation of cellulose supramolecular structure by 13C CP-MAS NMR, Lenzinger Berichte. 87 (2009) 38–46.

[166] A. Idström, S. Schantz, J. Sundberg, B.F. Chmelka, P. Gatenholm, L. Nordstierna, C NMR assignments of regenerated cellulose from solid-state 2D NMR spectroscopy, Carbohydr. Polym. 151 (2016) 480–487.

[167] Å. Östlund, A. Idström, C. Olsson, P.T. Larsson, L. Nordstierna, Modification of crystallinity and pore size distribution in coagulated cellulose films, Cellulose. 20 (2013) 1657–1667.

[168] X. Tan, L. Chen, X. Li, F. Xie, Effect of anti-solvents on the characteristics of regenerated cellulose from 1-ethyl-3-methylimidazolium acetate ionic liquid, Int. J. Biol. Macromol. 124 (2019) 314–320.